Characterization of putative RCK domain channel proteins in *Arabidopsis thaliana*

Dissertation

zur Erlangung des
Doktorgrades der Agrarwissenschaften (Dr. agr.)

der

Naturwissenschaftlichen Fakultät III
Agrar- und Ernährungswissenschaften,
Geowissenschaften und Informatik

der Martin-Luther-Universität Halle-Wittenberg

vorgelegt von

Xuefeng Gong

Geb. am 06.02.1983 in Xi´an, VR China

Gutachter: 1. Prof. Dr. Edgar Peiter (Halle/ Saale)
2. Prof. Dr. Nicolaus Von Wirén (Gatersleber)
3. PD. Dr. Feng Yan (Gießen)

Verteidigung am: 16.12.2013

Table of Contents

List of Abbreviations

$[Ca^{2+}]_{cyt}$	activity of cytosolic free Ca^{2+}
½ MS	½ strength Murashige and Skoog medium
ABA	abscisic acid
AM	*arbuscular mycorrhiza*
Amp	Ampicilin
Arabidopsis	*Arabidopsis thaliana*
BiFC	bimolecular fluorescence complementation
BSA	bovine serum albumin
cDNA	complementary DNA
C-terminal	carboxy terminal
d	day(s)
DMSO	dimethly sulfoxide
DNA	desoxyribonucleic acid
dNTPs	desoxyribonucleotides
EDTA	ethylenediamine tetraacetic acid
EYFP	enhanced yellow fluorescent protein
GFP	green fluorescent protein
GUS	β-glucuronidase
kb	kilo base pairs
LB medium	Luria-Bertani medium
MAPK	mitogen-activated protein kinase
MIPS	Munich Information Center for Protein Sequences
mRNA	messenger RNA
NCBI	National Center for Biotechnology Information
NFs	Nod factors
N-terminal	amino-terminal
PAMPs	pathogen-associated molecular patterns
PCR	polymerase chain reaction
PTI	PAMP-triggered immunity
rH	relative humidity
Rif	rifampicin

List of Abbreviations

RNA	ribonucleic acid
rpm	rotations per minute
RT	room temperature
SD	standard deviation
SDS	sodium dodecyl sulfate
SEM	scanning electron microscope
SOC	Super Optimal broth medium with Catabolite repression
Spc	Spectinomycin
TAIR	The Arabidopsis Information Resource
U	Unit
WT	Wild type
X-Gluc	5-bromo-4-chloro-3-indolyl-β-D-glucuronic acid
YC3.6	Yellow Cameleon 3.6

1. Introduction

In recent years, huge progress has been made in unraveling the function of many genes in plant genomes. This led to a better understanding of plant developmental processes and plant signalling pathways involved for example in stress tolerance, and in the end this knowledge can also contribute to the generation of stress-tolerant crops needed for human nutrition. Uncovering the function and role of plant genes thus is of great importance. While some have been examined in detail, the role of others is still completely unknown. The current work deals with three as yet uncharacterized genes from *Arabidopsis thaliana*, which are homologues to the leguminous calcium signal modulator DMI1 from *Medicago truncatula*.

1.1 MtDMI1 – a calcium signal modulator in symbiotic signalling pathways

Leguminous plants are able to establish two different kinds of symbiotic interactions, namely with arbuscular mycorrhizal (AM) fungi and with rhizobial bacteria, which help the plant to aquire phosphorus or nitrogen, respectively. Strigolactones and flavonoids released from the host roots attract fungi or bacteria, which then themselves produce signalling molecules called mycorrhizal factors (Myc factors) or nodulation factors (Nod factors) (Oldroyd, 2013). Both are lipochitooligosaccharides. The perception of the Nod factors by root hair cells through signal transduction in the end leads to the establishment of the special organs comprising the bacteria, called nodules (Oldroyd and Downie, 2008). Recognition of the Nod factors by root hair cells initially occurs via receptor-like kinases of the LysM (Lysine Motif) type, such as NFR (Nod-Factor Receptor) 1 and 5 from *Lotus japonicus* or SYM2 from pea (Madsen et al., 2003, Radutoiu et al., 2003, Limpens et al., 2003). Following perception, a signal cascade is induced, which ultimately results in changes in gene expression. An essential component of this signal cascade

are Ca^{2+} oscillations in the nucleus and in the perinuclear region (Oldroyd, 2013, Oldroyd and Downie, 2008). MtDMI1 (*Medicago truncatula* Doesn't Make Infections 1) is involved in generating these Ca^{2+} oscillations (Peiter et al., 2007). Mutants for this protein were first identified in a screen for nodulation-defective plants, therefore its name (Catoira et al., 2000). MtDMI1 has first been localized to the periphery of the nucleus in epidermal cells of *Medicago truncatula* using GFP fusion proteins (Riely et al., 2007) and has recently been reported to be preferentially situated at the inner nuclear envelope by using immunogold labeling (Capoen et al., 2011). How exactly MtDMI1 modulates the Ca^{2+} signals has not been completely unraveled yet. It is assumed that MtDMI1 is not the Ca^{2+} channel itself (Peiter et al., 2007, Capoen et al., 2011). Two possibilities are discussed: DMI1 might act as a K^+ channel, which in the signalling cascade is activated by a second messenger and then leads to a change in membrane potential of the nuclear membrane. This could then activate a yet unidentified voltage-gated Ca^{2+} channel. Alternatively, DMI1 may act as a counter-ion channel to the Ca^{2+} channel. A combination of both is also possible (Charpentier et al., 2013). The Nod and Myc factor-induced Ca^{2+} spiking is decoded by a Ca^{2+}- and calmodulin-dependent protein kinase (CCaMK, DMI3 in Medicago), which together with the transcription factors NSP1 (Nodulation Signalling Pathway 1) and NSP2 transduces the signal into gene expression (Mitra et al., 2004, Levy et al., 2004, Hirsch et al., 2009).

1.2 Homologues of MtDMI1 in other plant species

MtDMI1 has homologues in different plant species, monocots as well as dicots. Homologues can be found in many agriculturally relevant plant species such as maize or rice, and also in the model plant *Arabidopsis thaliana* (Fig.1). Only few of those genes have been experimentally analyzed.

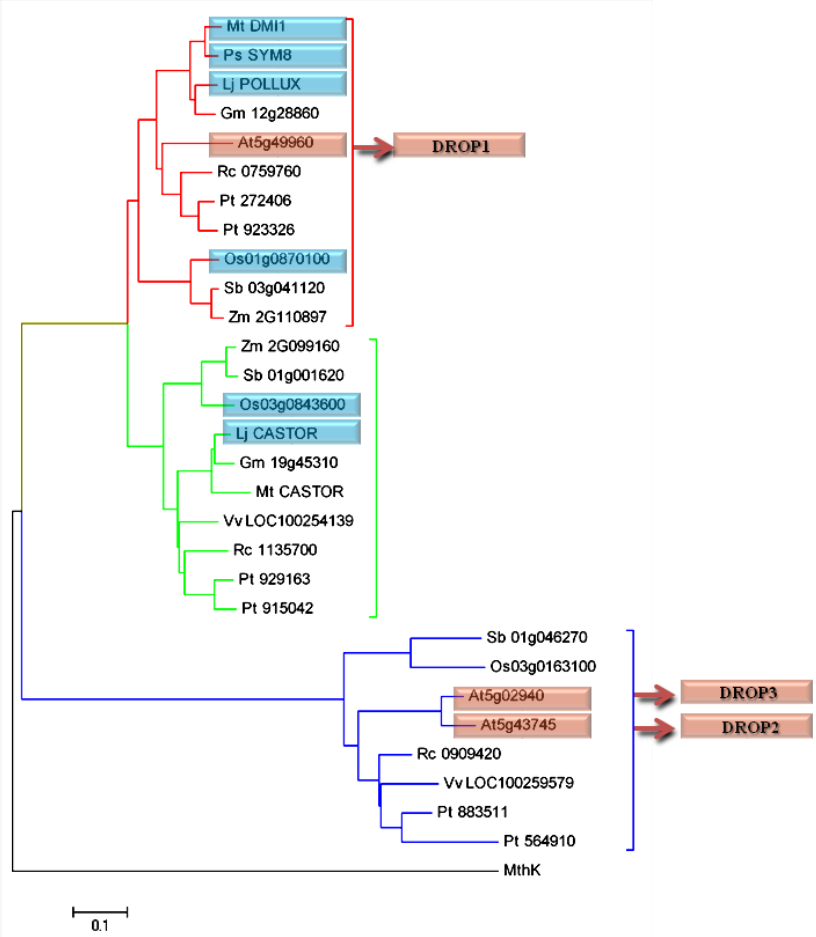

Fig.1: Phylogenetic relationship between MthK, MtDMI1, AtDROP1, AtDROP2 and AtDROP3 as well as orthologues from several crop species (Thor, unpublished). The tree was constructed using MEGA 4 (Tamura et al., 2007). Blue boxes indicate proteins mentioned in the text, red boxes indicate the proteins which are the subject of this thesis. At *Arabidopsis thaliana*, Gm *Glycine max*, Lj *Lotus japonicus*, Mt *Medicago truncatula*, Os *Oryza sativa*, Ps *Pisum sativum* , Pt *Populus trichocarpa*, Rc *Ricinus communis*, Sb *Sorghum bicolor*, Vv *Vitis vinifera*, Zm *Zea mays*.

In the legume model species *Lotus japonicus* for example, CASTOR and POLLUX have been identified as homologues to MtDMI1 by phylogenetic analysis (Ané et al., 2004). They are both essential for Ca^{2+} spiking during arbuscular mycorrhizal and rhizobial symbioses, and thereby seem to act in the same way as MtDMI1. CASTOR and POLLUX have an identical selectivity filter region and form homo- but not heterocomplexes (Ané et al., 2004, Imaizumi-Anraku et al., 2005, Charpentier et al., 2008). Electrophysiological studies and yeast complementation assays suggest that CASTOR and POLLUX are K^+-permeable channels. GFP-fusion proteins of both of them localize to the nuclear region, and CASTOR, similar to MtDMI1, has been confirmed to localize in the nuclear envelope (Charpentier et al., 2008).

Among the two, POLLUX is the one which is more closely related to MtDMI1, but interestingly POLLUX alone cannot fulfill the function that MtDMI1 exerts in Medicago (Venkateshwaran et al., 2012). CASTOR and POLLUX together are needed, which is due to an amino acid replacement in the filter region of MtDMI1 compared to POLLUX. It is currently hypothesized that during Nod and Myc factor signalling a second messenger activates CASTOR and POLLUX, which together are responsible for influx of K^+ into the perinuclear space. This then leads to hyperpolarization and activation of voltage-gated Ca^{2+} channels. Ca^{2+} ions then flow out of the perinuclear space into the cytoplasm resulting in Ca^{2+} spiking eventually. Because of the amino acid substitution, MtDMI1 has a higher net K^+ flux and thus is able to cause the hyperpolarization on its own (Venkateshwaran et al., 2012).

SYM8 is an additional MtDMI1 homolog from *Pisum sativum*. *SYM8* is able to functionally substitute Mt*DMI1* in *M. truncatula* mutants (Edwards et al., 2007). There are also homologues of MtDMI1 in non-legume plants, for example OsCASTOR and OsPOLLUX in rice. Rice mutants of *OsCASTOR* and *OsPOLLUX* cannot establish an AM symbiosis. This indicates that the two genes are essential components of the AM symbiosis signalling pathway in grasses, too. In addition, OsPOLLUX is able to restore nodulation, but not rhizobial infection, in the *M. truncatula dmi1-1* mutant (Chen et al., 2009).

All of the DMI1 homologues mentioned here share to a certain degree a common feature, the RCK domain. RCK stands for “Regulator of Conductance of K^+”. In the bacterial channel MthK, the C-terminal RCK domain is essential for opening of the channel. The MthK complex has eight RCK domains, which form a gating ring at the intracellular membrane surface. Four of the domains belong to full-length MthK subunits and four are soluble domains. Ca^{2+} binding to the domains leads to opening of the pore (Jiang et al., 2002, Chakrapani and Perozo, 2007, Pau et al., 2011). Importance of the RCK domain for correct function of MtDMI1 has also been demonstrated in work on *dmi1* mutants and *MtDMI1*-expressing yeast (Peiter et al., 2007). Another domain, which overlaps considerably with the RCK domain, is Domain of Unknown Function (DUF) 1012 in the pfam database (Punta et al.,

2012). Therefore the homologous proteins can also be found in the DUF1012 family of proteins (Ané et al., 2004, Punta et al., 2012).

In Arabidopsis, three proteins with homology to MtDMI1 can be found (Ané et al., 2004, Fig.1): At5g49960, At5g43745 and At5g02940. As they also possess the C-terminal RCK-domain, they will be referred to in the current study as DROPs (DMI1-like RCK domain Proteins). Among the three, DROP1 (At5g49960) is most closely related to MtDMI1, SYM8 from pea and POLLUX, with 80% identity to MtDMI1 on protein level. DROP2 (At5g43745) and DROP3 (At5g02940) are closely related to each other, but with only around 37% identity more distantly related to MtDMI1 (Ané et al., 2004, Fig.1).

The Arabidopsis membrane protein database ARAMEMNON (http://aramemnon.botanik.uni-koeln.de) indicates that DROP1 has four transmembrane domains, whereas DROP2 and DROP3 most likely have three transmembrane domains (Fig. 2). Predictions point to a mitochondrial or secretory pathway localization in the case of DROP1 and to a chloroplast localization in the case of DROP2 and DROP3 (http://aramemnon.botanik.uni-koeln.de).

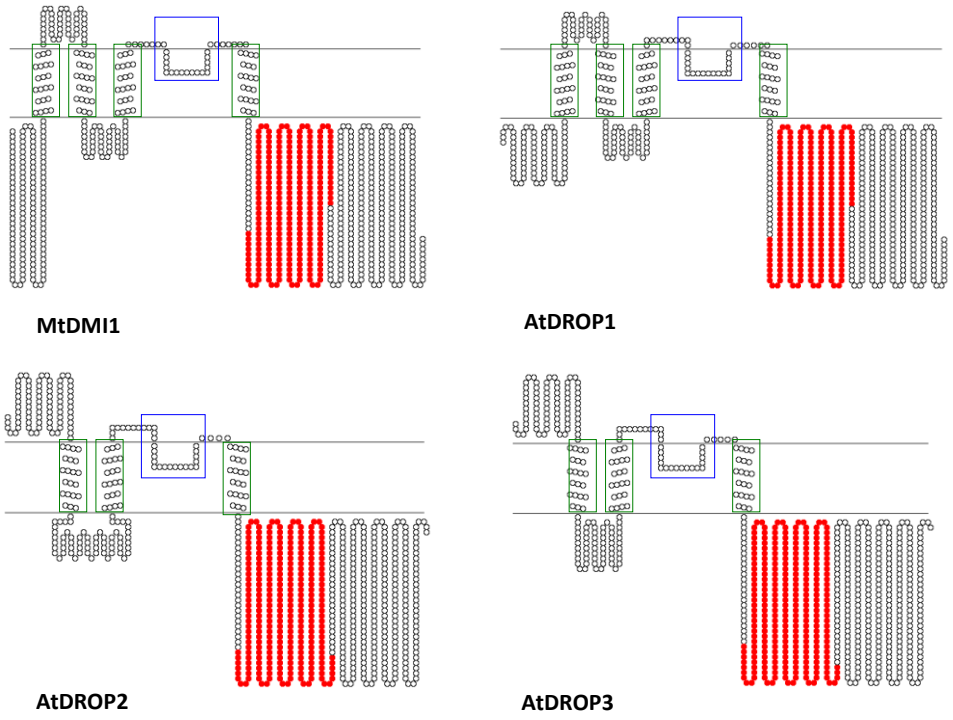

Fig. 2: Predicted topology of MtDMI1 from *Medicago truncatula* and the Arabidopsis DROP1, DROP2, and DROP3 proteins (E. Peiter and K. Thor, unpublished). Transmembrane spans (green boxes) were calculated by TmConsens from predictions of 18 algorithms (http://aramemnon.botanik.uni-koeln.de), and pore regions (blue boxes) were predicted by alignment with the putative pore region of MtDMI1 (Ané et al., 2004). Putative RCK domains (red residues) were predicted by pfam queries and aligments. The figure was drawn in TOPO2 (http://www.sacs.ucsf.edu/TOPO-run/wtopo.pl)

1.3 Calcium signalling is involved in many different processes

As mentioned above, MtDMI1 is involved in generating the Ca^{2+} signal during the nodulation process and has homologs in other plant species. The proteins share structural similarities, indicating that these homologs may also have a function in Ca^{2+} signalling, yet in the case of *Arabidopsis thaliana* this cannot lie in nodulation or mycorrhization. Ca^{2+} however is a second messenger involved in many different processes other than nodulation or mycorrhization. Some Ca^{2+}-dependent aspects of plant function that are of relevance for this work are outlined in the following.

1.3.1 Stress tolerance and stomatal regulation

Plants are exposed to a wide variety of stress situations during their life, including biotic stress, which is brought about by other organisms such as pests or pathogens, and abiotic stress, which is caused by unfavourable environmental conditions such as cold or drought. As sessile organisms, plants don't have the ability to run away from the stress. They thus have developed specific mechanisms for sensing and responding to the stress conditions in order to tolerate them. When a stress is sensed by a plant cell, a molecular signal is transduced to the nucleus, which leads to changes in gene expression. These then lead to physiological and developmental changes, which help the plant to survive (Bray et al., 2000). One important component standing at the centre of signal transduction in many abiotic stress responses is the plant hormone abscisic acid (ABA) (Umezawa et al., 2010). A second messenger which is highly important in signal transduction during both abiotic and biotic stress is Ca^{2+}. Changes in the cytosolic Ca^{2+} concentration ($[Ca^{2+}]_{cyt}$) have been observed in response to many stimuli, e.g. cold, osmotic shock, salt, or pathogens (Knight et al., 1991, Knight et al., 1997, Plieth et al., 1999, Lecourieux et al., 2002). Characteristic oscillations in $[Ca^{2+}]_{cyt}$ thereby induce specific downstream responses. It is assumed that the specificity of the response is determined by the duration, period, frequency, and amplitude of the Ca^{2+} rises. They are therefore also called Ca^{2+} signatures (McAinsh and Hetherington, 1998).

Stomatal guard cells are a cell type in which signalling cascades in response to stress have been studied extensively. Stomata are microscopic pores formed by pairs of guard cells in the epidermis of the plant leaf. Water loss and gas exchange between the plant and the atmosphere are regulated by modulating the aperture of the stomatal pore through turgor changes in the guard cells. Therefore, they react very sensitively to changing environmental conditions. Conditions in which water availability for the plant is limited, like drought or salinity, induce closing of the stomata in order to prevent high transpiration and dehydration of the plant. Low CO_2 concentrations on the other hand lead to stomatal opening in order to keep photosynthetic processes going (Young et al., 2006).

Stomatal closure during drought is induced by the plant hormone ABA, which triggers $[Ca^{2+}]_{cyt}$ elevations. This Ca^{2+} signal leads to activation of two types of anion channels at the plasma membrane, slow-activating sustained (S-type) and rapid transient (R-type) anion channels (Schroeder and Keller, 1992). Activation of these channels induces an anion efflux, which in turn leads to membrane depolarization. Changes in membrane potential lead to K^+ efflux from the guard cells through voltage-dependent outward-rectifying K^+ channels. The loss of ions from the cell causes water to flow out of the cell; the turgor of the cell is reduced and the pore closed (Kim et al., 2010). Stomatal opening on the other hand requires the activity of the H^+-ATPase at the plasma membrane. This activity causes membrane hyperpolarization and in this way induces K^+ uptake into the guard cell through inward-rectifying K^+ channels. Influx of K^+ and other ions increases turgor and volume of the guard cell and thus opens the stomatal pore. This process is inhibited by ABA and Ca^{2+} because they inhibit the H^+-ATPase (Kim et al., 2010).

Stomatal closure not only is a reaction to abiotic stress; it also is part of the plant immune response in order to prevent bacterial invasion (Melotto et al., 2006). In general, the plant innate immune system protects the plants from pathogens through a complex network of responses which can be divided roughly into two major branches (Muthamilarasan and Prasad, 2013): PAMP-triggered immunity (PTI) and effector-triggered immunity (ETI). PTI constitutes a basal defense, whereas ETI relies on specific interactions between effector proteins and resistance proteins and can induce a hypersensitive response (HR) (Ma and Berkowitz 2012, Muthamilarasan and Prasad, 2013, Newman et al., 2013). Both reactions rely on the recognition of conserved microbial constituents called pathogen-associated molecular patterns (PAMPs), such as the bacterial flagellin. Moreover, a 22 amino acid conserved region of flagellin (flg22) is sufficient to serve as PAMP (Felix et al., 1999, Gómez-Gómez et al., 1999). PAMPs are detected by PRRs (pattern-recognition receptors) on the plasma membrane (Jones and Dangl, 2006). For example, the receptor recognizing flg22 is FLS2 (Flagellin Sensing 2) and constitutes an LRR-type receptor kinase (Zipfel et al., 2004, Gómez-Gómez and Boller, 2000). Following elicitor recognition, a $[Ca^{2+}]_{cyt}$ transient is induced, which in the case

of flg22 is characterized by a steep increase and a sustained elevation lasting several minutes (Grant et al., 2000, Ranf et al., 2011). Components decoding the Ca^{2+} signal include Ca^{2+}-dependent protein kinases (CPKs), mitogen-acitvated protein kinase (MAPK) cascades, calmodulin (CaM) and CaM-binding proteins. Downstream of the Ca^{2+} signal, other messengers like reactive oxygen species (ROS) or nitric oxide (NO) are produced (Ma and Berkowitz 2012, Boudsocq and Sheen, 2010, Lecourieux et al., 2006). Physiological and morphological outcomes of the signalling cascade include early responses like stomatal closure (Melotto et al., 2006) and late responses such as seedling growth arrest or callose deposition (Boller and Felix, 2009).

1.3.2 Tip growth processes

Ca^{2+} as signalling molecule is not only involved in stress responses. Prominent examples for plant developmental processes relying on $[Ca^{2+}]_{cyt}$ changes are tip growth processes such as pollen tube and root hair growth.

Pollen tube growth is essential for plant fertilization, and a tip-focused $[Ca^{2+}]_{cyt}$ gradient has been shown to be important for pollen tube growth (Miller et al., 1992). Such gradients have been observed years ago in, for example, pollen tubes from *Agapanthus umbellatus* using fluorescence ratio imaging (Malhó et al., 1994). In pollen of *Lilium longiflorum* $[Ca^{2+}]_{cyt}$ oscillations in one-minute intervals have been observed, which go along with pollen tube growth fluctuations (Pierson et al., 1996). Application of the Ca^{2+} chelator BAPTA, which abolishes the Ca^{2+} gradient, also abolishes the tube growth, which shows that tube growth is dependent on the Ca^{2+} gradient (Miller et al., 1992, Pierson et al., 1994). To accomplish fertilization of the egg, pollen tubes also have to reorient direction and this reorientation has been shown to also be dependent on the Ca^{2+} gradient: if $[Ca^{2+}]_{cyt}$ is increased on one side of the tube apex, the tube grows in this direction (Malhó and Trewavas,1996).

A similar phenomenon to that observed in pollen tubes can be seen in growing root hairs. In these cells, an oscillating tip-focussed $[Ca^{2+}]_{cyt}$ gradient is linked to oscillations of ROS and pH required to activate or deactivate Ca^{2+}-permeable channels (Monshausen et al., 2007).

Ca^{2+} has also been shown to be required for the transport of auxin, a plant hormone that mediates growth and gravitropism of root tips. By applying Ca^{2+} chelators to root tips, Ca^{2+} was deduced to play a key role in linking gravity detection to gravitropic curvature in roots (Lee et al., 1983). Auxin transport interacts with $[Ca^{2+}]_{cyt}$ in the gravitropic response (Plieth and Trewavas, 2002).

1.4 The generation of $[Ca^{2+}]_{cyt}$ signals

In the cytosol of plant cells, stimulus-specific Ca^{2+} signals are generated by Ca^{2+} influx from the apoplast or Ca^{2+} release from internal Ca^{2+} stores, such as vacuole, ER, mitochondria, nucleus, or plastids (Hepler et al., 2005, Sai and Johnson., 2002, White and Broadley., 2003, Wyatt et al., 2002, Jammes et al., 2011). The intracellular Ca^{2+} store involved in a specific response has only been assigned in very few cases. Mitochondria have been defined as the source of anoxia-induced $[Ca^{2+}]_{cyt}$ elevations (Subbaiah et al., 1998). In addition, a chloroplast-localized Ca^{2+} sensor protein (CAS), which has originally been assigned to the plasma membrane (Han et al., 2003), plays a role in the modulation of $[Ca^{2+}]_{cyt}$ and the regulation of stomatal movements (Weinl et al., 2008).

Ca^{2+} influx into the cytosol is brought about by the activation of Ca^{2+} channel proteins at different cellular membranes (Kudla et al., 2010). At the plasma membrane, cyclic nucleotide-gated channels (CNGCs) and glutamate receptors (GLRs) are types of ligand-gated channels that may mediate Ca^{2+} influx (Kudla et al., 2010, Frietsch et al., 2007, Ali et al., 2007, Qi et al., 2006). At the vacuolar membrane, or tonoplast, the slow vacuolar channel, encoded by *Two Pore Channel 1* (*TPC1*), is thought to contribute to $[Ca^{2+}]_{cyt}$ signal generation and has been shown to be involved in the regulation of seed germination and stomatal aperture of Arabidopsis (Peiter et al., 2005, Peiter, 2011).

Although the generation of $[Ca^{2+}]_{cyt}$ signals has been described for many stimuli and stresses, the underlying molecular mechanisms are largely unknown.

1.5 *Arabidopsis thaliana* as a model system

Many of the channels and other proteins involved in the processes mentioned before have been characterized in the model plant *Arabidopsis thaliana*. *Arabidopsis thaliana* is a small flowering plant of the *Brassicaceae* family, which also includes economically important crops, such as broccoli, cauliflower, or oilseed rape (Meinke et al., 1998). It has been used as model organism in laboratories of different disciplines ranging from plant genetics, physiology and developmental biology to biochemistry all over the world. Some of its properties make it ideal as model organism. These are for example its small size, a short life cycle and huge seed production, which make propagation in the greenhouse or climate cabinets easy. Arabidopsis contains 25,498 genes organized on five chromosomes (Meinke et al., 1998, Arabidopsis, 2000), without much of the repetitive DNA present in the genomes of other higher plant species (Salinas and Sanchez-Serrano, 2006). Huge collections of knock-out mutants are commercially available, and a large variety of protocols for molecular and phenotypic analysis can be found. The whole genome was sequenced by the year 2000 (Arabidopsis Genome Sequencing Initiative, 2000), and as a result the information on specific genes found in online databases has enlarged. In this thesis, TAIR (The Arabidopsis Information Resource, www.arabidopsis.org) has been used for information on sequences, Genevestigator (www.genevestigator.com/gv) and the eFP (Electronic Fluorescent Pictograph) Browser (http://bar.utoronto.ca/efp/cgi-bin/efpWeb.cgi) for microarray data on expression of the genes under different conditions, and the plant membrane protein database ARAMEMNON (aramemnon.botanik.uni-koeln.de) for predictions of protein topology and subcellular localization.

1.6 Aim of the thesis

The aim of this thesis is to characterize the three as yet uncharacterized genes, At5g49960 (*DROP1*), At5g43745 (*DROP2*), and At5g02940 (*DROP3*) from *Arabidopsis thaliana.* As explained before, these genes are homologues to the leguminous Ca^{2+} signal modulator *MtDMI1*, with DROP2 and DROP3 being very closely related to each other but more distantly related to DROP1 and MtDMI1. *Arabidopsis thaliana* is a plant, which does not establish rhizobial or mycorrhizal symbioses. Coming from the phylogenetic relationship and the fact, that all three genes possess an RCK domain, which is a characteristic of ligand-gated channels, it is hypothezised that the three Arabidopsis genes encode channels with a function in Ca^{2+} signalling or ion homeostasis in processes other than nodulation or mycorrhization. To test this assumption, the following approaches will be employed:

- Subcellular localization using YFP-fusion proteins:
Knowledge about the precise destination of a protein in the cell is indispensable for determining its function in the cell.

- A thorough analysis of information available in databases:
The focus will lie on expression data from publically available microarray data under non-stress and stress-conditions. Information obtained here will guide directions for experiments to be performed.

- Promoter-GUS expression studies:
The results obtained here will provide knowledge about tissues and organs in which or developmental stages and environmental conditions during which the genes are expressed. These data will complement information obtained from databases and are necessary to understand the role the genes play in the plant.

- Phenotypic characterization of T-DNA mutants:

Physiological and developmental analyses of mutants are key experiments in the characterization of plant genes. They will determine the involvement of the genes or corresponding proteins in specific processes of plant development or acclimation. The focus will lie on processes in which Ca^{2+} signalling or ion flux in general are known to be involved.

Combining and linking the results of these different approaches will help to understand the role that DROP1, DROP2 and DROP3 fulfill in the plant.

2. Materials and Methods

2.1 Materials

2.1.1 Chemicals

Substance	Company	Cat. No.
Acetic acid $C_2H_4O_2$	Apolda	579-94-2
Agar-Agar, Kobe I	Sigma-Aldrich	5210.2
Agarose	Biozym Scientific	840004
Ampicillin sodium $C_{16}H_{18}N_3O_4SNa$	Duchefa	A0104
Boric acid BH_3O_3	Fluka	15665
Calcium chloride dihydrate $CaCl_2 \cdot 2H_2O$	Sigma-Aldrich	31307
Calcium nitrate $Ca(NO_3)_2$	Sigma-Aldrich	C2786
Cellulase Onozuka R-10	Duchefa	C8001
D(+)-Glucose $C_6H_{12}O_6$	Carl Roth	HN06.2
Dimethly sulfoxide $C_2H_6O_3$	Duchefa	D1370
D-Mannitol $C_6H_4O_6$	Sigma-Aldrich	M1902
EDTA disodium salt dihydrate $C_{10}H_{14}N_2NaO_3 \cdot 2H_2O$	Carl Roth	8043.1
Formaldehyde solution CH_2O	Sigma-Aldrich	F8775
Isopropanol C_3H_8O	Carl Roth	T910.1
Macerozyme R-10	Duchefa	M8002
Magnesium chloride $MgCl_2$	Fluka	63068
Magnesium sulfate $MgSO_4 \cdot 7H_2O$	Fluka	63140

Meat extract	Sigma-Aldrich	X975.1
MES (2-[*N*-Morpholino] ethanesulfonic acid) hydrate $C_6H_{13}NO_4S{\cdot}xH_2O$	Sigma-Aldrich	M2933
MS salts+vitamins	Duchefa	M0231
PEG3350 Poly(ethylene glycol) 3350	Sigma-Aldrich	88276
PEG4000 Poly(ethylene glycol) 4000	Fluka	95904
Phyto-Agar	Duchefa	P1003
Potassium dihydrogen phosphate KH_2PO_4	Fluka	60220
Potassium chloride KCl	Duchefa	PO515
Sodium dodecyl sulfate $C_{12}H_{25}NaO_4S$	Carl Roth	2326.2
Sucrose $C_{12}H_{22}O_{11}$	Carl Roth	4621.1
Sodium chloride NaCl	Carl Roth	3957.1
Tryptone	Formedium	TRP02 or 11/MFM/1029
X-GlcA cyclohexylammonium	Duchefa	X1406.1000
Yeast extract	Formedium	YEM02 or 11MFM/1014

2.1.2 Enzymes for molecular cloning

Enzyme	**Company**	**Cat. No.**
*BamH*I-HF	New England Biolabs	R3136S
Invitrogen SuperScript II Reverse Transcriptase	Invitrogen	108064-022
Phusion Polymerase	Finnzymes	F-540S
RNAse A	MBI Fermentas	EN0531
Taq Polymerase (Go Taq DNA polymerase)	Promega	M3175
TSAP (Thermosensitive alkaline phosphatase)	Promega	M9910
T4 DNA ligase	New England Biolabs	M0202S
*Xma*I	New England Biolabs	R0180S

2.1.3 Kits for molecular cloning

Kit	Company	Cat. No.
DNeasy Plant Mini kit	Qiagen	69104
NucleoBond Xtra Midi Plasmid DNA Purification kit	Macherey-Nagel	740410.10
Spectrum Plant Total RNA kit	Sigma-Aldrich	STRN50
Wizard Gel Clean-Up and Purification System	Promega	A9282
Wizard Plus SV Miniprep DNA Purification kit	Promega	A1460

2.1.4 Oligonucleotides

All oligonucleotides were synthesized by Eurofins MWG Operon (Ebersberg, Germany).

Oligo name	Sequence	Gene	Restr.	Purpose
DMI1fw_XmaI	AAAAAACCCGGGATGCCGATTCATACCCCTAGAAG	DROP1	XmaI	EYFP cloning
DMI1rv_no_STOP_XmaI	AAAAAACCCGGGCTGACTTGAGGCGATGACAACAA	DROP1	XmaI	EYFP cloning
DMI1fw_XmaI(A)	AAAAAACCCGGGAATGCCGATTCATACCCCTAGAAG	DROP1	XmaI	EYFP cloning
DMI1rv_XmaI	AAAAAACCCGGGTTACTGACTTGAGGCGATGACAAC	DROP1	XmaI	EYFP cloning
DMI2fw_XmaI	AAAAAACCCGGGATGATGGTGGCTGTTCAGTTGT	DROP2	XmaI	EYFP cloning
DMI2rv_no_STOP_XmaI	AAAAAACCCGGGTAGTGTGATTGGTTGGTCTCCT	DROP2	XmaI	EYFP cloning
DMI2fw_XmaI(A)	AAAAAACCCGGGAATGATGGTGGCTGTTCAGTTGT	DROP2	XmaI	EYFP cloning
DMI2rv_XmaI	AAAAAACCCGGGTCATAGTGTGATTGGTTGGTCTCCT	DROP2	XmaI	EYFP cloning
DMI3fv_XmaI	AAAAAACCCGGGATGGTGGCTGTTCAGTTGTTTAC	DROP3	XmaI	EYFP cloning
DMI3rv_no_STOP_XmaI	AAAAAACCCGGGTAGTGTGATAACTTGGTCTCCTTCA	DROP3	XmaI	EYFP cloning
DMI3fv_XmaI	AAAAAACCCGGGATGGTGGCTGTTCAGTTGTTTAC	DROP3	XmaI	EYFP cloning
DMI3rv_XmaI	AAAAAACCCGGGTCATAGTGTGATAACTTGGTCTCCT	DROP3	XmaI	EYFP cloning
DMI1fw-BamHI 745	AAAAAAGGATCCTGCCACACTAAGACCAGCCAAT	DROP1	BamHI	GUS cloning
DMI1rv-BamHI 746	AAAAAAGGATCCCGGGTTGAAGTAAGTAAATTGAGAAACAG	DROP1	BamHI	GUS cloning
DMI2fw-BamHI 747	AAAAAAGGATCCAGTGAAAGATTATGCCCTCCACATG	DROP2	BamHI	GUS cloning
DMI2rv-BamHI 748	AAAAAAGGATCCTTATCTCTTCTCCTCGCTCTCTCTTTGT	DROP2	BamHI	GUS cloning
DMI3fw-BamHI 749	AAAAAAGGATCCTCGCATCATAGCAAGGAAAGCAAG	DROP3	BamHI	GUS cloning
DMI3rv-BamHI 750	AAAAAAGGATCCCTTTCTTAATCTTCTCCTTGATTTATCTTACGC	DROP3	BamHI	GUS cloning
SALK_LBa117	TGGTTCACGTAGTGGGCCATCG	SALK TDNA	Confirmation of homozyous insertion	
SAIL_LB1_short 245	CAGAAATGGATAAATAGCCTTGCTTC	SALK TDNA	Confirmation of homozyous insertion	
DMI1-B08-LP 503	CCACTTTCTTTCCACCATCTTC	DROP1	Confirmation of homozyous insertion	
DMI1-B08RP 504	TTGCTCTGCAACTGTCTGATG	DROP1	Confirmation of homozyous insertion	
DMI2-267-LP2 528	TTACACAGGGATCAGATTCCG	DROP2	Confirmation of homozyous insertion	
DMI2-267-RP2 529	CTCGTTCAGTTCGCTGTTTTC	DROP2	Confirmation of homozyous insertion	
DMI3-415-RP 261	AGGACAGGAGATACAGAGCCG	DROP3	Confirmation of homozyous insertion	
DMI3-415-LP 260	CTAGGACTTGCATATGTGCCC	DROP3	Confirmation of homozyous insertion	
pBI101-3_F 39	GCGGATAACAATTTCACACAGGA	pBI101.3	Colony PCR	
pART7-MCS_F 52	CAATCCCACTATCCTTCGCAAGA	pART7	Colony PCR	

2.1.5 Bacterial strains

Strain	Species	Aim	Source	Selection
Top 10	*E. coli*	general cloning	Invitrogen Darmstadt, Germany No. C4040	Streptomycin
GV3101	*Agrobacterium tumefaciens*	plant transformation	Peiter lab stock	Rifampicin, Gentamicin

2.1.6 Vectors

Vector	Antibiotic resistance	Source
pART7-EYFP	Ampicillin	(Gleave, 1992; Peiter et al., 2007)
pART7-EYFP(no stop)	Ampicillin	(Gleave, 1992; Peiter et al., 2007)
pBI101.3	Kanamycin	(Bevan, 1984; Bevan et al., 1983; Jefferson et al., 1986)

2.2 Methods

2.2.1 Subcellular localization of DROP proteins

2.2.1.1 Extraction of RNA

For RNA extraction, leaves (for cloning *DROP2*) or roots (for cloning *DROP1*) of four-week-old *Arabidopsis* plants (ecotype Col-0) were harvested in liquid nitrogen. Tissue samples were ground to a fine powder in liquid nitrogen using a mortar and pestle. Approximately 100 mg of the resultant powder was filled into a 1.5 ml Eppendorf tube. The Spectrum Plant Total RNA kit was applied to extract the RNA according to the manufacturer`s instructions: 500 µl of lysis solution including 2-mercaptoethanol were added to the tissue powder, and the mixture was vigorously vortexed for at least 30 seconds. The sample was incubated at 56°C for three to five minutes and then centrifuged at maximum speed in a Minispin centrifuge (Eppendorf, Hamburg, Germany) for three minutes to pellet cellular fragments. The lysate supernatant was pipetted into a filtration column seated in a collection tube. The cap of the tube was closed and then the tube was centrifuged at maximum speed for one minute to remove residual debris. The clarified flow-through lysate was saved. 300 µl of wash solution 1 was pipetted onto the binding column and then centrifuged at maximum speed for one minute. The flow-through liquid was decanted and

the collection tube briefly tapped on a clean absorbent paper to drain the residual liquid. The column was returned to the collection tube and 500 µl of wash solution 1 was again pipetted onto the binding column and centrifuged again at maximum speed for 1 minute. The flow-through liquid was decanted and the collection tube was briefly tapped on a clean absorbent paper to drain the residual liquid, then the column was returned to the collection tube. 500 µl of the diluted wash solution 2 was pipetted onto the column. The cap was closed and the tube with column centrifuged at maximum speed for 30 seconds. The flow-through liquid was discarded, and the tube was briefly tapped on a clean absorbent paper to drain the residual liquid, then the column was returned to the collection tube. The washing step with wash solution 2 was repeated. After another centrifugation at maximum speed for 1 minute, the column was carefully removed to a new 2-ml collection tube. 50 µl of MilliQ-purified H_2O were used to dissolve the purified RNA by centrifuging at maximum speed for one minute. The resulting RNA was stored at -70°C.

2.2.1.2 cDNA synthesis

RT-PCR was performed using the Invitrogen SuperScript II Reverse Transcriptase. One microgram of RNA was used for cDNA synthesis. 2 µl oligo(dT)$_{24}$ primers (50 µM) and 1 µl dNTPs (10 mM each) were added to the RNA, and the reaction was filled up to 12 µl with H_2O in a sterile PCR microtube. The tube was incubated at 65°C for 5 minutes and then put on ice immediately. Four µl of 5× first strand buffer, 1 µl of 0.1 M DTT and 1 µl of RNaseOUT were added to the PCR reaction, followed by quickly flicking and spinning the microtube. After two minutes of incubation at 42°C, one microliter of reverse transcriptase (200 units) was added. Afterwards, the following incubation steps were applied: 90 minutes at 65°C; 15 minutes at 70°C. After adding 1 µl of RNAse A, the reaction was incubated at 37°C for 20 minutes. The reaction was filled up with 29 µl of H_2O stored at -20°C.

2.2.1.3 Cloning of EYFP fusion constructs

Full length cDNA sequences of At5g49960 (*DROP1*), At5g43745 (*DROP2*), and At5g02940 (*DROP3*) were obtained from the Munich Information Center for Protein Sequences (MIPS) (http://mips.helmholtz-muenchen.de/plant/athal/searchjsp/index.jsp), and corresponding primer pairs bearing *Xma*I restriction sites were designed. These primer pairs, shown in 2.1.4 were used for amplifying full-length cDNAs of *DROP1* and *DROP2* with added *Xma*I restriction sites from cDNA. *DROP3* was amplified from the plasmid pYES2-DROP3 (K. Thor, unpublished). The amplification of the cDNA fragments was carried out by PCR using the Phusion high-fidelity polymerase.

The vectors pART7-EYFP and pART7(no stop)-EYFP (Gleave, 1992; Peiter et al. 2007) were used for constructing N-terminal and C-terminal EYFP fusion plasmids, respectively. Vector and PCR products were digested with *Xma*I and purified using the Wizard Gel Clean up and Purification System. Vectors were dephosphorylated with TSAP (Thermosensitive alkaline phosphatase) to prevent self-ligation after digestion. Ligation of vectors and inserts with T4 DNA ligase was carried out at 16°C overnight. Transformation into *E. coli* was performed by electroporation using an Elektroporator 2510 (Eppendorf, Hamburg, Germany) with a voltage of 2.5 KV. In each transformation assay, 2 µl of ligation was mixed with 60 µl competent *E. coli* cells in an electroporation cuvette (2 mm electrode gap, PEQLAB, Erlangen, Germany), which was chilled on ice before. After the pulse, 400 µl SOC medium was added immediately to the cuvette. Cells were pre-cultured at 37 °C and 200 rpm for about 1 hour before plating them on selective LB plates containing 50 µg/ml ampicillin. Plates were incubated at 37 °C overnight. Positive colonies were confirmed by colony-PCR (with one primer binding to the vector and one to the insert) and use to inoculate liquid LB medium. Plasmid DNA was extracted from those cultures using the Promega Wizard Plus SV Minipreps Purification system according to the manufacturer's instructions. 1 µg of plasmid was digested with *Xma*I again to confirm the presence of the insert. The sequences of the insertions were checked by Sanger sequencing (Sanger et al., 1977) using the ABI PRISM BigDye Terminator V1.1 Cycle Sequencing kit (Platt et al., 2007). After the sequencing PCR, 10 µl of the product were

incubated with 1 µl of 125 mM EDTA (pH 8.0), 1 µl of 3 M Na-acetate and 25 µl of 100% ethanol for 15 minutes at room temperature to precipitate the DNA, followed by centrifuging at 14000 rpm and 4°C for 45 minutes (5415R, Eppendorf). After that, the supernatant was carefully removed. The pellet was washed with 60 µl of 70% ethanol and centrifuged at 14000 rpm, 4°C for 15 minutes. The supernatant was removed and the pellet was dried at 80°C for about 10 minutes. Electrophoresis and fluorescence detection were performed commercially. Results were evaluated by Sequence Scanner software (Life Technologies, Darmstadt, Germany). Correct constructs were amplified using the Nucleo Bond Xtra midiprep kit according to the manufacturer`s instructions.

Amplification of *DROP*s:

H_2O	30.5 µl
5× Phusion HF Buffer	10.0 µl
10 mM dNTPs	1.0 µl
10 µM forward primer	2.5 µl
10 µM reverse primer	2.5 µl
cDNA	3.0 µl
Phusion hot start DNA polymerase	0.5 µl
Total	50.0 µl

98°C for 30 s
98°C for 10 s
62°C for 20 s } 35 cycles
72°C for 90 s
72°C for 5 min

*Xma*I-digestion of purified PCR product

Phusion PCR product	30 µl
10× NEB Buffer 4	4 µl
10× BSA	4 µl
H_2O	1 µl
10U *Xma*I	1 µl
Total	40 µl

*Xma*I-digestion of purified vector

Vector	(1 µg)
10× NEB Buffer 4	3 µl
10× BSA	3 µl
H_2O	× µl
10U *Xma*I	1 µl
Total	30 µl

TSAP dephosphorylation

1 µg DNA	30 µl
10x Multi-core buffer	3.5 µl
1.5 U TSAP	1.5 µl
Total	35 µl

Ligation of vectors and inserts

10× ligase buffer	1 µl
100 ng vector	
× ng insert *	
5U T4 ligase	1 µl
Total	10 µl

*: ng insert = (100 ng vector × 2500 bp (fragment of cDNA insert) / 5500 bp (vector)) x 3

LB medium

Tryptone	10 g
Yeast extract	5 g
NaCl	10 g
H_2O	ad 1 l

Solid medium was supplemented with 8 g agar.

Colony PCR

10× Taq buffer	2.5 µl
10 mM dNTPs	0.5 µl
10 µM forward primer	1.0 µl
10 µM reverse primer	1.0 µl
H_2O	19.0 µl
1U/µl Taq polymerase	1.0 µl
Total	25 µl

94 °C for 5 min
94 °C for 30 s
55 °C for 20 s } 35 cycles
72 °C for 90 s
72 °C for 5 min

SOC medium

Tryptone	20 g
Yeast extract	5 g
1M NaCl	10 ml
2.5 M KCl	2.5 ml
1M $MgCl_2$	10 ml
1M $MgSO_4$	10 ml
H_2O	ad 1 l

BigDye sequencing reaction	
5× sequencing buffer	2 µl
H_2O	× µl
plasmid	(200ng)
primer (3.2 µM)	2 µl
BigDye	0.5 µl
Total	10 µl

Note: Primers for sequencing see Tables S 1 and S2 (Appendix)

96 °C hot-start
96 °C for 1 min
96 °C for 10 sec
50 °C for 5 sec
} 15 cycles
60 °C for 1 min 15 sec
96 °C for 10 sec.
50 °C for 5 sec
60 °C for 1 min 30 sec
} 5 cycles
96 °C for 10 sec
50 °C for 5 sec
60 °C for 2 min
} 5 cycles

2.2.1.4 Transformation of Arabidopsis mesophyll protoplasts

Mesophyll protoplasts were isolated from 4-week old *Arabidopsis* plants (ecotype Col0) according to a protocol modified from Abel and Theologis (1994): five to eight well-expanded rosette leaves were placed into plasmolysis buffer and cut into 0.5 to 1 mm strips by using a fresh razor blade. The leaf strips were transferred into enzyme solution, vacuum-infiltrated two times for 5 min, and incubated in darkness for 3 hours at 23°C. Protoplasts were separated from undigested tissue by filtration through a 70 µm nylon mesh (BD Falcon, Dresden, Germany). The protoplast filtrate was diluted with 0.5 volumes of 200 mM $CaCl_2$. Protoplasts were precipitated by centrifugation (5804R, Eppendorf) at 100 *g* for 5 min. The protoplast pellet was resuspended

in 5 ml cold W5 solution, and cell yield was determined by using a hematocytometer (Fuchs-Rosenthal chamber, Marienfeld, Lauda-Königshofen, Germany) under an Axioskop microscope with 10× objective (Carl Zeiss, Jena, Germany). The suspension was diluted with cold W5 to approximately 2×10^5 cells ml^{-1}, and the tubes were placed horizontally on ice and kept in darkness for at least 30 minutes. Before starting the transformation, protoplasts were precipitated from the W5 solution by centrifugation (1 min at 100 *g*) and resuspended in MaMg solution to 2×10^5 cells ml^{-1}. 100 µl of the protoplast suspension was added to 10 µg of plasmid DNA in a 2-ml low-bind tube (Eppendorf). 110 µl PEG-CMS solution was immediately added, and everything was mixed gently. The transformation mixture was incubated at room temperature for 20 min and then carefully diluted with 0.5 ml W5 solution. Subsequently, it was centrifuged at 1200 rpm (Minispin, Eppendorf) and diluted with 1 ml protoplast culture medium for washing. It was resuspended in 225 µl new protoplast medium after 1200rpm centrifugation. Finally, the transformed protoplast suspension were pipetted into a 35 mm glass-bottom dish (MatTek, Ashland, MA, USA), which was sealed with parafilm (Sigma-Aldrich, St. Louis, USA) and incubated overnight without shaking in darkness at 23 °C.

Plasmolysis buffer

500 mM mannitol

10 mM MES-KOH pH 5.6

10 mM $CaCl_2$

Enzyme solution

1% Cellulysin R-10

0.3% Macerase

0.4 M mannitol

20 mM KCl

20 mM MES, pH 5.6

10 mM $CaCl_2$

0.1%BSA

W5 solution

154 mM NaCl

125 mM $CaCl_2$

2 mM MES-KOH pH 5.6

5 mM KCl

MaMg solution

400 mM mannitol

15 mM $MgCl_2$

5 mM MES-KOH, pH 5.6

PEG-CMS solution

300 mM mannitol

150 mM $Ca(NO_3)_2$

60% PEG4000 (Fluka95904)

Protoplast culture medium

4.4 g/l MS salts + vitamins (sigma M0404)

350 mM mannitol

50 mM glucose

3 mM $CaCl_2$

0.1 mg/ml ampicillin, pH 5.8

2.2.1.5 Microscopical observation of EYFP fluorescence

Fluorescence microcopy was performed by using a LSM 510 Meta confocal laser scanning microscope (Carl Zeiss, Jena, Germany). Fluorescence was excited by using the 488 nm laser line, and emission was recorded in lambda mode. First, spectra of chloroplast autofluorescence, EYFP and GFP were recorded using untransformed protoplasts or such expressing only one of the two fluorophores, respectively. Spectra were saved and used for spectral unmixing of the pictures obtained in lambda mode. Absence of bleed-through of fluorescence signals with the applied laser settings was confirmed. DIC pictures of the same cells were obtained in channel mode.

2.2.2 Expression analysis of *DROP* genes

2.2.2.1 Cloning of promoter-GUS constructs

Genomic DNA was isolated from 4-week old *Arabidopsis thaliana* (ecotype Col-0) leaves by using the DNeasy Plant Mini kit. Genomic sequences of At5g49960 (*DROP1*), At5g43745 (*DROP2*), and At5g02940 (*DROP3*) were acquired from TAIR (http://www.arabidopsis.org/), and approximately 2 kb upstream of the start codon were defined as promoter region (*DROP1*: 1941 bp, *DROP2*: 2029 bp, *DROP3*: 2035 bp). Primer pairs used for amplifying the three promoters contained *BamH*I restriction sites. The amplification was carried out by Phusion PCR, as described in 2.2.1.3, but with altered cycling conditions:

Cycling conditions

98°C for 30 s
98°C for 10 s
X °C for 20 s } 35 cycles
72°C for 90 s
72 °C for 5 min

X = 57°C for *DROP1* and *DROP3*; 60°C for *DROP2*

The plasmid pBI101.3, a binary vector containing the β-glucuronidase (GUS) cassette was digested with *BamH*I and dephosphorylated with TSAP before ligation. Phusion PCR products were also digested with *BamH*I and ligated into the dephosphorylated pBI101.3 vector. Ligation, transformation, colony PCR, plasmid amplification, and sequencing were performed as described in 2.2.1.3. Kanamycin was used as selective antibiotic. For sequencing primers see Table S. 2 (Appendix).

2.2.2.2 Agrobacterium-mediated transformation of Arabidopsis and screening of transformants

Transformation of *Agrobacterium tumefaciens* (strain GV3101; Logemann et al., 2006) was performed by electroporation in an Electroporator 2510 (Eppendorf). To 50 µl electrocompetent bacteria, 0.5 µl plasmid (100-200 ng μl^{-1}) was added into the cuvette. 300 µl SOC (see 2.2.1.3) was added immediately after electroporation. Cells were incubated for 2 h at 28°C and 200 rpm in a shaking incubator (Certomat IS, Sartorius, Göttingen, Germany). Subsequently, 50 µl of the cells were plated on YEB plates, which contained rifampicin (100 mg l^{-1}), gentamicin (25 mg l^{-1}), and kanamycin (50 mg l^{-1}). Plates were sealed with Parafilm and incubated in darkness at 28°C for 2 to 3 days. Resulting colonies were picked and resuspended in 25 µl sterile MilliQ-purified water. Five µl of the suspension was used for colony-PCR analysis (see 2.2.1.3), and 20 µl were plated onto a selective kanamycin-containing YEB plate. The plate was sealed with Parafilm and incubated in darkness at 28 °C for 2 to 3 days. The densely grown bacterial lawn was collected from the plate by scraping and resuspended in 30 ml liquid YEB. For transformation of Arabidopsis, 120 ml of a sucrose solution (50 g l^{-1}) containing 0.03 % Silwet L-77 was prepared and the bacterial suspension added into it.

Agrobacterium-mediated transformation of *A. thaliana* was carried out by floral dip (Clough and Bent, 1998). Arabidopsis plants (ecotype Col-0) were grown in soil under long-day greenhouse conditions (approximately 65% rh, 16 h day / 8 h night, 22°C / 18°C) for 5 weeks. First emerging shoots were cut in order to encourage the growth of more shoots with inflorescences. The inflorescences of the plants were dipped into the *Agrobacterium* suspension for 30 s under gentle agitation. Dipped plants were covered with a lid for 16 h to maintain humidity and further grown under long-day conditions. Seeds of transformed plants (i.e. the T1 generation) were harvested and sown onto ½ MS 0.8 % agar plates containing 50 mg l^{-1} kanamycin. Plates were cultivated for around 2 weeks under long-day conditions in a plant cabinet until non-transformed seedlings died. Remaining seedlings were transferred to soil,

cultured in the long-day greenhouse, and their seeds (i.e. the T2 generation) were harvested. Eight lines were chosen for histochemical GUS staining.

YEB

Beef extract	5 g
Yeast extract	1 g
Peptone	5 g
Sucrose	5 g
$MgSO4 \times 7H_2O$	0.49 g
agar	20 g
H_2O	ad 1 l

Ajust pH to 7.2

2.2.2.3 Histochemical GUS staining

Tissue was submerged in X-Gluc staining solution, vacuum-infiltrated two times for 5 min, and incubated at 37 °C for about 12 h. For destaining of chlorophyll, samples were placed into 80% ethanol, which was exchanged several times. Photographs were taken using a stereo microscope (SteREO Discovery.V20, Carl Zeiss) or an inverted microscope (Axiovert 40 CFL, Carl Zeiss). Both microscopes were equipped with an AxioCamMRc camera (AxioCamMR Rev.3, Carl Zeiss).

X-Gluc staining solution

100 mM sodium phosphate pH 7.0
10 mM EDTA
3 mM potassium ferricyanide
0.5 mM potassium ferrocyanide
0.1 % Triton X-100
2 mM X-Gluc (in DMSO)

2.2.3 Analysis of T-DNA mutants

2.2.3.1 Genotypical analysis

PCR reactions were performed on genomic DNA to verify the genotype of mutant plants used in physiological assays. For DNA extraction, a piece of leaf was harvested by closing the cap of a 1.5 ml Eppendorf tube, and 400 µl of extraction buffer were added into the tube. The leaf material was mashed several times by using an autoclaved micro-pestle, and the tube was centrifuged for 5 min at maximum speed in a Minispin centrifuge (Eppendorf). 300 µl of the supernatant were transferred into a new tube. After addition of 300 µl isopropanol the tube was briefly vortexed and centrifuged for 10 min at maximum speed. The supernatant was discarded, and the pellet was washed with 300 µl of 70% ethanol. The ethanol was removed after centrifuging for 10 minutes at maximum speed. The final pellet was air-dried for about 30-45 min and dissolved in 50 µl 10 mM Tris-HCl (pH 8.5). For PCR, different primer combinations were used, containing genespecific primers spanning the insertion site or one genespecific plus one T-DNA-specific primer (see 2.1.4) in order to confirm the homozygosity of the plants for the insertion. Products of the PCR reactions were loaded onto 1 % agarose gels for electrophoresis.

Extraction buffer

200 mM Tris-HCl (pH 7.5)

250 mM NaCl

25 mM EDTA

5 g l^{-1} SDS

PCR reaction	
10× Taq buffer	2.5 µl
10 mM dNTPs	0.5 µl
10 µM forward primer	1.0 µl
10 µM reverse primer	1.0 µl
DNA product	2.0 µl
H2O	17.0 µl
5 U/µl Taq	1.0µl
Total	25.0µl

94°C for 5min
94°C for 30 s
60°C for 20 s
72°C for 90 s
} 35 cycles
72°C for 5 min

2.2.3.2 Pollen germination and tube growth assays

Seeds of Arabidopsis wild type and mutant lines were sown onto soil (Profi substrate, Patzer, Sinntal-Altengronau, Germany, mixed 1:2 with vermiculite) and stratified for 2 d at 4°C in the dark. Plants were cultured in the greenhouse (approximately 65% rh, 16 h day / 8 h night, 22°C / 18°C) for about 7 weeks until they reached the flowering stage. To confirm the plant genotypes, a piece of leaf was harvested from each plant, and a control PCR was performed (see 2.2.3.1). Fifty flowers (stage 12 to 15; Smyth et al., 1990; Irish, 2010) from 8 different plants of the same genotype were collected randomly into a 2.0 ml tube. Collections took place in the morning. Six replicate tubes were prepared per genotype (50 flowers × 6 replicates = 300 flowers in total). In the laboratory, 1 ml germination medium (Footitt et al., 2007) was added to the flowers in the tubes. Each tube was vortexed for 10 seconds. Subsequently, the pollen was concentrated by centrifugation (MiniSpin, Eppendorf) with maximum speed for 5 min. Flowers floating on top and the supernatant were carefully removed. Pollen pellets in six replicate

tubes were resuspended in approximately 100 µl pollen germination medium to one tube. Two 20 µl drops of the pollen suspension were pipetted onto a glass slide (76×26 mm, Carl Roth, Karlsruhe, Germany). Three slides were prepared per genotype and each of six time points (0, 2, 4, 6, 10, 14 h). To get a high rate of pollen germination and homogenous tube growth, measures were taken to obtain a high humidity: Slides were gently turned onto their back and stuck onto two blue pipette tips in a square petri dish (12×12 cm, Greiner, Frickenhausen, Germany), which contained a paper tissue that had been wetted with 30 ml Milli-Q-purified H_2O. Petri dishes were sealed with Parafilm. To avoid experimental variation between wet chambers, slides with wild-type and mutant pollen were placed together in the same square petri dish. Three dishes were prepared for one time point. Pollen was incubated in a plant growth cabinet (Percival, Perry, IA, USA) at 65 % rH, continuous illumination at 120 µmol m^{-2} s^{-1}, and a temperature of 22 °C. At each time point, 3 plates were taken out of the cabinet, and the slides carrying the pollen suspension drops were inverted and covered with cover slips (22×40 mm, VWR, Darmstadt, Germany). Lengths of the germinated pollen tubes was measured using a 10× objective on an upright Axioskop microscope and the online measurement software tool of Axiovision 4.7 (Carl Zeiss). 100 pollen tubes were measured on three replicate slides, on average 33 pollen tubes per slide. The germination rate was counted from images taken under the microscope with an an AxioCamMRc. Slides with wild-type and mutant pollen were observed alternately. 300 grains were counted for the determination of the germination rate. To confirm the results, all experiments were repeated three times.

Pollen germination medium

18 % (w/v) PEG3350

1 mM $CaCl_2$

1 mM $Ca(NO_3)_2$

0.5 mM $MgSO_4$

0.015 % (w/v) boric acid

2 % (w/v) sucrose

2.2.3.3 Pollen observation by scanning electron microscopy

Flowers (stage12-15) of wild type or mutant plants were removed and gently dipped onto one side of a 5 mm^2 double-sided sticker, the backside of which was stuck to a 10 mm^2 aluminum alloy plate. Samples were dried at room temperature for 1 d. Three replicate plates were prepared. Before observation, the plates with the dried samples were coated with a copper membrane with a sputter coater (Cressington Sputter Coater 108auto, Watford, UK). Samples were observed by Xiaopeng Li at the Max-Planck-Institut für Mikrostrukturphysik using a JEOL JSM-6700F scanning electron microscope (Jeol, Tokyo, Japan).

2.2.3.4 Silique and seed set analysis

Plants were cultured in the greenhouse (conditions see 2.2.3.2) for up to eight weeks to produce flowers and siliques. About eight siliques emerging from the primary shoot were acquired from eight different plants per genotype. The length of the siliques was measured immediately after removal. Ten yellow but not open siliques were collected from eight plants per genotype for counting of seeds. Another ten such siliques were collected and submerged in 10 % acetic acid in EtOH for destaining of chlorophyll and tissue fixation for about 24-48 h. Subsequently, they were observed under a stereo microscope and photographed as described in 2.2.2.3. The experiments were repeated 2 times.

2.2.3.5 Root growth analysis

Six mutant seeds and six wild type seeds were sown onto square petri dishes (12x12 cm, Greiner) containing ½ MS medium supplemented with 0.8% agar and stratified for 2 d at 4°C in darkness. Plants were grown under long day conditions (16 h light / 8 h dark, 120 µmol m^{-2} s^{-1}, 22 °C /18 °C) in a growth cabinet (Percival). Main root lengths were measured every two days with a transparent plastic ruler. The experiment was performed three times with three replicate plates each time.

2.2.3.6 Stomatal aperture assays

Wild type and mutant plants were grown under short day conditions (120 µmol m^{-2} s^{-1}, 10 h light / 14 h dark, 22 °C /18 °C) for 5 weeks in an ATC-26 growth cabinet (Conviron, Winnipeg, Canada). To obtain flat leaves, trays were covered with a lid in order to keep a high and constant humidity. Single, fully expanded rosette leaves from three Arabidopsis plants (three leaves per plant) were floated for 2 h in petri dishes of 6 cm diameter containing stomata opening solution (10 mM MES-KOH (pH 6.15), 50 mM KCl, 50 µM $CaCl_2$) and in the light (120 µmol m^{-2} s^{-1}). Subsequently, ABA, $CaCl_2$ or flg22 were added to a final concentration of 10 µM, 10 mM or 1 µM, respectively, and the plates were incubated for another 2 h. Equal volumes of solvent (H_2O or EtOH) were added into the control Petri dishes. Stomatal apertures of leaves treated with flg22 were also measured directly, without pre-incubation, as described by Melotto et al. (2006). In all stomatal bioassays, epidermal strips were peeled from the treated leaves, placed in buffer on glass slides, and covered with cover slips. 30 stomatal apertures were measured per slide in about 30 minutes using the 63× objective of an Axioskop (Carl Zeiss) and the Zeiss AxioVision online measurement tool. The assays were performed as blind assays and two or three repeats were performed for every treatment.

2.2.3.7 Porometer measurements

To determine the effect of flg22 on transpiration, Arabidopsis plants were cultivated in a AR-75 growth cabinet (Percival) under short-day conditions (10 h light / 14 h dark, 120 µmol m^{-2} s^{-1}, 22 °C /18 °C). Six-week-old plants were taken for the assay. Each plant was sprayed with 5 ml of a 2 µM flg22 solution supplemented with 0.05% Silwet-L77. The same volume of H_2O supplemented with 0.05% Silwet-L77 was sprayed onto control plants. Per plant, three leaves of the same age were labeled, and the stomatal conductance of these leaves was measured at different time points (0, 24, 72, 120, 168 h after flg22-spraying). Measurements were performed using an AP-4 porometer (Delta-T Devices, Cambridge, UK). The experiment was performed on three replicate plants per line.

For measurements of stomatal conductance under drought stress, plants were cultured in a walk-in climate chamber under short-day conditions (10 h light / 14 h dark, 120 µmol m^{-2} s^{-1}, 22°C / 18°C). Each pot contained the same volume of soil and was watered to a weight of 75 g. The 9th and 10th leaf of each plant were marked with a colour string, and stomatal conductance of these leaves was measured for 8 days after watering had been stopped in the 6th week of cultivation. Measurements were performed with the AP-4 porometer and always started at 12:00. For each line, 4 plants were measured.

2.2.3.8 Callose deposition assay

Seedlings were grown in liquid culture under short-day conditions (10 h light / 14 h dark, 120 µmol m^{-2} s^{-1}, 22°C / 18°C). Seeds were first germinated for 5 days on ½ MS agar (0.8%) plates supplemented with 2% sucrose after stratification for 2 days. On each agar plate four genotypes were sown in four rows in random order. Four replicate plates were prepared. At day 8, seedlings were transferred to a 24-well plate containing liquid ½ MS with 1.5% sucrose. After one day in this culture, seedlings were treated with 1µM flg22 and incubated for another 24 hours. Seedlings then were fixed in formaldehyde/acetic acid/alcohol (FAA) for 24 h, cleared in ethanol, and stained with 0.01% aniline blue staining solution for 1 hour in the dark. Stained seedlings were transferred to slides and mounted with glycerol mounting solution. Fluorescence was observed by using an Axioskop (Zeiss) microscope equipped with a 4x lens, a HBO50 light source, and a UV filter set. Photographs were taken by using an Axiocam MRc camera (Zeiss). The assay was repeated four times.

<u>FAA (formaldehyde/acetic acid/alcohol)</u>

35 % H_2O

50 % ethanol

5 % glacial acetic acid

10 % formaldehyde

Aniline blue staining solution

0.01% aniline blue	5mg
67 mM K_2HPO_4 pH12	50ml

Glycerol mounting solution

70 % glycerol

30 % staining solution

2.2.3.9 Statistical analyses

The statistical significances of mutant versus wild type results were determined by calculating the P-value using single factor ANOVA.

3. Results

3.1 Subcellular localization of DROP proteins

Transient expression assays with Arabidopsis mesophyll protoplasts were used to analyze the subcellular localization of DROP proteins in Arabidopsis. C- and N-terminal fusions of DROPs to enhanced yellow fluorescent protein (EYFP) were tested. Fluorescence was observed by confocal laser scanning microscopy. To examine the localization of DROP1, protoplasts were isolated from an Arabidopsis marker line which expresses GFP fluorescence from the ER (Fig. 3). Confocal images of the transformed protoplasts provide evidence that ER-GFP and DROP1-EYFP colocalize to the same compartment. In contrast, EYFP-DROP1 localization did not coincide with ER-GFP.

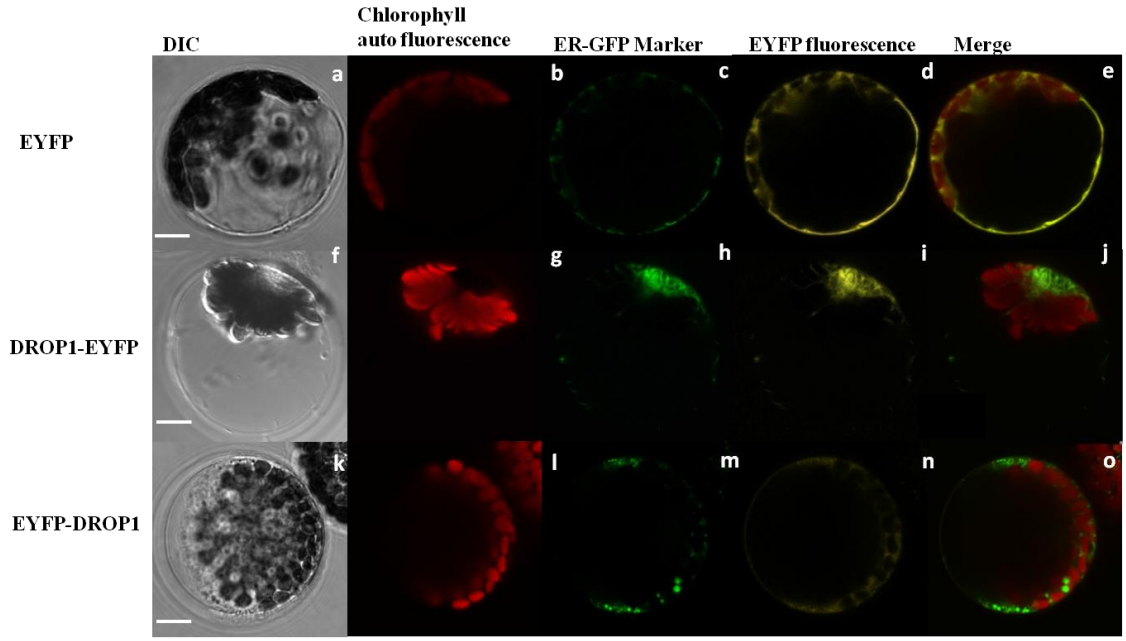

Fig. 3. Subcellular colocalization of EYFP (a-e), DROP1-EYFP (f-j) and EYFP-DROP1 (k-o) with an ER-GFP marker in protoplasts. Scale bars: 10µm.

Fig. 4 demonstrates that fluorescence of DROP2-EYFP and DROP3-EYFP was clearly associated with chloroplasts, which are shown in red. In contrast, EYFP-DROP2 and EYFP-DROP3 localized to a non-chloroplastic membrane of unknown origin.

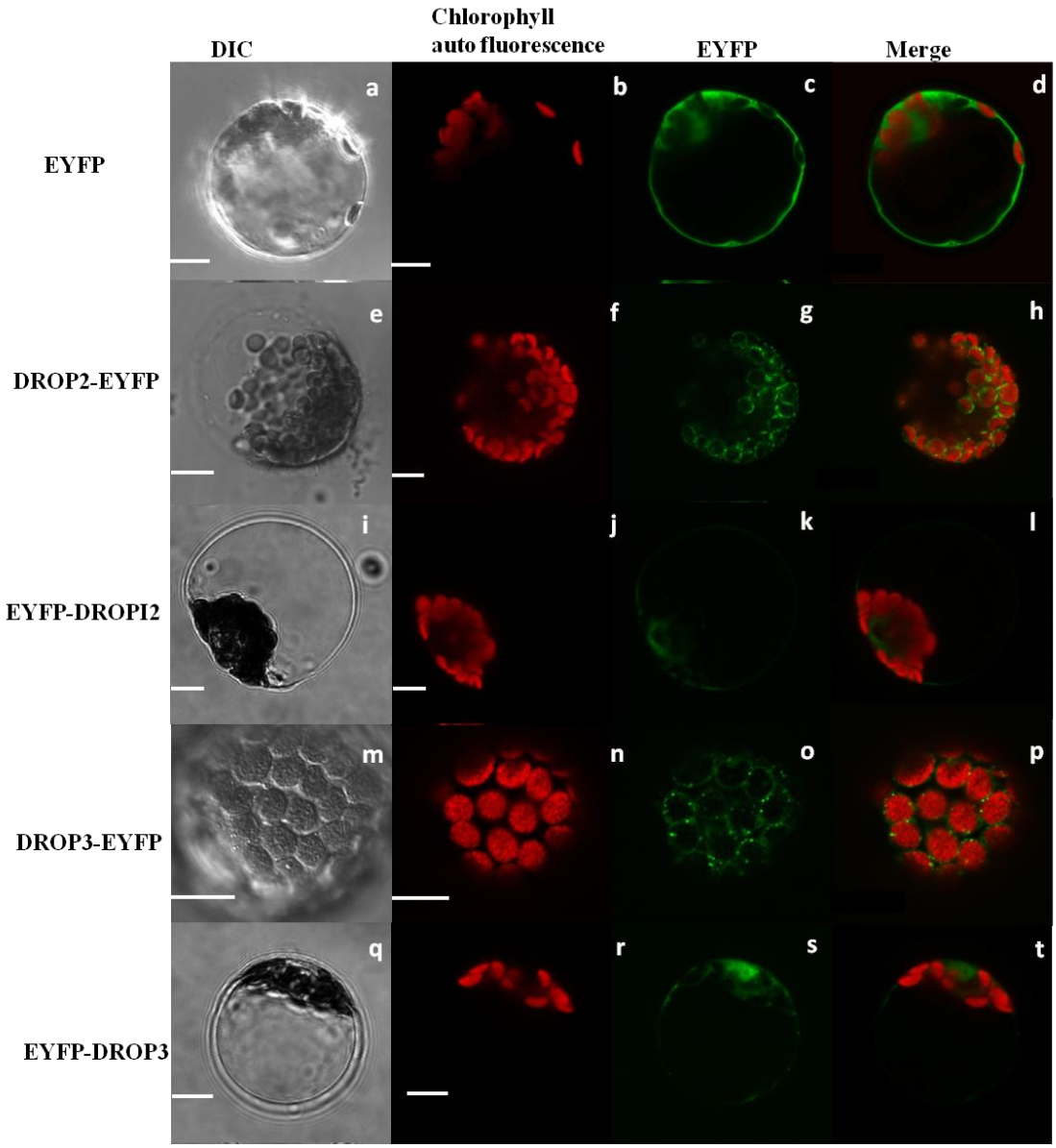

Fig. 4. Subcellular localization of EYFP (a-d), DROP2-EYFP (e-h), EYFP-DROP2 (i-l), DROP3-EYFP (m-p), and EYFP-DROP3 (q-t) in transiently transformed Arabdopsis mesophyll protoplasts. Scale bars: 10µm.

3.2 Expression of *DROP* genes

3.2.1 *In silico* analysis of publically available microarray data

To reveal their role in the plant, the expression of the *DROP* genes in different tissues of Arabidopsis was analysed. Expression data were acquired from Genevestigator (https://www.genevestigator.com/gv/plant.jsp) and the

Arabidopsis eFP browser (http://bar.utoronto.ca/efp/cgi-bin/efpWeb.cgi). Genevestigator is a web-based application which contains several tool sets for searching and analyzing the expression of genes of interest. Its results are based on Affymetrix microarray experiments. Arabidopsis eFP browser (electronic Fluorescent Pictograph browser) displays expression data obtained from the AtGenExpress Consortium by pictographic representations (Winter et al., 2007). Expression values of *DROP*s under non-stress conditions suggest that the highest expression of *DROP1* is in the root system, whereas *DROP2* and *DROP3* are most highly expressed in floral organs (Fig. 5 a). For flower tissues, the gene expression value is represented by a pictograph obtained from eFP browser (Fig. 5 b-d). The colour of the tissues represents the ratio of the averaged replicate samples to the maximum. The colour scales range from yellow to red, corresponding to gene expression values of 0 to maximum. Among the three *DROPs, DROP2* (Fig. 5 c) and *DROP3* (Fig. 5 d) showed higher expression values than *DROP1* (Fig. 5 b).

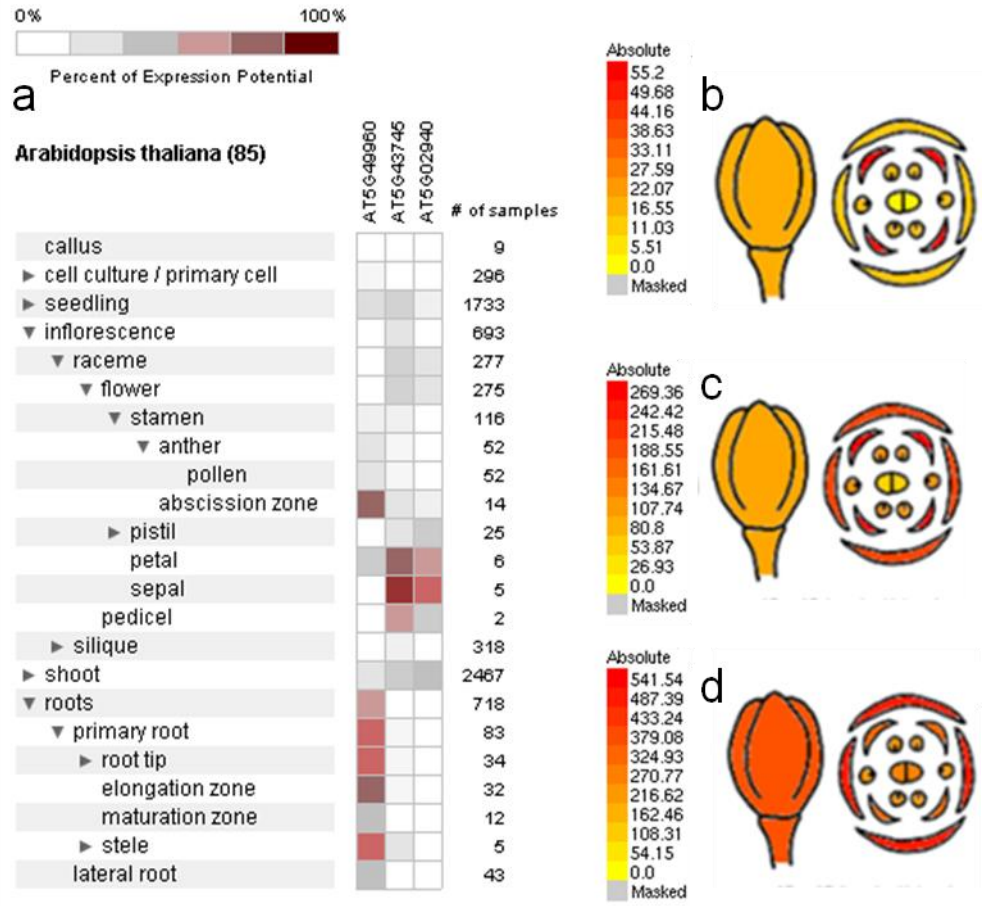

Fig. 5. Microarray data for *DROP*s obtained from Genevestigator (a) and Arabidopsis eFP browser (b-d). *DROP2* (At5g43745; c) and *DROP3* (At5g02940; d) exhibit a high relative expression in floral organs. Absolute values for these two genes in these tissues are quite high. *DROP1* (At5g49960; b) shows a relative high expression in the root system (a), but the absolute expression level values are very low.

Fig. 6, obtained from Genevestigator, showed that *DROP1* is expressed only at low levels throughout all developmental stages.

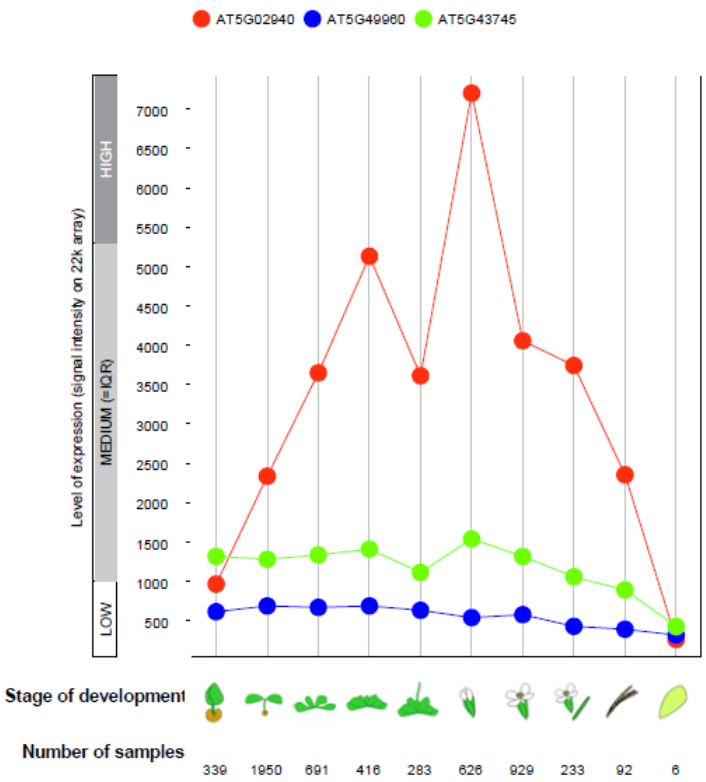

Fig. 6. Expression level of *DROP1*, *DROP2* and *DROP3* at different developmental stages. blue: *DROP1* (At5g49960); green: *DROP2* (At5g43745); red: *DROP3* (At5g02940).

Microarray data also indicate that the *DROP* genes are differentially regulated under some biotic and abiotic stress conditions (Fig. 7). After treatment with *Pseudomonas syringae* bacteria, for example, the expression of *DROP2* showed a higher value. Exposing seedlings to drought stress by putting them under the air stream of a sterile bench for 15 minutes leads to a very high *DROP3* expression.

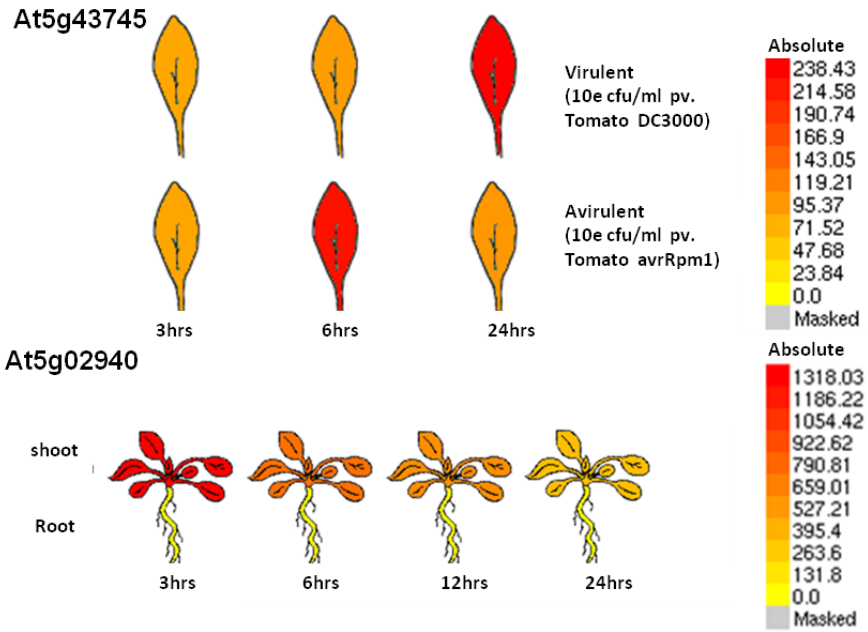

Fig. 7. *DROP2* (At5g43745) shows an increased expression in Arabidopsis leaves treated with *P. syringae* DC3000 and avrRpm1. Under drought stress, *DROP3* (At5g02940) shows an increased expression in seedlings. Arabidopsis eFP Browser data.

3.2.2 *PrDROPx::*GUS expression in non-stressed tissues confirms the microarray data

To further examine the expression patterns of *DROPs*, fragments of around 2000 bp upstream of the coding regions of *DROP1*, *DROP2,* and *DROP3* were amplified and cloned upstream of the β-glucuronidase (*GUS*) gene to obtain the constructs *PrDROPx::GUS*. These constructs were transformed into wild type Arabidopsis in order to obtain plants in which the *GUS* gene is driven under the control of a *DROP* promoter. GUS activity was made visible by incubation in a solution containing X-Gluc as substrate. Eight transgenic lines were tested per gene. The expression patterns and the staining intensities of replicate lines were comparable. Detailed information on lines of which photos are shown can be found in Supplementary Table S 3 (Appendix). In order to assess the spatial and temporal expression pattern of the *DROPs*, the transgenic plants were stained at different developmental stages ranging from one week-old seedlings to flowering plants. In *PrDROP2::GUS* and *PrDROP3::GUS* plants strong *GUS* expression was

detected in leaves, roots, and floral organs, namely sepals, petals, stigmata and pollen, as well as siliques (Figs. 8 and 9). In contrast, no obvious GUS activity was detected in leaves, stems, floral organs (data not shown) and seedlings (Fig. 8 d) of *PrDROP1::GUS*-plants, but an expression could be detected in 30 day-old roots and the rosette base (Fig. 8 a-c).

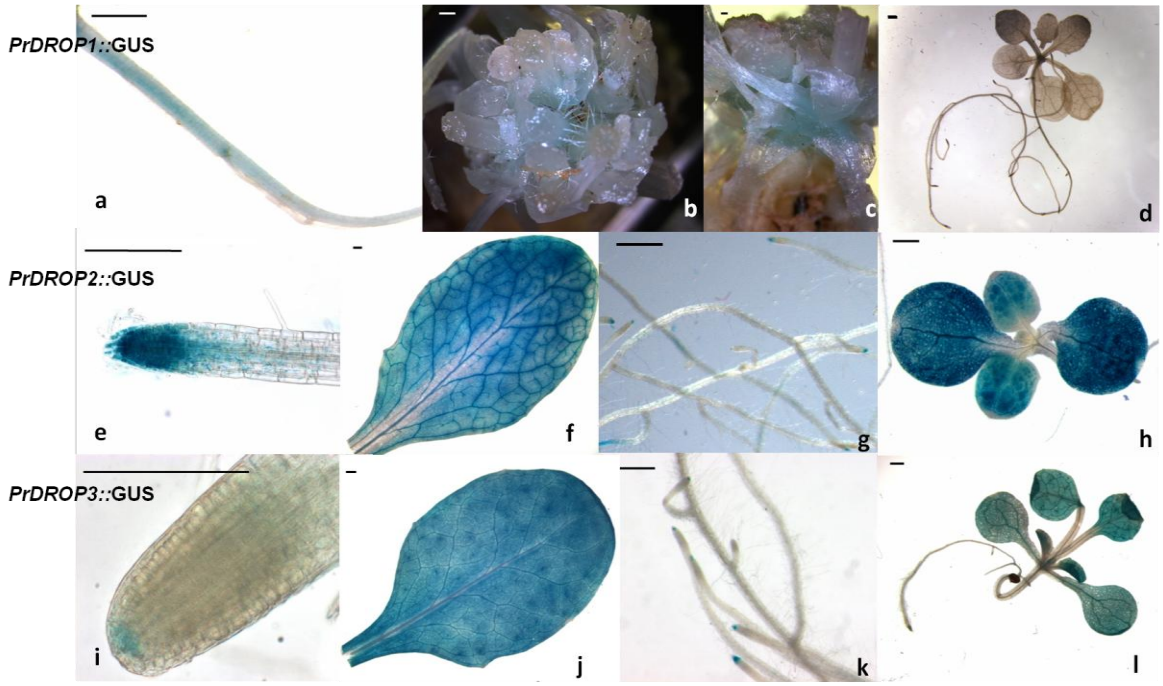

Fig. 8. GUS expression in vegetative tissues. (a) *PrDROP1::*GUS expressed in 4 week-old lateral root. (b, c) *PrDROP1::*GUS expression in the rosette base; (b) cross section, (c) vertical profile. (d) *PrDROP1::*GUS did not show expression in seedling. (e-h) *PrDROP2::*GUS expression in root tips (e, g), leaves (f) and seedling (h). (i-l) *PrDROP3::*GUS expression in root tips (i, k), leaves (j) and seedling (l). Scale bars: 500µm.

In inflorescences of *PrDROP2::GUS* and *PrDROP3::GUS* plants GUS staining was apparent not only in sepals and petals, but also in pollen (Fig. 9).

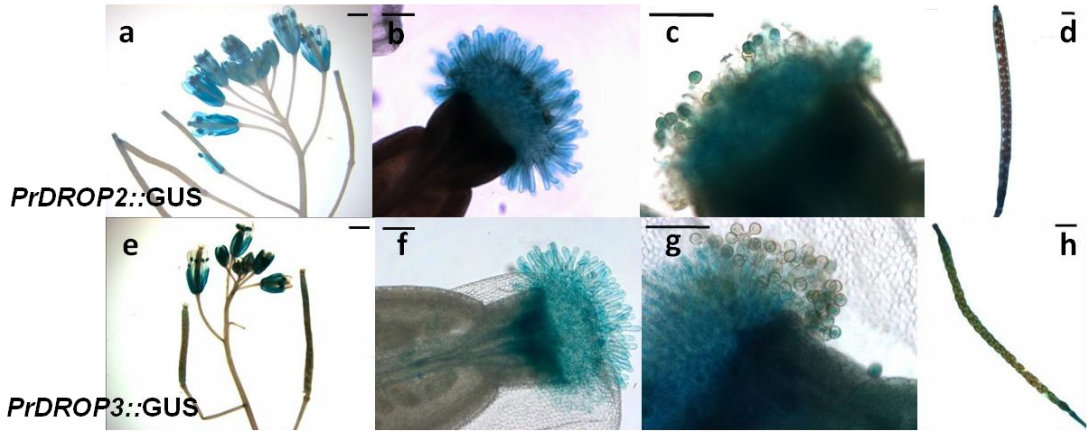

Fig. 9. GUS expression in reproductive tissues. The two promoter-GUS fusions *PrDROP2::*GUS (a-d) and *PrDROP3::*GUS (e-h) showed a comparable expression pattern in inflorescence, stigma, and silique. (a, e) Inflorescences showing GUS staining in sepals, petals, and siliques. (b, f) stained stigmas. (c, g) Stigmas with adhering pollen. (d, h) Siliques. Scale bars: 500µm.

In order to know the expression pattern of *PrDROP2/3::GUS* during pollen development, different stages of flowers were examined. For a better understanding, first the stages of Arabidopsis flowers were defined by taking photos of a well-developed inflorescence of a Col-0 Arabidopsis plant under a stereomicroscope (Fig. 10).

Fig. 10. Definitions of different flower developmental stages. Stage 1 to 5: primordia of sepals, petals, and stamen have developed. Stage 6 to 8: stamen develop and enlarge rapidly. Stage 9 to 12: petals and gynoecium develop, and anthers reach final developmental stage; the flower is fully developed. Stage 13 to 15: buds open, petals become visible. Stage 16: petals and sepals are withering, then siliques begin to develop (Irish, 2010; Smyth et al., 1990).

Flowers from the stained inflorescences of the *PrDROP2/3::GUS* plants were allocated to one of the four classes 1-5, 6-8, 9-12, or 13-15. As can be seen in Fig. 11 for *PrDROP2::GUS* and in Fig. 12 for *PrDROP3::GUS*, GUS activity in pollen was not detected up to developmental stage 8. This suggested that *PrDROP2::GUS and PrDROP3::GUS* expression occurs mainly in mature pollen grains, which implies that DROP2 and DROP3 might be involved in processes like pollen germination rather than pollen development.

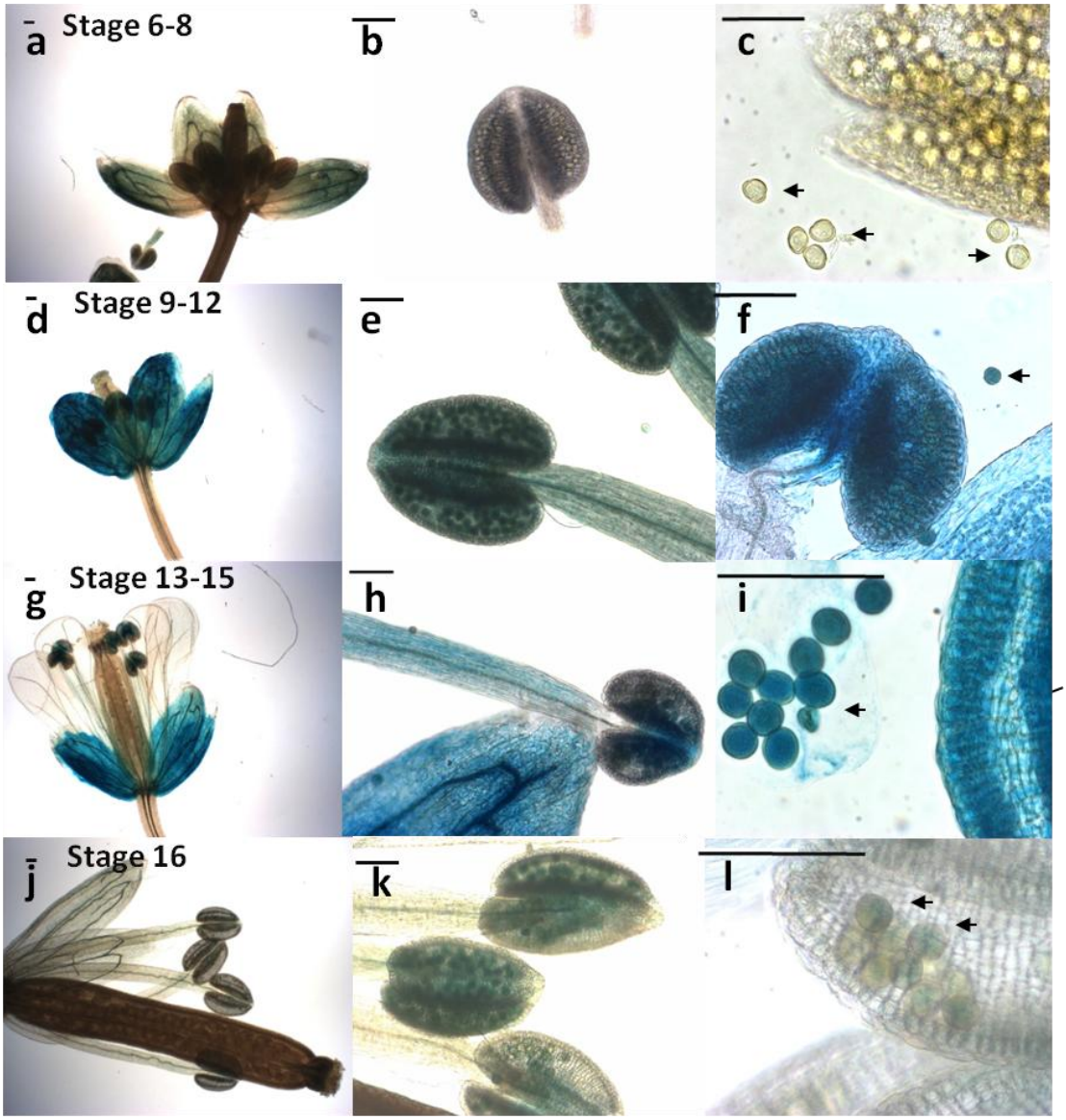

Fig. 11. *PrDROP2::*GUS expression analysis of different flower and pollen stages. (a-c) flower stage 6 to 8, (d-f) flower stage 9 to 12, (g-i) flower stage 13 to 15, (g-l) flower stage 16. Single flowers (a, d, g, j), stamen (b, e, h, k), and pollen (c, f, i, l; arrows) are displayed. No pollen in stage 6 to 8 (c) showed *prDROP2::*GUS expression, while expression was visible in all other stages. Scale bars: 500µm.

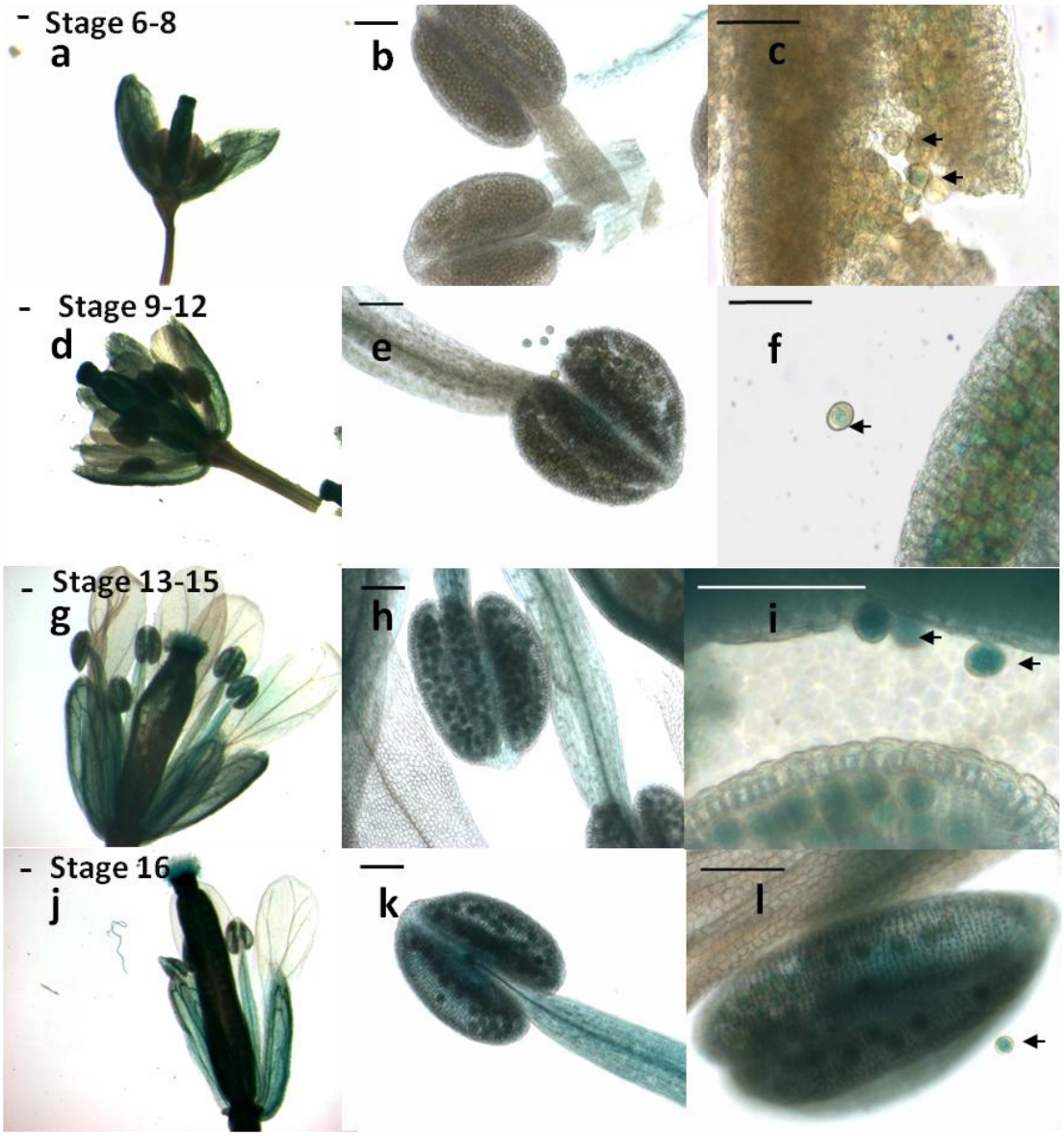

Fig. 12. *PrDROP3::*GUS expression analysis in different stages of flower and pollen. (a-c) flower stage 6 to 8, (d-f) flower stage 9 to 12, (g-i) flower stage 13 to 15, (g-l) flower stage 16. Single flowers (a, d, g, j), stamen (b, e, h, k), and pollen (c, f, i, l; arrows) are displayed. Almost no pollen stained in stage 6 to 8 (c) showed *prDROP3::*GUS expression, while expression was visible in all other stages. Scale bars: 500µm.

3.2.3 *PrDROP2::GUS* expression during biotic stress

10-day-old seedlings expressing *PrDROP2::GUS* showed an increased staining under flg22 treatment (Fig. 13), which was performed as described in 2.2.3.8.

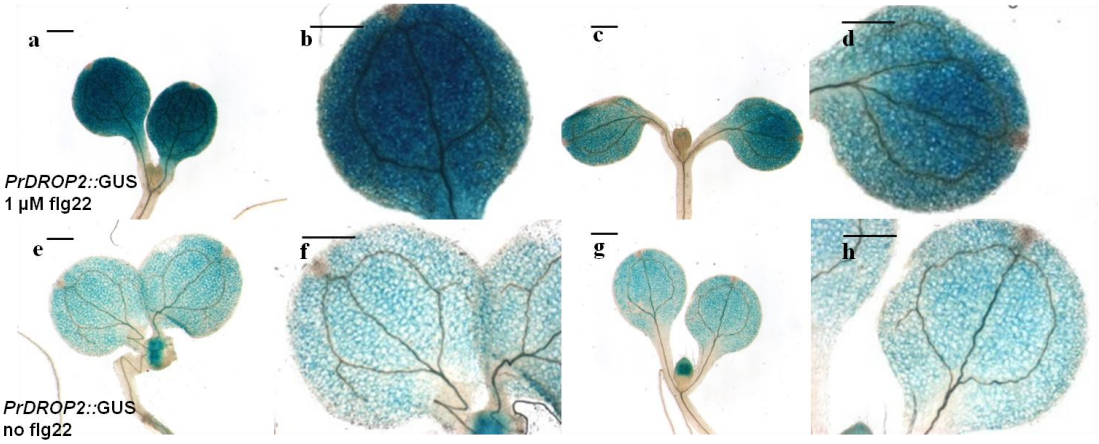

Fig. 13. Flg22-induced *PrDROP2::*GUS expression in seedling leaves. (a, c) 10 day-old seedling leaves treated for 12 hours with 1 µM flg22. (b, d) single leaf magnified from (a) and (c), respectively. (e, g) 10 day-old seedling leaves without flg22 treatment. (f, h) single leaf magnified from (e) and (g), respectively. All photos were taken with the same camera settings to allow for quantitative evaluation of the staining intensity. Scale bars: 1 mm.

To examine the flg22 response of mature plants, detached *PrDROP2::GUS* leaves were treated with flg22 for two hours (Fig. 14). Treatments were the same as applied for the stomatal assay (2.2.3.6). As in seedlings, flg22-treated *PrDROP2::*GUS leaves displayed a stronger blue staining as compared to control leaves.

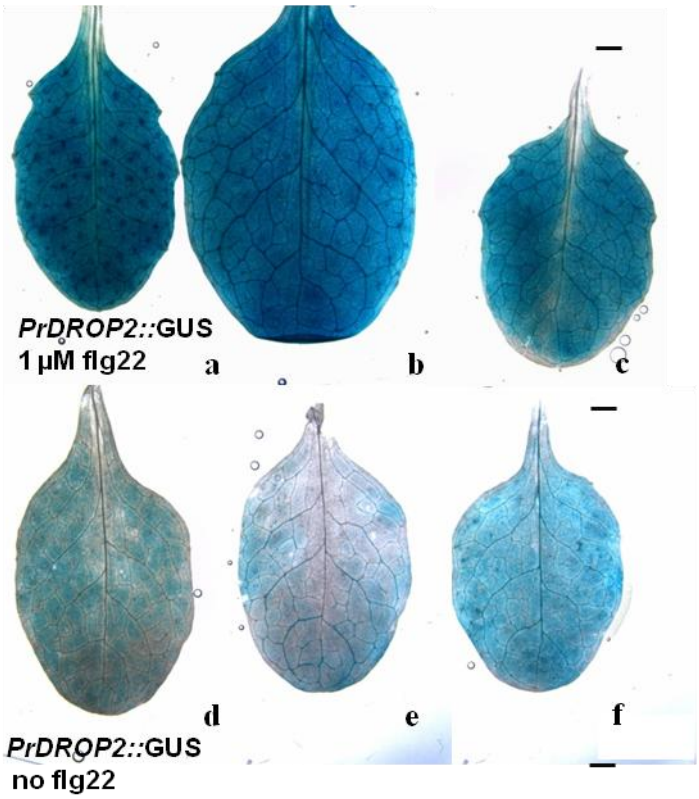

Fig. 14. Flg22-induced *PrDROP2::*GUS expression in mature leaves. (a-c) 30-day-old detached leaves treated for 2 hours with 1µM flg22. (d-f) control leaves without flg22 treatment. All photos were taken with the same camera settings to allow for quantitative evaluation of the staining intensity. Scale bars: 1 mm.

3.2.4 *PrDROP3::*GUS expression during abiotic stress

According to eFP browser data, *DROP3* is upregulated under drought stress (Winter et al., 2007). The underlying experiment was repeated with *PrDROP3::GUS* lines. Plants were cultured for 13 days in a 24-well plate containing ½ MS medium with 0.5% agar and 0.5% sucrose. Seedlings were then exposed to a stream of air in a laminar flow hood for 15 min. It was calculated that during this time period the plants lost 10% of their fresh weight (Kilian et al., 2007). Afterwards, they were transferred back into the medium and cultured for another 2 days. Seedlings were then stained with x-Gluc for 12 hours. Drought stressed seedlings of all three lines tested showed a stronger GUS expression than non-stressed control seedlings (Fig. 15).

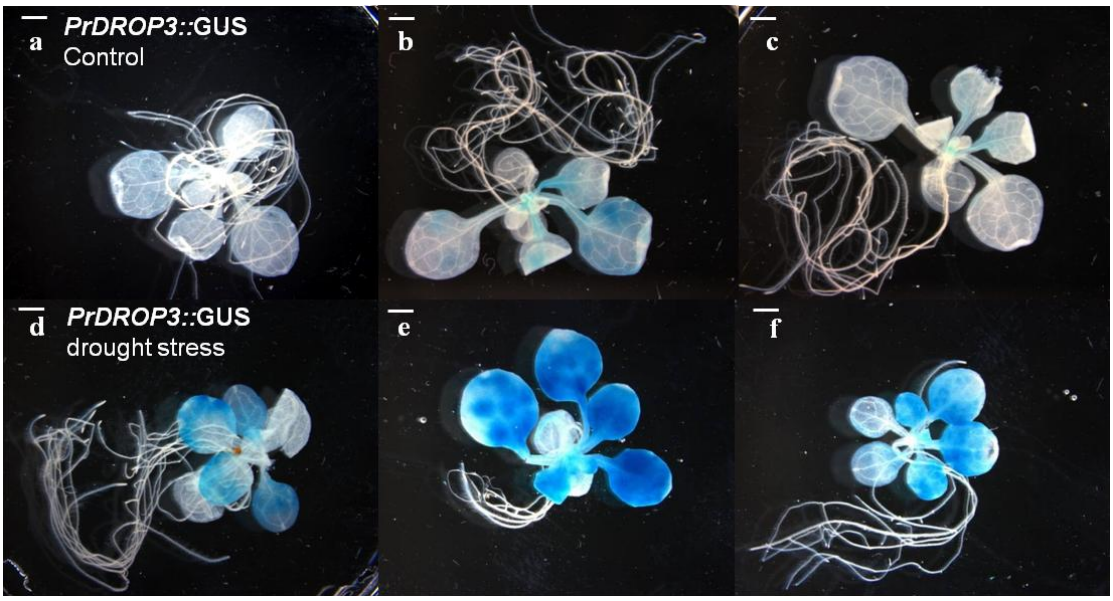

Fig. 15. Drought induces *PrDROP3::*GUS gene expression. Under drought stress seedlings show more intensive GUS staining in comparison with non-stressed plants. Three tested lines (a, d: 3-1; b, e: 3-2; c, f: 3-3) all show the same expression pattern. All photos were taken with the same camera settings to allow for quantitative evaluation of the staining intensity. Scale bars: 1 mm.

3.3 Roles of DROPs in plant development

To get a deeper insight into the roles that DROPs play in the plant, T-DNA insertion lines have been employed. Screenings for homozygous plants, localization of the insertion by PCR and sequencing, and verification of the absence of the corresponding transcript had been performed prior to the experiments (K. Thor, unpublished). To reveal the physiological roles of DROP2 and DROP3 in reproductive organs, two T-DNA insertion lines, *drop2-1* (SALK_102200) and *drop3-1* (SALK_013399) and their double knock-out mutant (*drop2-1 drop3-1*) were used. In line *drop2-1* the insertion is located in the seventh exon of the genomic DNA sequence of At5g43745; in *drop3-1* the insertion lies in the fourth intron of the genomic DNA sequence of At5g02940. To examine the roles of DROP3 in roots and guard cells, besides line *drop3-1*, the T-DNA insertion lines *drop3-2* (SALK_118260) and *drop3-3* (SALK_045095) were employed as well. In line *drop3-2* the insertion is located in eighth intron in the genomic DNA sequence, in line *drop3-3* in the twelfth exon. In experiments examining the role of DROP2 in biotic stress, two further T-DNA insertion lines were used, *drop2-2* (SALK_02267) and

drop2-3 (GABI_346CO3). In both lines the insertion is located in the 18th intron of the genomic DNA sequence.

3.3.1 Developmental phenotypes of pollen and siliques

Pollen germination and tube growth as well as proper silique and seed development are essential processes that ensure the reproduction of flowering plants. As promoter-GUS data showed expression of *DROP2* and *DROP3* in flowers, especially pollen, stigma and siliques (Figs. 9, 11, and 12), an involvement of these two genes during flower development and reproduction might be assumed. Hence, *in vitro* pollen germination and tube growth assays as well as an analysis of silique length and seed set were performed to investigate a possible role of the two genes in these processes.

In vitro germination of pollen from *drop2-1*, *drop3-1,* and wild type plants was tested. Fig. 16 a and c show the germination rate over time. The pollen germination rates of *drop2-1* and *drop3-1* mutants show constantly lower values in comparison with the wild-type. Decreased values of pollen germination of *drop2-1* and *drop3-1* are accompanied by the reduced pollen tube lengths (Fig. 16 b and d).

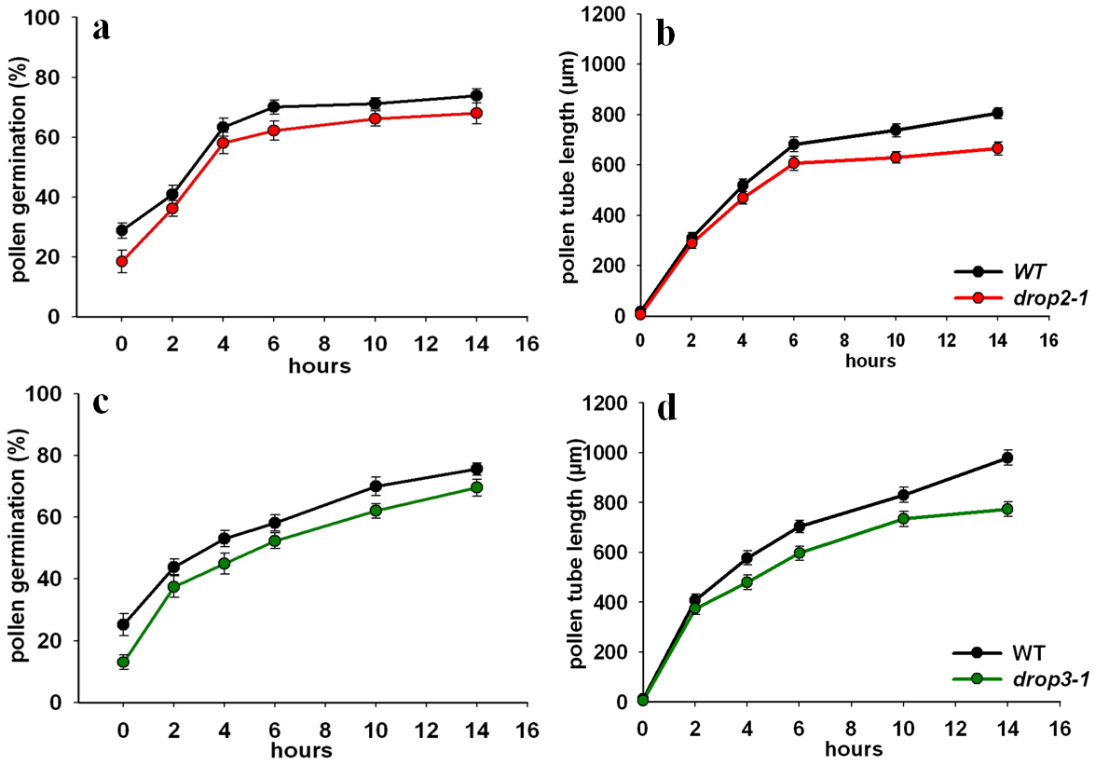

Fig. 16. Pollen germination and tube length over time in wild-type, *drop2-1, and drop3-1*. (a, c) pollen germination rate. (b, d) pollen tube growth. Data represent the mean ± SE of three independent experiments. n=100 (germination), n=300 (tube growth).

To analyse whether the defects of *drop2-1* and *drop3-1* are additive, pollen germination assays were carried out on the *drop2-1 drop3-1* double mutant. After 16 hours of incubation, the double mutant exhibited a germination rate of 60% as compared to 70% in the wild type, again indicating a significant decrease in the mutant ($P<0.05$; Fig.17 a). Fig. 17 b shows that the average tube length of the double knock-out was 510 µm as compared to 720 µm of the wild type, yielding a difference of 210 µm between the two ($P< 0.01$). Fig. 17 c (*drop2-1 drop3-1*) and d (wild-type) are typical images of the pollen tubes and clearly show the reduced length of the mutant tubes. Scanning electron micrographs show that the morphology of the pollen was not altered in the double mutant (Fig. 17 e-h).

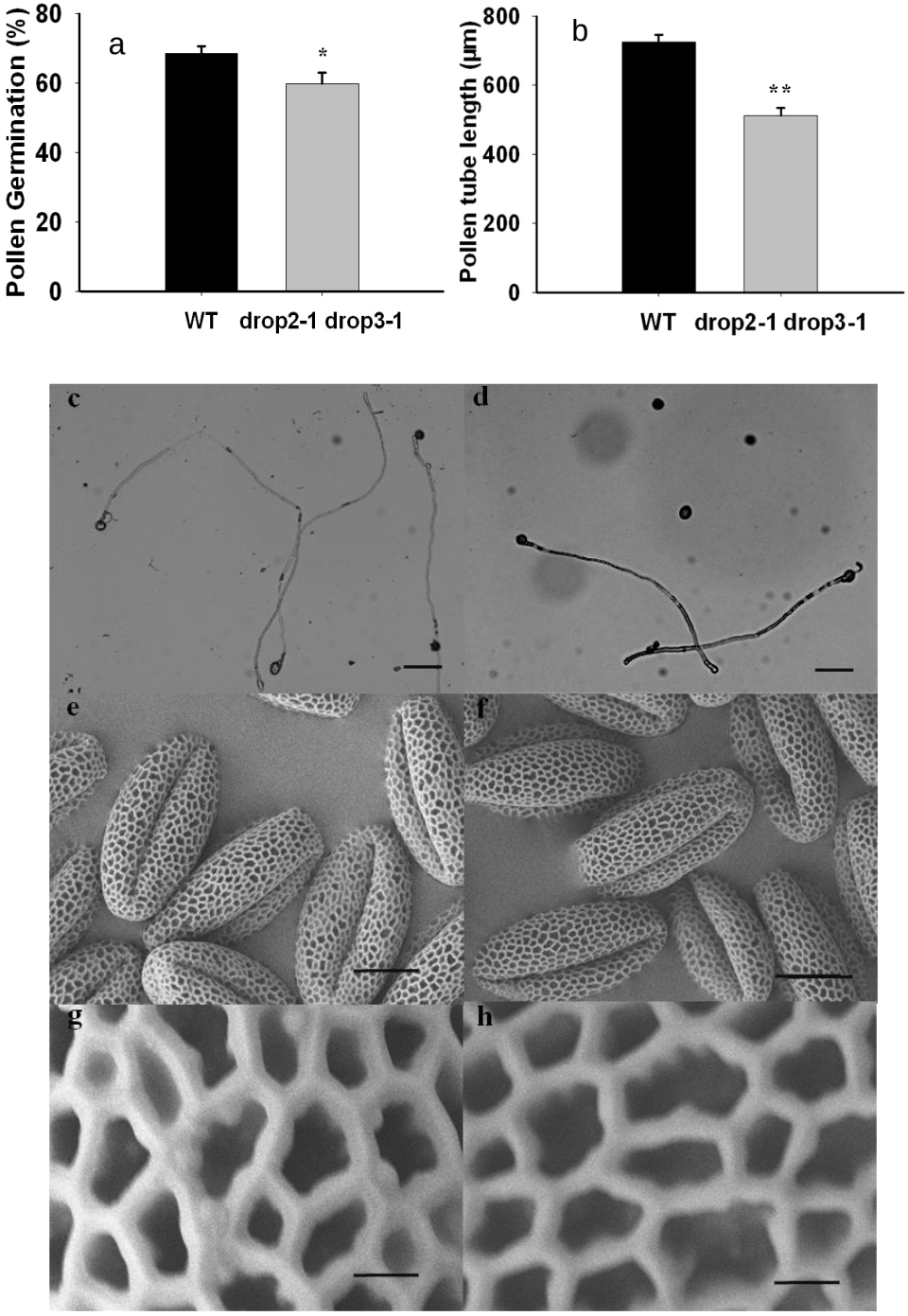

Fig. 17. Pollen germination and tube length of double knockout mutant plants are decreased *in vitro*, but pollen morphology is not affected. (a, b) Pollen germination rate and tube length of wild-type and the *drop2-1 drop3-1* mutant after 16 h of incubation. All data represent the mean ±SE (n=300 for germination rate and n=100 for tube length). **: significantly different at 0.01 level, *: significantly different at 0.05 level. (c, d) Germinated pollen of wild type (c) and the *drop2-1 drop3-1* mutant (d) after 16 h of incubation. Scale bars: 500 µm. (e, h) Scanning electron microscope (SEM) pictures of pollen grains of Col-0 wild-type (e) and the *drop2-1 drop3-1* mutant (h), 5.0 kV. Bar=10 µm. (f, i) Magnifications of (e) and (h), respectively, 5.0 KV. Scale bars: 1µm.

In continuation of the pollen assays, silique length and seed content in both *drop2-1* and *drop3-1* single mutants and the *drop2-1 drop3-1* double mutant were analyzed. The number of seeds per silique was decreased in the line *drop3-1* (Fig. 18 b) while siliques of *drop2-1* (Fig. 18 a) contained the same amount of seeds as the wild-type. However, both single mutants showed a decreased silique length (Fig. 18 c, d).

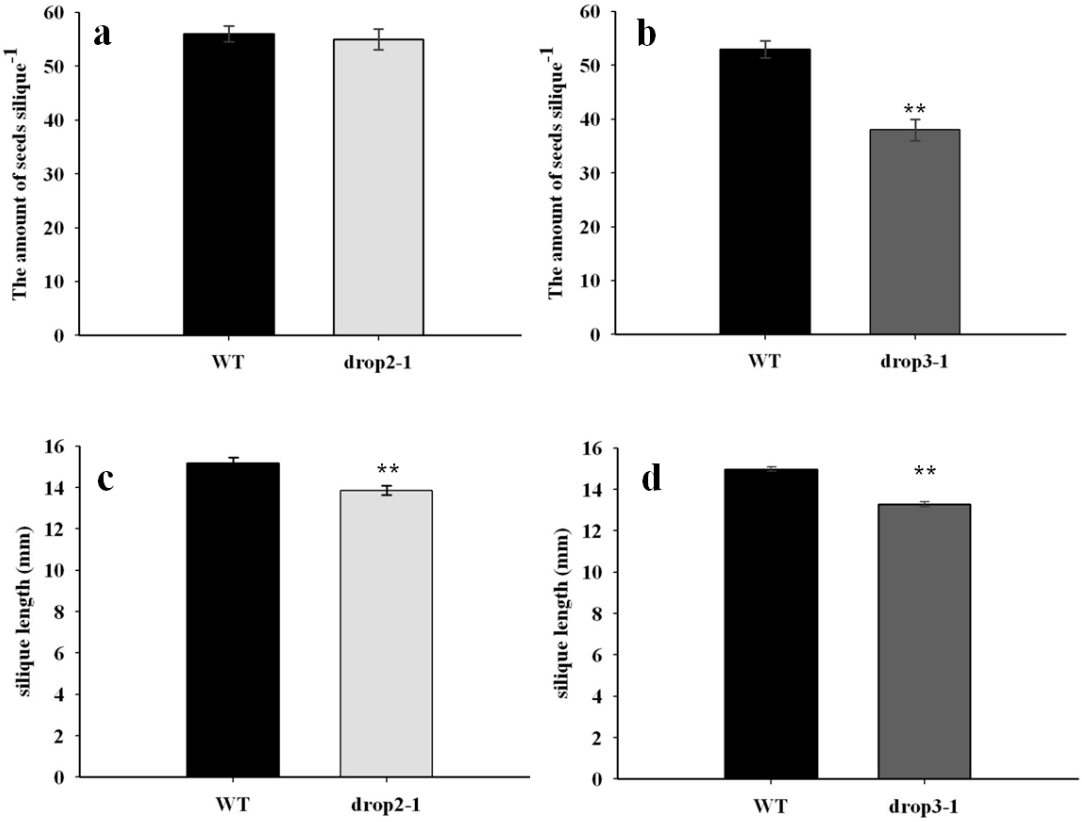

Fig. 18. Siliques of *drop*2*-1* and *drop*3*-1* mutants show developmental defects. (a, b) amount of seeds per silique (a) and silique length (b) in *drop 2-1*; (c, d) amount of seeds per silique (c) and silique length (d) in *drop 3-1*. (a, b) Data represent the mean of the amount of seeds per silique ± SE (n=10). (c, d) Data represent the mean of silique length ± SE (n=40). **: significantly different at 0.01 level. Experiments were repeated twice with comparable results.

Like the single mutants, the double mutant contained less seeds per silique (Fig. 19 a) and exhibited a shorter silique length (Fig. 19 b). Moreover, the reduction of the number of seeds per silique was in the same range as for the line *drop3-1*. Differences were significant for both number of seeds ($p < 0.01$) as well as silique length ($p < 0.01$).

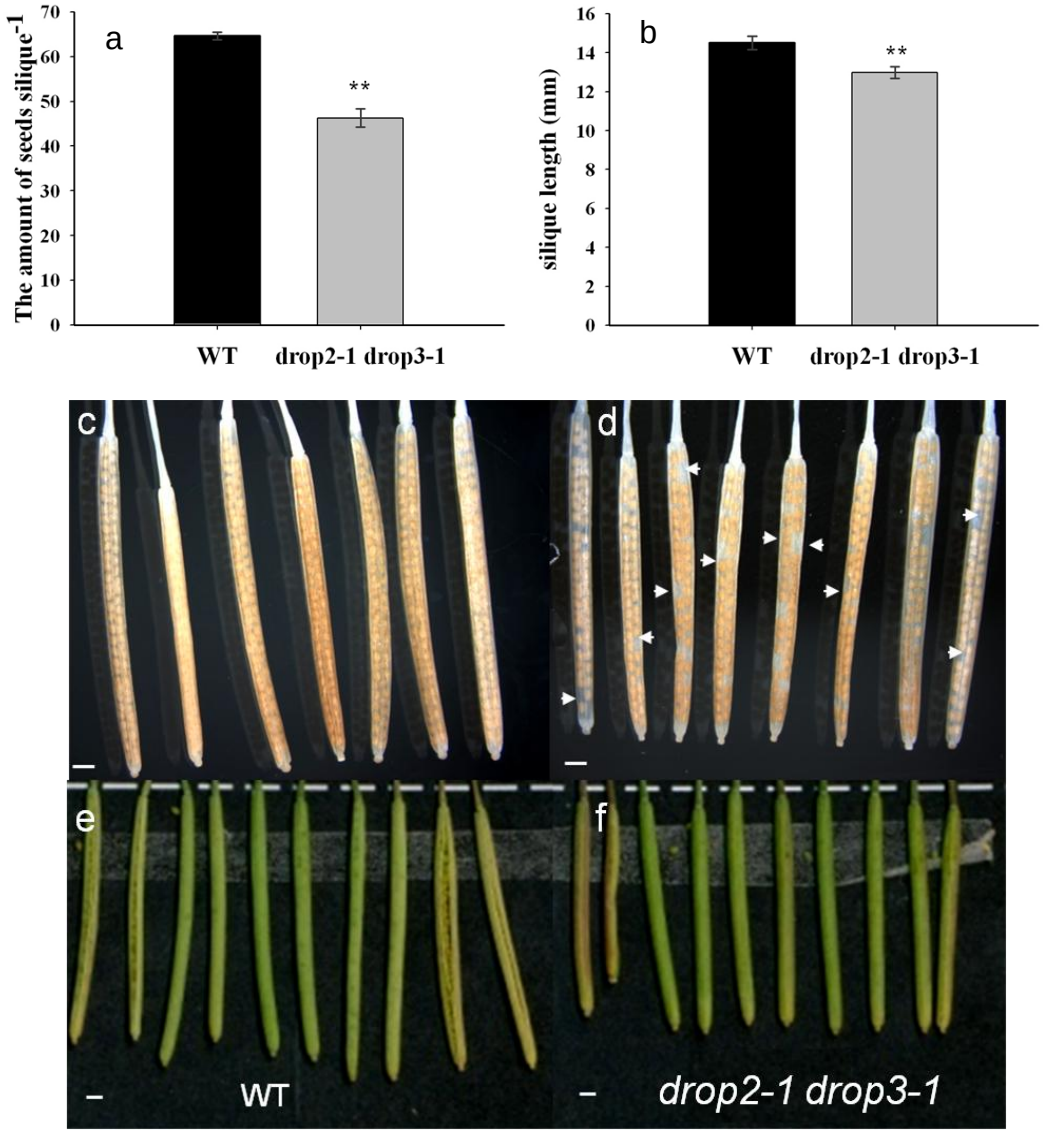

Fig. 19. Siliques of the *drop2-1 drop3-1* double mutant and the wild-type show developmental differences. (a, b) Number of seeds per silique (a) and silique length (b) of the double mutant as compared to the wild-type. (a) Data represent the mean of the amount of seeds per silique ± SE (n=10). (b) Data represent the mean of silique length ± SE (n=200). **: significantly different at 0.01 level. Experiments were repeated twice with comparable results. (c, d) Siliques of wild-type (c) and double mutant (d) fixed in acetic acid. Arrows indicate sites of undeveloped seeds in the double mutant. (e, f) Freshly excised siliques of wild-type (e) and mutant (f). Scale bars: 1mm.

Photographs of siliques, which were fixed in acetic acid, show that in the mutant siliques, ovules from which no seeds have developed can be found throughout the silique. In contrast, in wild-type siliques, all seeds developed

well (Fig. 19 c, d). Fig. 19 e and f show freshly harvested siliques of wild-type and double mutant, respectively. Siliques were taken from the same region of the shoot. The reduced length of the siliques quantified in Fig.19 b can be clearly seen.

3.3.2 Developmental phenotypes of roots

The root system functions in the absorption of water and nutrients from the soil and is thus a crucial plant organ. Promoter-GUS data indicated an expression of *DROP3* in an area of the root apex termed the root stem-cell niche (3.2.2, Fig. 8 i). This area is involved in root growth and differentiation. T-DNA insertion lines of *drop3* were compared with the wild-type to get an insight into which role these genes might play in roots. Root growth is best observed on agar plates. So, mutant lines were sown on ½ MS agar plates together with wild type plants as shown in Fig. 20. The two *drop3* knock-out mutant lines tested (*drop3-1, drop3-2*) showed the same trend, namely a faster root growth than the wild type.

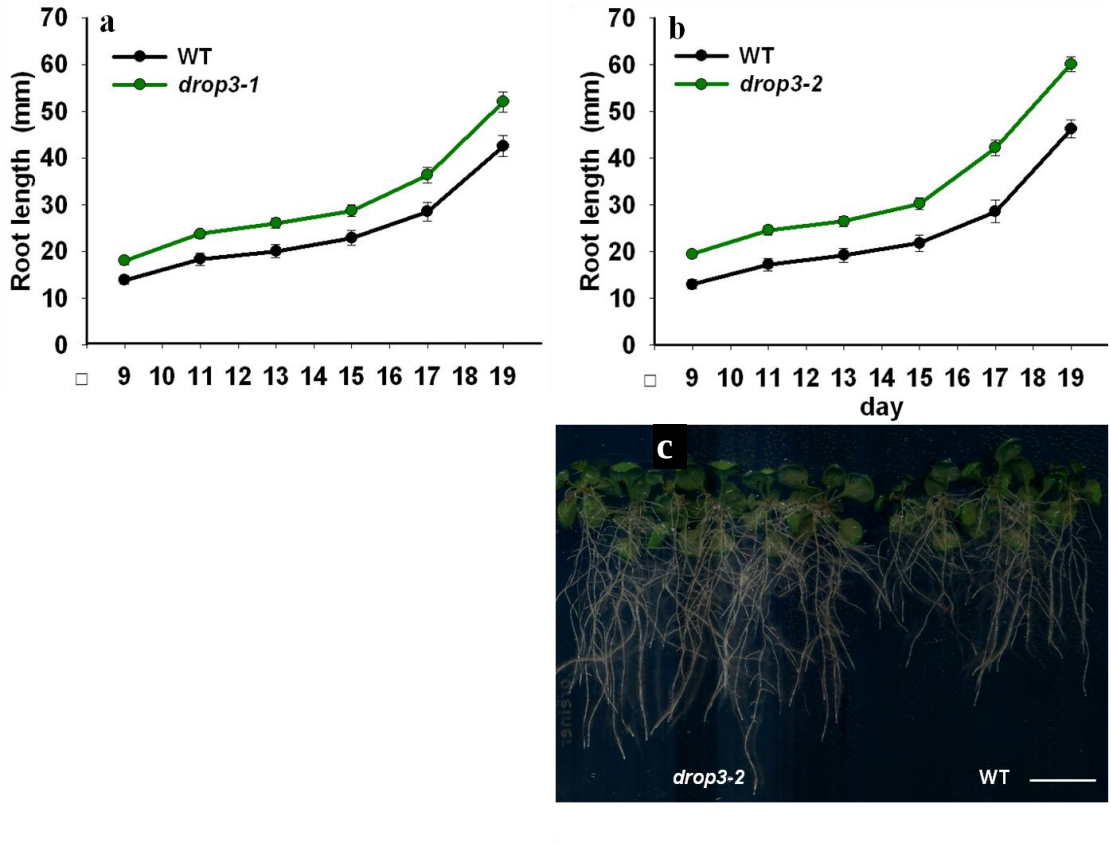

Fig. 20. Root growth assay. Length of main roots of wild-type (black lines) and *drop3* mutants (green lines) was measured on six consecutive time points within 19 days of growth. Error bars represent standard error of the mean values of triple-time repetition. Two independent mutant lines were observed: *drop3-1* (a) and *drop3-2* (b). Data represent the mean ±SE (n=18, three independent experiments). (c) shows a representative agar plate with *drop3-2* plants (left) and wild-type plants (right). *drop3-2* plants exhibit longer roots than the wild-type. Scale bar: 10 mm.

The root tip is a site of relatively high auxin concentration and sensitivity, which is a main determinant of root development (Overvoorde et al., 2010). The physiological phenomenon of gravitropsim is regulated by auxin. To examine wether DROP3 is involved in gravitropsim, the *drop3-1* mutant was sown on ½ MS agar plates, and two-week-old plants were rotated by 90° (Fig. 21). We did not find any difference in gravitropic responses of wild-type and *drop3-1* roots.

Fig. 21. Gravitropsim analysis of *drop3-1*. When ½ MS plates of two-week-old seedlings were turned by 90º and plants grown further for 2 days, roots of both wild-type and mutant responded in an identical way.

3.4 Roles of DROPs under stress conditions

3.4.1 Stomatal aperture changes in response to ABA, $CaCl_2$, and flg22

Stomatal pores are formed by guard cells in the leaf epidermis. The function of guard cells is to respond to environmental changes by opening and closing the stomatal pores. In guard cells, a network of signal transduction mechanisms integrates water status, hormone responses, light, CO_2, and other environmental factors (Hetherington and Woodward, 2003; Kwak et al., 2008; Schroeder et al., 2001). Abscisic acid (ABA) is a trigger which increases the cytosolic Ca^{2+} concentration. It actives Ca^{2+}-permeable channels in the plasma membrane of guard cells and induces stomatal closure (Jakab et al., 2005; Kwak et al., 2008). Fig. 22 clearly shows that the aperture of stomata decreases when epidermal strips are treated with 10 µM ABA.

A high concentration of extracellular Ca^{2+} also evokes a rise in $[Ca^{2+}]_{cyt}$ that precedes the loss of turgor by the guard cells and leads to stomatal closing (McAinsh and Hetherington, 1998; McAinsh and Pittman, 2009). Fig. 22 likewise clearly shows that the aperture of stomata decreased when leaf epidermal strips were treated with 10 mM $CaCl_2$.

During the infection of plants, bacterial entry is restricted by the closing of stomata. Stomatal closure therefore is part of the plant innate immune response and acts as a barrier against bacterial infection (Melotto et al., 2006). Flg22 is a bacterial elicitor which stands at the beginning of the guard cell signalling cascade leading to stomatal closure. Flg22-induced stomatal closure was also observed in the present study (Fig. 22).

As DROPs may participate in Ca^{2+} signalling, we investigated in stomatal bioassays, if those proteins may be involved in guard cell responses. Several knock-out mutant lines for *drop2* and *drop3* were used for the stomatal assays. Fig. 22 a and c show that stomatal aperture was decreased by ABA and $CaCl_2$ in the wild-type and the mutants in a similar way. Therefore, DROP2 and DROP3 are probably not involved in the ABA or $CaCl_2$-triggered guard cell signalling pathway. Stomatal aperture of the *drop2-1* mutant exposed to 1 µM flg22 was also comparable to that of the wild-type (Fig. 22 b). Therefore, DROP2 does not seem to be involved in the signalling pathway leading to stomatal closure during the *Arabidopsis* innate immune response.

Interestingly, stomatal aperture of untreated controls of *drop3-1* was consistently larger than that of the wild type. Measurements of stomatal width and length indicated that *drop3-1* possesses somewhat larger stomata as compared to the wild-type (Fig. 22 d).

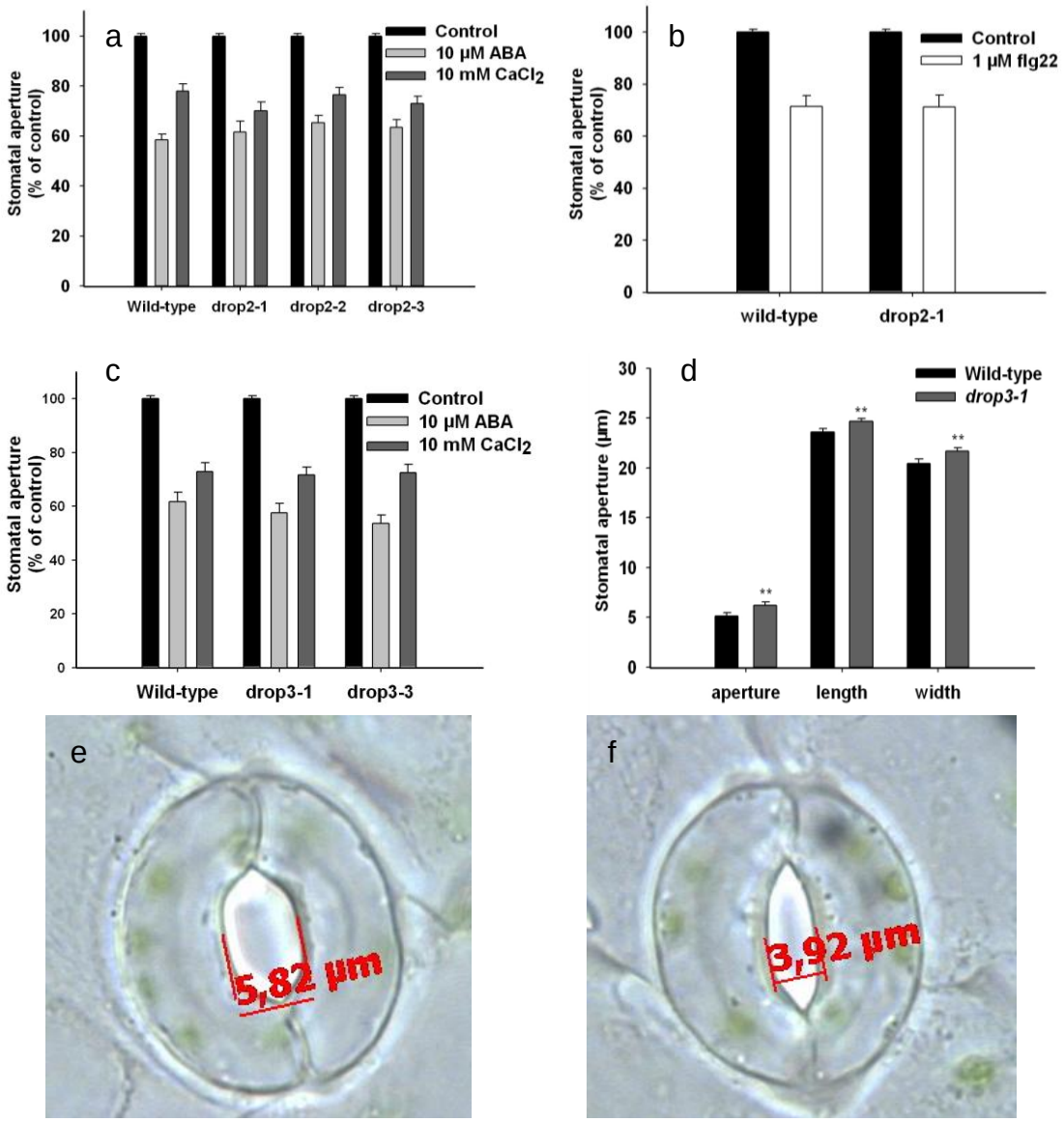

Fig. 22. Stomatal aperture assay under different stress-related treatments. (a, c) Stomatal aperture values of *DROP* mutants in the presence of 10 µM ABA (light grey bars), 10 mM $CaCl_2$ (dark grey bars), and without any treatment (black bars). All data represent the mean ± SE (n=30, three independent experiments, each consisting of 30 stomatal aperture measurements per line and treatment). Absolute values of stomatal apertures in control medium were 5.9 µm, 6.2 µm, 6.5 µm, 6.0 µm, 6.1 µm and 6.6 µm for wild-type, *drop2-3*, *drop2-1*, *drop2-2*, *drop3-3,* and *drop3-1* respectively. (b) Stomatal aperture values for *drop2-1* in the presence of 1 µM flg22 (white bar). All data represent the mean ± SE (n=30, two independent experiments). Absolute values of stomatal apertures in control medium were 5.6 µm and 5.6 µm for wild type and *drop2-1,* respectively. (d) Stomatal size in the *drop3-1* mutant. All data represent the mean ± SE (n=30, two independent experiments) (e) Example of opened stomata without a treatment. (f) Example of stomata in the presence of a treatment.

3.4.2 Stomatal conductance in response to flg22 treatment or drought stress

The stomatal pores present in the epidermis of terrestrial plant organs determine gas exchange and transpiration of water. Stomatal conductance in principle is the speed at which water evaporates from those pores and is directly related to the stomatal aperture. (It must be noted that humidity, the hydration status of the plant and light intensity are also factors that affect stomatal conductance.) Stomatal aperture is the dominant factor in the diffusion conductance of leaf surfaces (Farquhar and Sharkey, 1982; Mott et al., 1982). During plant-pathogen interactions, stomata also constitute one entry point for bacteria, which need to reach the apoplastic space to multiply and cause disease. Measurements of conductance are therefore important indicators of plant water status and provide a valuable insight into plant growth and plant adaptation to environmental variables. The AP-4 leaf porometer measures stomatal conductance by comparing the rate of humidification provided by a leaf within a small cuvette to readings obtained with a calibration plate. In this thesis, the stomatal conductance of wild type and mutant lines in response to flg22 treatment or drought was determined.

As can be seen in Fig. 23, flg22 treatment of plants grown in soil in general decreased stomatal conductance in comparison with untreated plants, and this decrease was stable for several days. However, stomatal conductance measured upon flg22 treatment in line *drop2-1* was lower than that of wild-type plants (Fig. 23 b), while values measured for line *drop2-2* were slightly higher (Fig. 23 d). This discrepancy may be due to experimental deficiencies or an additional insertion in a gene other than *DROP2* in one of the two lines. More experiments will be needed to dissect this. Thus, from the currently existing porometer data, a clear statement about a possible influence of *DROP2* on stomatal conductance upon flg22 treatment cannot be made.

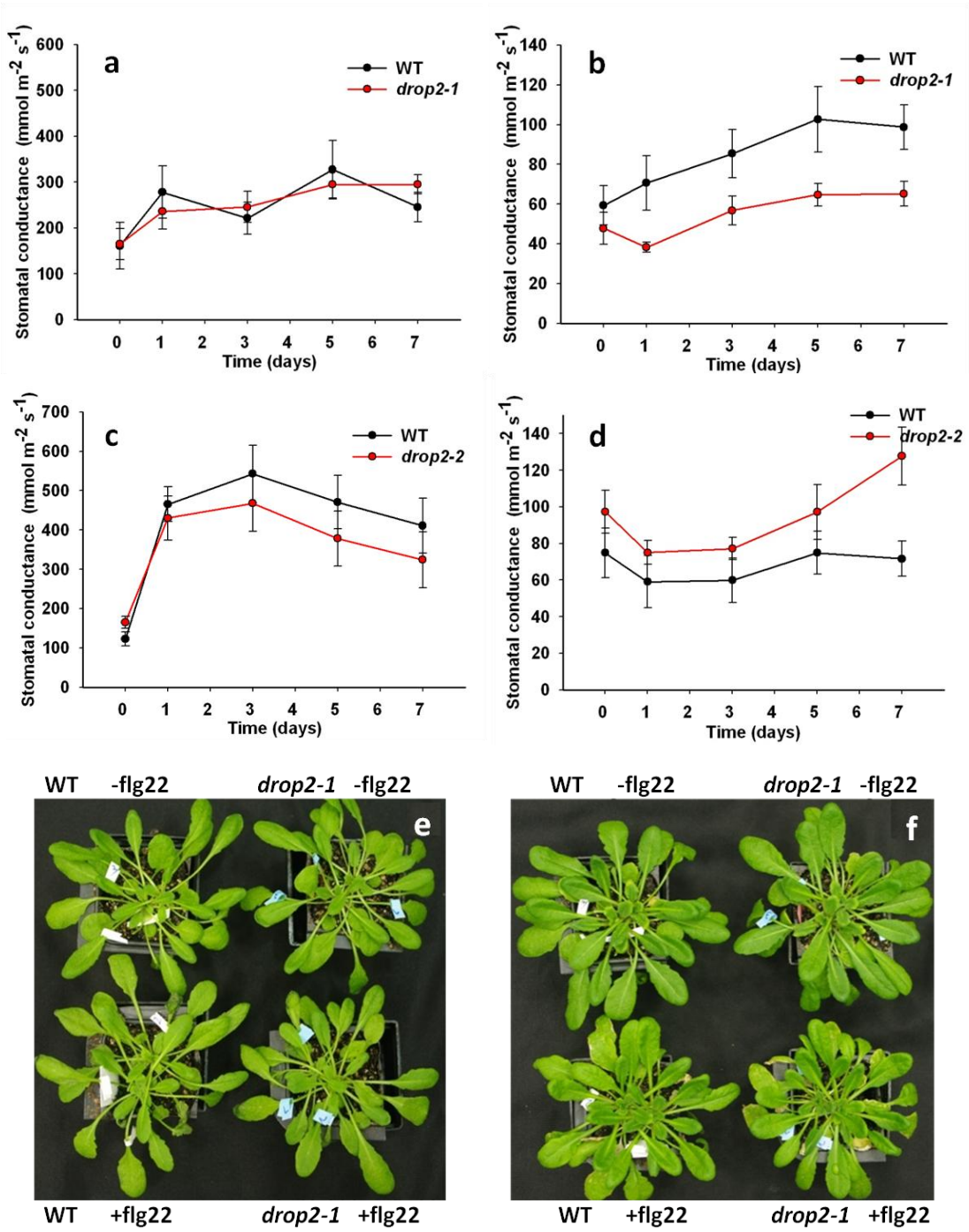

Fig. 23. Stomatal conductance under flg22 stress as determined by porometry. Stomatal conductance values of *drop2-1* (a, b) or *drop2-2* (c, d) and wild type plants over time. Plants were sprayed with 2 µM flg22 (a, c) or water only (b, d). "Day 0" value was determined 3 h after spraying. (e) Photos of *drop2-1* and wild type plants at 1 day after flg22 application. (f) Photos of *drop2-1* and wild type plants at 8 days after flg22 application.

A drought stress experiment was performed with the lines *drop2-1* and *drop3-1* (Fig. 24). On day 0, watering was stopped. Stomatal conductance of *drop2-1* and *drop3-1* plants was initially the same as that of wild-type plants.

Values for *drop2-1* plants remained similar to the ones for the wild-type during the next seven days, whereas *drop3-1* plants showed slightly lower values (Fig. 24 a, b). However, this slight reduction did not result in visibly longer drought survival (Fig. 24 c).

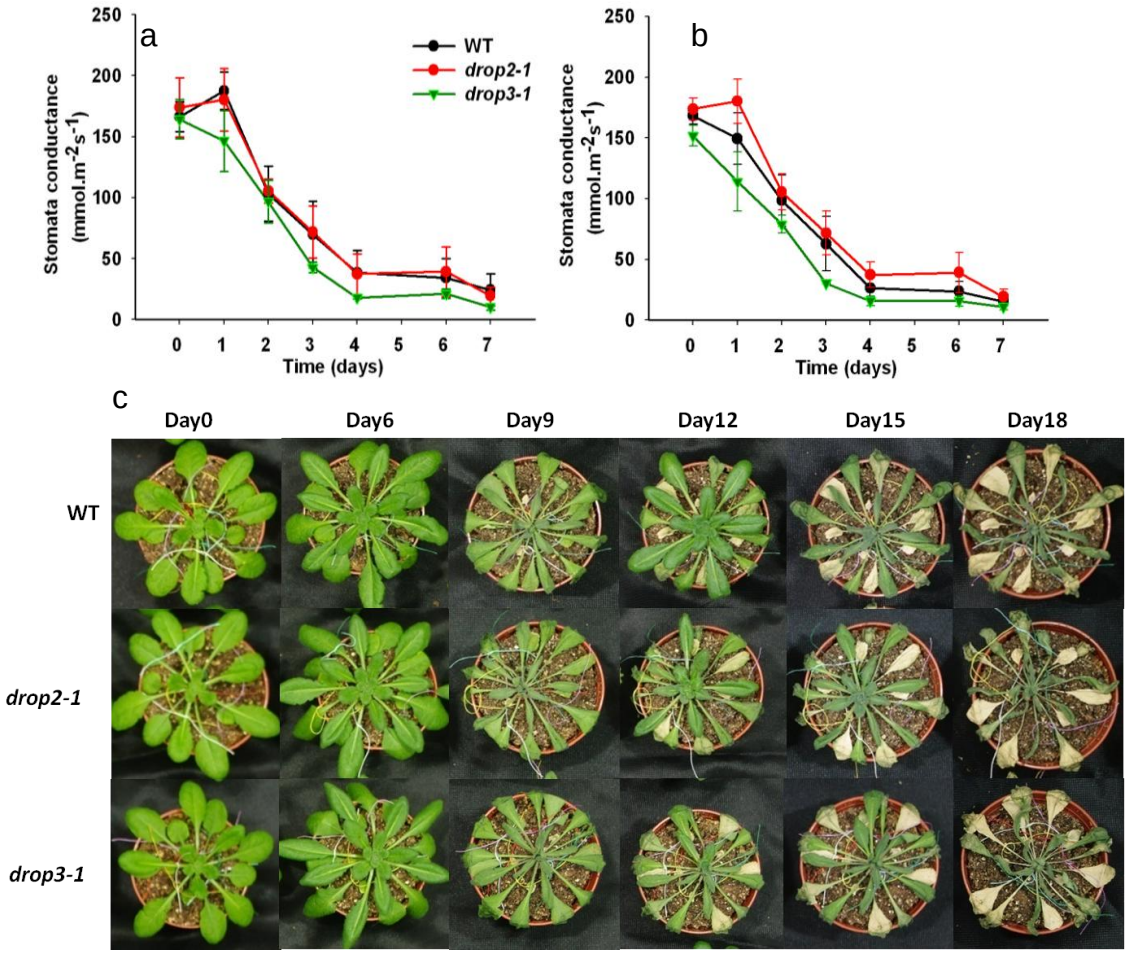

Fig. 24. Stomatal conductance under drought as determined by AP-4 porometer. (a) Values of stomatal conductance over time for the 10th leaves; (b) values of stomatal conductance over time for the 9th leaves. Watering of plants was stopped at day 0. Plants were rewatered with 5 ml once at day 5. All data represent the mean ±SE (n=4). (c) Representative plants of wild-type and the lines *drop2-1* and *drop3-1* at 0, 6, 9, 12, 15, and 18 days of drought.

3.4.3 Callose formation by flg22 treatment

Callose deposition has emerged as a popular read-out to quantify plant immune responses (Luna et al., 2011). The accumulation of callose, a plant β-1,3-glucan polymer synthesized between the cell wall and the plasma membrane, is a classical marker of PTI (PAMP-triggered immunity)

responses after treatment with infectious or noninfectious pathogens in the perception of PAMPs (Pathogen-Associated Molecular Patterns) (Brown et al., 1998; Gómez-Gómez et al., 1999; Nicaise et al., 2009).

In the pathogen signalling pathway, Ca^{2+} signals are produced by Ca^{2+} influx into the cytosol. The Ca^{2+} chelator EGTA was used to determine the relevance of external Ca^{2+} for callose deposition. Seedlings of wild type were treated with 1 µM flg22 for 24 h, and callose deposition was determined by aniline blue staining. Staining was documented by taking photographs under UV light. As can be seen in Fig. 25, 1 mM EGTA decreased flg22-induced callose deposition markedly. This clearly demonstrated that part of cytosolic Ca^{2+} influx is derived from extracellular space.

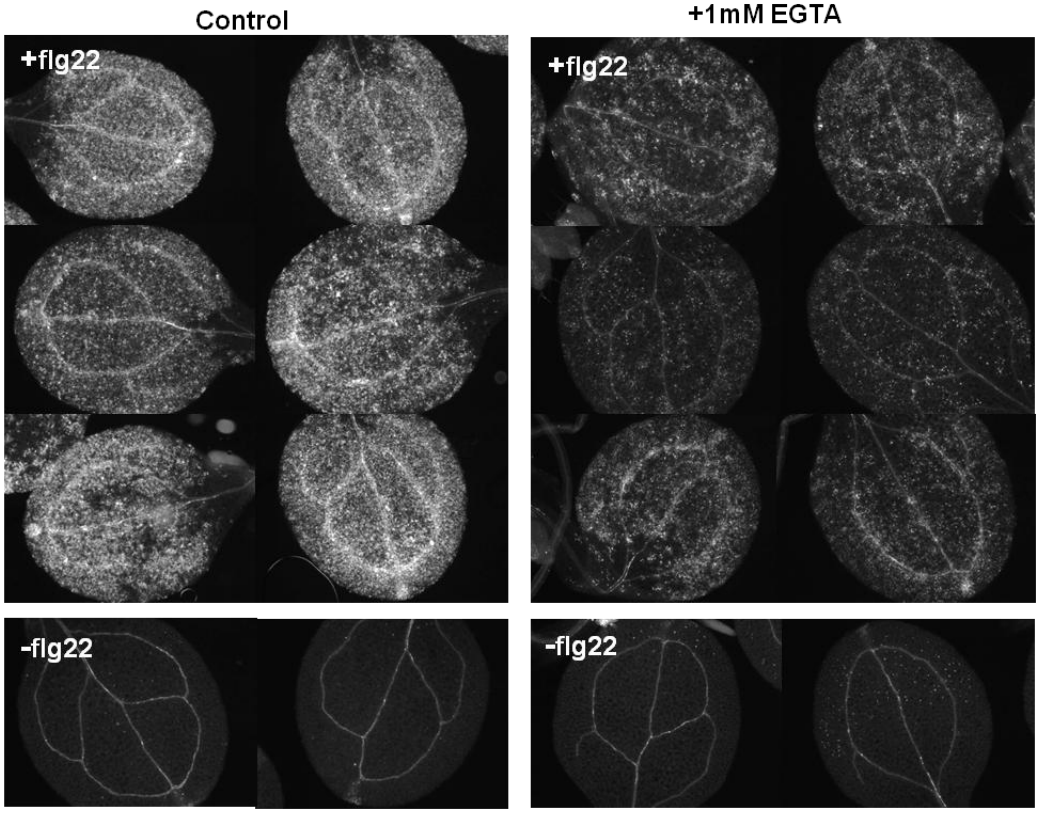

Fig. 25. EGTA inhibition of callose deposition. 10 days-old wild type Arabidopsis seedlings were exposed for 24 h to 10 µM flg22. 1mM EGTA was added to chelate extracellular Ca^{2+}.

DROP2 may regulate callose deposition by regulating the inital Ca^{2+} fluxes or by an alternative mechanism downstream of the initial Ca^{2+} signal. To test this, seedlings of wild type and *drop2* mutants were treated with 1 µM flg22 for 24 h, and callose deposition was determined as described above (Fig. 26 a-d). The wild type clearly showed a stronger aniline blue fluorescence than the three independent *drop2* knockout mutants (Fig. 26 a-d), which means that leaves of the mutants accumulate less callose than wild type leaves. Seedlings without flg22 treatment did not show fluorescence. Quantified fluorescence intensity values demonstrated a significant difference between wild-type and *drop2* mutants (Fig. 26 e).

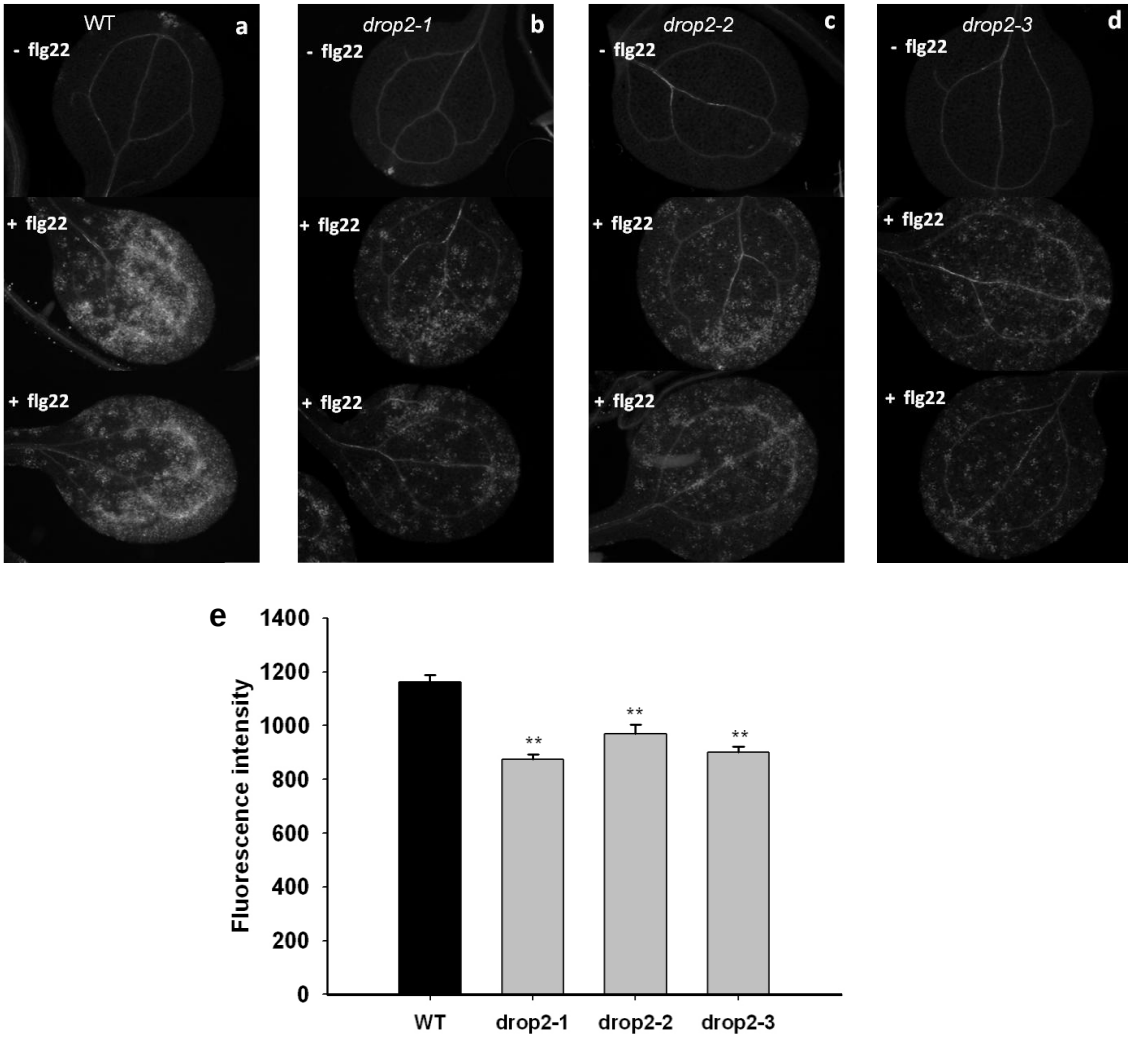

Fig. 26. Callose deposition assay. (a-d) Fluorescence microscopy pictures of leaves stained with aniline blue to reveal callose deposition after 24 h of flg22 treatment. Shown are the wild type and three independent *drop2* mutants. (e) Fluorescence intensity reflecting callose deposition in wild type and *drop2* mutant leaves. Data represent the mean of 14 seedling leaves ±SE. **: significantly different at 0.01 level.

4. Discussion

Signalling, that means transmitting information within the cell, is an important process in plants, for example during stress responses. An elicitor thereby activates a specific receptor protein on the cell membrane, and a second messenger transmits the signal within the cell, inducing changes in gene expression and physiological responses. An important second messenger is Ca^{2+}. Changes in the cytosolic Ca^{2+} concentration describe patterns, which are specific for a defined stimulus and induce specific downstream responses (Kudla et al., 2010; McAinsh and Pittman, 2009). The Ca^{2+} thereby has to be released from external or internal stores through the action of channel proteins and brought back to a basal level afterwards. A prominent example of Ca^{2+} signalling is the symbiosis pathway induced by Nod factors, which leads to nodulation in leguminous plants. MtDMI1 from *Medicago truncatula* has been shown to be a Ca^{2+} signal modulator in this pathway (Peiter et al., 2007). This protein has been shown to be located in the nuclear membrane and probably acts as K^+ channel, which is activated by other second messengers, and induces a membrane hyperpolarization, which in turn opens voltage-gated Ca^{2+} channels. In this way it contributes to the nuclear and perinuclear Ca^{2+} spiking, which is essential for a successful nodulation (Peiter et al. 2007, Oláh et al., 2005). In *Arabidopsis thaliana* three uncharacterized genes exist, which are homologs to *MtDMI1* (Ané et al., 2004). These genes have been named here *DROP1*, *DROP2,* and *DROP3* for DMI1-like RCK domain proteins. As is mentioned in the name, the corresponding proteins all carry an RCK domain. In MtDMI1 and in bacterial channels like MthK, this domain is responsible for activation by ligands. It is therefore likely that the three proteins constitute channels which might also act as Ca^{2+} signal modulators. Arabidopsis has been established as a model plant in reverse genetics (Reski, 1998). However, as Arabidopsis is a non-symbiotic plant, DROP1, 2, and 3 cannot play a role in symbiotic signalling. Therefore, the current study elucidated their potential role in other plant signalling pathways or developmental processes, with an emphasis on processes which are known

to involve Ca^{2+} signals. An important part was the detection of phenotypes of T-DNA mutants. These, combined with online database searches, subcellular localization of EYFP fusion proteins, and promoter-GUS expression studies contributed to unraveling the role of DROP1, DROP2, and DROP3 in the plant and therefore to a better understanding of molecular processes underlying plant development and stress responses.

4.1 DROPs – putative channel proteins located at organellar membranes

The results of the subcellular localization assay show that C-terminal EYFP fusion proteins of DROP1 colocalize with the ER-GFP marker (Fig. 3). This subcellular localization of DROP1 to the ER displays similarity to the localization of MtDMI1 in yeast: Here, immunogold labeling also assigned MtDMI1 to the ER as well as to the nuclear envelope (Peiter et al., 2007). In plants, MtDMI1 is localized to the nuclear envelope (Riely et al., 2007, Capoen et al., 2011). Derived from functional assays in yeast and plants, MtDMI1 is assumed to be a cation channel modulating the activity of Ca^{2+} channels (Peiter et al., 2007, Oldroyd and Downie, 2008, Capoen et al., 2011). From the observed localization, it could therefore be speculated that DROP1 fulfils a similar function at the ER. However, as DROP1 expression levels are very low throughout all developmental stages of the plant, the role of this protein was not analysed in this study.

N-terminal fusion proteins of DROP1, but also DROP2 and DROP3, exhibited diffuse localization patterns that were different from the C-terminal fusions. It is a well-known phenomenon that GFP fusions at the N-terminus are prone to mistargeting, probably due to masking of the signal peptide by the GFP (Palmer and Freeman, 2004). As hydropathy plots for the DROP proteins show that they possess transmembrane domains, the proteins have to be associated with a membrane, which, for the N-terminal fusions, may be some part of the ER or secretory pathway.

Fluorescence of C-terminal EYFP fusion proteins of DROP2 and DROP3 was clearly associated with chloroplasts (Fig. 4). This result is also supported by subcellular localization predictions for both proteins in the ARAMEMNON database (Schwacke et al., 2003) and by proteomics data. In recent years, proteomics have moved from just unraveling the complete expressed and translated genome to subcellular studies in order to obtain information on protein location and therefore implications on their function (Jung et al., 2000). However, subcellular proteomics data need to be validated by independent approaches, because the likelyhood of false assignments is relatively high (Dreger, 2003). Published data of the *Arabidopsis thaliana* chloroplast proteome indicated that the DROP3 protein is located in the chloroplast envelope (Ferro et al., 2003, Ferro et al., 2010, Froehlich et al., 2003), and in one publication also the DROP2 protein was detected in the envelope fraction (Froehlich et al., 2003). Chloroplasts are chlorophyll-containing plastids enclosed by an envelope which is composed of an outer and an inner membrane. While for a long time it was thought that only the inner membrane contains specific transport proteins and the outer membrane merely acts as mesh with pores, it has now become clear that regulated proteins with specific functions also exist in the outer membrane. Outer Envelope Porins (OEPs) for example are channel proteins with different substrates located in the outer envelope (Vothknecht and Soll, 2005, Inoue, 2007, Bölter et al., 1999, Bölter and Soll, 2001). The chloroplast is the place of important metabolic reactions such as photosynthesis or fatty acids synthesis. It has also been known for a long time that chloroplasts are able to accumulate Ca^{2+} in the millimolar range and that the Ca^{2+} influences metabolic reactions such as the Calvin cycle (Charles and Halliwell, 1980). The chloroplast also contributes to homeostasis of other ions such as magnesium (Portis Jr and Heldt, 1976). Ca^{2+} levels within the chloroplast change dependent on the light conditions. Light-dark transition induces stromal Ca^{2+} fluxes, as has been shown with the Ca^{2+} reporter aequorin (Sai and Johnson, 2002). Apparently, chloroplasts receive Ca^{2+} from the cytosol during the light (Kreimer et al., 1985). The ion is stored and, when light is replaced by darkness, moves back into cytosol (Sai and Johnson, 2002). Evidence is rising that chloroplasts not only are involved in

ion homeostasis but also in Ca^{2+} signalling. The 'calcium-sensing receptor' of Arabidopsis (CAS), a thylakoid-localized protein, has been shown to be involved in the generation of the cytosolic Ca^{2+} oscillations induced by external Ca^{2+}, which lead to stomatal closure (Han et al., 2003, Nomura et al., 2008, Vainonen et al., 2008). A very recent study has proven that CAS regulates stress-induced chloroplastic and cytosolic Ca^{2+} signals in the plant immune response (Nomura et al., 2012). Taken together, previous studies have already shown that chloroplasts can sense and influence cytoplasmic Ca^{2+} levels in plant physiological processes, but much more research on the molecular mechanisms behind these processes has to be done. DROP2 and DROP3 are homologs to a known Ca^{2+} signal modulator, show structural characteristics of ligand-gated channels, and in this work have been shown to localize to chloroplasts. Therefore they are good candidates for chloroplastic Ca^{2+} signal modulators. First experiments with *drop2* mutants bearing the Ca^{2+} reporter aequorin show that cytosolic Ca^{2+} signals in response to the fungal elicitor chitin are altered in these mutants (K. Thor, unpublished), underlining such a modulator function for DROP proteins. More detailed functional analysis as for example planar lipid bilayer experiments will have to be performed to get a closer insight into their channel character.

4.2 Expression patterns and roles of *DROP*s in plant development

Publically available microarray data from Genevestigator (Hruz et al., 2008; Zimmermann et al., 2004) show that *DROP1* is expressed at low level in different developmental stages (Fig. 6). In promoter-GUS expression studies expression of *DROP1* could only be demonstrated in roots and rosette base at a very low level in 4-week-old plants (Fig.8 a-d). In contrast to this low expression of *DROP1*, Genevestigator (Hruz et al., 2008, Zimmermann et al., 2004) as well as eFP browser data (Winter et al., 2007) state that *DROP2* and *DROP3* are expressed at higher levels in every developmental stage tested, especially during flowering (Fig. 6, Fig. 5 c and d). Consistent with that,

PrDROP2::GUS and *PrDROP3*::GUS expression could be observed in both, vegetative tissues, such as root tips and leaves (Fig. 8 e-h and i-l), as well as reproductive tissues, i.e. flowers and siliques (Fig. 9 a-h). Due to the low expression of *DROP1*, phenotyping experiments in the current study then concentrated on *drop2* and *drop3* mutants.

4.2.1 DROP2 and DROP3 are essential for pollen germination and tube growth

Promoter-GUS expression analysis revealed that both, *DROP2* and *DROP3* are expressed in flowers, especially in the stigma and mature pollen grains, as well as in non-vascular tissue of petals and sepals (Fig. 9 a, e). Since it is known that pollen tube growth is a process dependent on a tip-focused Ca^{2+} gradient (Miller et al., 1992, Pierson et al., 1994), the expression in pollen was followed up in pollen germination assays in the current study. These assays revealed that *drop2-1* and *drop3-1* mutants exhibited a decreased pollen germination rate and reduced tube length compared to wild-type pollen (Fig. 16). The double mutant (*drop2-1 drop3-1*) exhibited a similar phenotype as the corresponding single mutants (Fig. 17 a, b). Therefore, although their expression pattern is quite similar, there seems to be no fuctional redundancy of DROP2 and DROP3. A possible reason for this might be that DROP2 and DROP3 form heteromers. A suitable method to test this hypothesis might be a BiFC (bimolecular fluorescence complementation) assay (Kerppola, 2006).

In mesophyll protoplasts, DROP2 and DROP3 were localized to chloroplasts (Fig. 4). Pollen does not contain these chlorophyll-containing plastids, but it has been shown that mature pollen contains plastids which have starch grains, i.e. amyloplasts (Inaba and Ito-Inaba, 2010). In recent years, these plastids have been tracked *in vivo* by using a construct in which GFP was fused to a plastid signal peptide and which was under the control of a vegetative cell-specific promoter. Fluorescence microscopy showed that Arabidopsis pollen grains contain around 40 plastids and that after germination of the grain they move into the growing tube. They also move back and forth with the cytoplasmic streaming in the tube (Tang et al., 2009, Fujiwara et al., 2010). It

needs to be determined whether the plastid localization of DROP2 and DROP3 observed in mesophyll cells is true for pollen, too.

Ion dynamics play an important role in regulating the rate and direction of pollen tube growth. Four major ions, Ca^{2+}, H^+, K^+ and Cl^-, are involved in the regulation of pollen tube growth (Feijó et al., 1995, Rounds et al., 2011). While H^+, K^+ and Cl^- seem to play a role mainly in osmoregulation and maintenance of the turgor in the growing tube (Rounds et al., 2011), Ca^{2+} plays a pivotal role as messenger. An apical $[Ca^{2+}]_{cyt}$ gradient is essential for tube growth (Malhó and Trewavas., 1996, Miller et al., 1992). It has been shown that the $[Ca^{2+}]_{cyt}$ at the tip oscillates with the same frequency as the pollen tube growth rate (Holdaway-Clarke et al., 1997, Messerli et al., 2000). Abolishing the Ca^{2+} gradient stops tube growth (Miller et al., 1992, Pierson et al., 1994). Proteins acting downstream of the Ca^{2+} signal during pollen germination and tube growth in Arabidopsis have already been identified. Pollen-specific CDPKs (calcium-dependent protein kinases) CPK11 and CPK24 for example are involved in Ca^{2+} -dependent regulation of inward-rectifying K^+ channels (Zhao et al., 2013). Information about channels creating the Ca^{2+} signal has improved in the last years, although it is still not complete. More precisely, CNGCs (cyclic nucleotide-gated channels), which are non-specific cation channels present in plants and animals (Kaupp and Seifert, 2002), have been reported to be indispensable for polarized tip growth of pollen and male fertility. *CNGC18*, for example, was shown to be expressed in pollen, and *cngc18* mutants showed abnormal pollen germination and tube growth, but normal seed set (Frietsch et al., 2007). *CNGC16* mutants exhibited reduced seed set and pollen viability under stress conditions, such as heat, and *cngc7 cngc8* double mutant pollen grains tend to burst instead of germinate (Tunc-Ozdemir et al., 2013a, Tunc-Ozdemir et al., 2013b, Zhao et al., 2013). All these CNGCs are plasma membrane channels. The current hypothesis therefore states that during growth of the tube towards the ovule, cNMP activates CNGCs, which by influx of Ca^{2+} over the plasma membrane contribute to create the Ca^{2+} gradient necessary for further tip growth (Frietsch et al., 2007). Experiments performed in the present study now revealed that also *drop2* and *drop3* mutants are defective in pollen

germination and tube growth. DROP2 and DROP3 are putative channels with homology to a known Ca^{2+} signal modulator. From the observed results it can therefore be concluded that the Ca^{2+} gradient needed for proper pollen tube growth might not only be established by influx from external Ca^{2+} but also from internal stores such as plastids via the action of DROP2 and DROP3. The two proteins might therein be Ca^{2+} channels themselves or, similar to MtDMI1, mediate cation fluxes leading to changes in the membrane potential, which then activates Ca^{2+} channels. To prove that these two proteins regulate $[Ca^{2+}]_{cyt}$ oscillations in pollen, $[Ca^{2+}]_{cyt}$ measurements with pollen from T-DNA mutants in comparison with wild-type pollen need to be performed in the future. For this purpose, the ratiometric Ca^{2+} reporter protein Yellow Cameleon 3.6 (YC 3.6) would be suitable. These measurements can be combined with for example removal of extracellular Ca^{2+} by chelators such as EGTA to get a closer insight into the contribution of different Ca^{2+} stores to the signal (Iwano et al., 2004, Iwano et al., 2009). Of course, an involvement of the DROPs in processes other than Ca^{2+} signalling, for example in uptake or reallocation of osmotica or nutrients during tube growth, cannot be excluded on the basis of the current data.

To determine whether the observed pollen phenotype of the mutants is related to a change in the morphology of the pollen, as has for example been observed in the Arabidopsis mutant *flp1* (*faceless pollen-1*; Ariizumi et al., 2003), pollen of the *drop2 drop3* double mutant was observed under the SEM (Fig. 17 e-h). No difference could be observed between wild type and mutant.

4.2.2 DROP2 and DROP3 are necessary for proper silique development and seed setting

During Arabidopsis reproduction, the pollen grain is transferred from the stamen onto the pistil´s stigma. Once the pollen grain sticks to the stigma, it germinates and its tube starts to elongate. Subsequently, the pollen tube grows in direction of the ovules in order to complete the process by double fertilization (Cheung, 1996, Palanivelu and Tsukamoto, 2012). After

fertilization is accomplished, a silique emerges and elongates from the gynoecium, and eventually seeds develop (Bennett et al., 2011, Ferrándiz et al., 1999).

Siliques of *drop2* and *drop3* single and double mutants exhibited a shorter length and a reduced seed set in comparison to the wild type (Figs. 18 and 19). This phenotype is similar to that of *aca9* mutants (Schiøtt et al., 2004). ACA9 (autoinhibited Ca^{2+}-ATPase 9) is a plasma membrane-localized Ca^{2+} pump, which is mainly expressed in pollen. Knock-out of *ACA9* results in a defect in pollen tube growth and this reduced pollen tube growth has been shown to be responsible for the reduced seed set of *aca9* mutants (Schiøtt et al., 2004). As has been shown in the current study, in *drop2* and *drop3* single as well as double mutants, pollen tube growth is also defective. It can therefore be assumed, that the defect in pollen tube length in the *drop* mutants is also responsible for the reduced silique length and seed set. However, in comparison with *aca9,* aborted seeds in siliques of *drop2 drop3* were distributed stochastically rather than at the lower part of the silique as in the *aca9* mutant and as would be expected when seed abortion resulted only from the fact that pollen tubes were too short to reach all ovules. Thus, in addition to pollen germination and tube growth, knock-out of *DROP2* and *DROP3* might also affect other organs or processes which influence seed setting. For example, it has been reported that the pod wall itself also contributes to seed growth and maturation. The pod wall contains a cell layer with many chloroplasts, which is photosynthetically active and delivers assimilates and nutrients to the growing seeds (Bennett et al., 2011). The result of the promoter-GUS studies showed that *PrDROP2*::GUS and *PrDROP3*::GUS were not only expressed in pollen but also in different silique stages (Fig. 7 d, h). Staining was observed in the silique wall, which could imply that DROP2 and DROP3 might contribute in a way to nutrient delivery or osmotic adjustment during seed filling, but from the data obtained here, this remains a matter of speculation. Seeds themselves did not show GUS staining, ruling out a direct influence of the female gametophyte. Nevertheless, GUS staining was observed in papilla cells of the stigma (Fig. 7 b, f). It has been shown, that in papilla cells, increases in $[Ca^{2+}]_{cyt}$ also occur during

pollination (Iwano et al., 2004). The increase can be seen after attachment of a pollen grain and in turn leads to an increase of $[Ca^{2+}]_{cyt}$ in the pollen grain, which then starts to germinate. Periodic changes in $[Ca^{2+}]_{cyt}$ in the papilla cell continue during penetration of the cell by the pollen tube and pollen tube growth (Iwano et al., 2004). According to their expression pattern, *DROPs* might therefore not only be involved in the establishment of the $[Ca^{2+}]_{cyt}$ gradient in the growing pollen tube, but also in stigmatic cells. Failure of establishment of the $[Ca^{2+}]_{cyt}$ gradient in papilla cells could lead to a reduced number of pollen grains, which start to germinate and therefore reduced number of fertilized ovules.

To clearly distinct between phenotypic effects due to aberrances of the female or the male plant organs, reciprocal crosses between the *drop2-1 drop3-1* mutant and wild-type plants need to be done in the future.

4.2.3 DROP3 is involved in root elongation, but not in gravitropism

The result of the promoter-GUS studies shows that both, *PrDROP2*::GUS and *PrDROP3*::GUS, are expressed in seedlings´ root tips (Fig. 8 e, g, i, k). Nevertheless, a slight difference can be seen between the expression patterns of the two genes (Fig. 8). *PrDROP2*::GUS is expressed in both the meristematic and the elongation zone, while *PrDROP3*::GUS is mostly expressed in the stem-cell niche of the meristematic zone. This region is the origin of cell division, and the different tissues of the root derive from here. In experiments performed in another context, root growth of a *drop2* mutant did not differ noticably from the wild type (K. Thor, unpublished). In contrast, in the present work, *drop3-1* and *drop3-2* exhibited a faster root growth over time in comparison with the wild-type, which after 19 days resulted in mutant roots that were around 1 cm longer than wild-type roots (Fig. 20). Interestingly, the stem-cell niche, where the *PrDROP3*::GUS expression was detected, also is a root region of high auxin biosynthesis and concentration, and auxin plays a major role in root growth (Garay-Arroyo et al., 2012, Nomura et al., 2012). Thus, a possible interplay between DROP3 function and auxin-mediated root growth should be further investigated. However, during root growth and

development, multiple hormones act together in a complex network. Apart from auxin these are cytokinins, gibberellins, brassinosteroids, ethylene and ABA (Garay-Arroyo et al., 2012). Thus, it may be interesting to study the involvement of DROP3 in hormonal relationships.

Another important point with relation to the enhanced root growth of *drop3-1* mutants is that in the stomatal assays, it could be shown that *drop3-1* plants had slightly larger apertures than wild type plants. In unstressed plants, stomatal aperture of *drop3-1* mutants was around 1 µm wider than that of wild type plants (Fig. 22 d). In higher plants, leaves perform photosynthesis and act as source tissues, which provide carbohydrates for transport to sink tissues such as roots (Roitsch, 1999). Larger stomatal aperture of *drop3* mutants would enhanced their ability for leaf photosynthesis and therefore their ability to translocate sugars to sink tissues. More sugar would mean more energy for the roots and therefore the ability to exhibit stronger root growth. However, the increased stomatal aperture found in the *in vitro* assays was not reflected in an increased stomatal conductance of the *drop3-1* mutant *in vivo* (Fig. 24). This discrepancy needs to be resolved by comparing plants growing side-by-side in both assays. In future studies the sugar concentration of roots should also be examined.

A root growth response with relation to plastids and Ca^{2+} is gravitropism (Fasano et al., 2000). Experiments with maize have shown that concentrations of apoplastic Ca^{2+} rise upon gravistimulation and that the curvature of roots seems to be dependent on this Ca^{2+} rise (Björkman and Cleland, 1991). Cytosolic Ca^{2+} elevations also seem to be essential for regulation of the gravireaction, and the involvement of internal Ca^{2+} stores, namely the ER, in their generation has been discussed (Pilet, 1989, Poovaiah et al., 1987, Takahashi et al., 1992). Amyloplasts found in roots have a high Ca^{2+} content (Chandra et al., 1982) and therefore could also be involved in the generation of the Ca^{2+} signal. In addition, a common hypothesis suggests that the sedimentation of amyloplasts in root cap cells is the trigger that is responsible for the subsequent root curvature (Fasano et al., 2002). Mutants of plastid proteins such as *sex1* (*starch excess 1*) are defective in the

gravitropic response (Inaba and Ito-Inaba, 2010, Vitha et al., 2007). *sex1* mutants, which exhibit a higher sensitivity to gravity, possess larger-size plastids (Vitha et al., 2007). In the current study, a gravitropism experiment was performed with the *drop3-1* mutant in order to test the hypothesis that this plastid protein might also be involved in the gravitropic response, possibly in the signalling leading from sedimentation to root curvature. *drop3-1* exhibited the same gravitropic response as the wild type (Fig. 21), thus exluding a role of DROP3 in the gravitropic signalling.

4.3 Expression patterns and roles of *DROP*s under biotic and abiotic stress conditions

4.3.1 DROP2 is involved in the flg22-induced immunity response

Flg22, which represents 22 amino acids of the conserved region of flagellin, elicits defense responses in Arabidopsis in the same manner as the full-length flagellin (Nicaise et al., 2009). Under flg22 treatment, *PrDROP2::*GUS seedlings showed a stronger blue staining compared to untreated seedlings (Fig. 13). Moreover, detached leaves of adult plants showed the same: when detached leaves were treated with flg22, *PrDROP2::*GUS expression was stronger than in untreated leaves (Fig. 14). Thus, *DROP2* expression is upregulated by flg22, indicating that *DROP2* might play a role in the plant immune response. To know more about the role of DROP2 in this response, callose deposition and stomatal aperture assays were carried out with *drop2-1* mutants. It has been reported that stomatal closure is part of the plant innate immune response to resist bacterial invasion (Melotto et al., 2006). Incubation of epidermal strips from *drop2*-1 mutants and wild type plants with flg22 did result in the same degree of stomatal closure in both lines (Fig. 22 b). DROP2 therefore is not involved in PAMP-induced stomatal closure. Experiments to detect effects of the knock-out of *DROP2* on long-term responses of stomatal conductance to flg22 did not yield unambiguous results (Fig. 23). A repetition of those experiments therefore is necessary. Due to the tight time frame, this

repetition could not be part of this thesis any more, but will be performed in the future.

Callose deposition is also part of the plant defense reaction, serving as barrier against bacterial invasion (Luna et al., 2011). In this study, callose deposition upon flg22-treatment was observed in *drop2-1* mutants and wild type plants. Aniline blue staining revealed that *drop2-1* mutants deposited less callose upon this treatment than wild type plants (Fig. 26), indicating that DROP2, although not being involved the regulation of stomatal aperture, is involved in callose deposition and therefore is part of the immune response.

Signalling events leading to defense responses in plant immunity constitute a complex network. After binding of flg22 to its receptor, a Ca^{2+} signal is generated, which can be decoded in several distinct ways, for example by the action of CDPKs (Ca^{2+}-dependent protein kinases) and MAP kinases or calmodulin, which then induce different downstream responses (Lecourieux et al., 2006). It is assumed that separate branches within the signalling network lead to different outputs (Lu et al., 2009). Many components of the signalling pathways included in the network have been identified; others and also the interplay between different paths within the network still have to be elucidated. Stomatal closure induced by flg22 is known to depend on NO production (Melotto et al., 2006). Callose deposition, on the other hand, has been reported to rely on the oxidative burst generated by apoplastic peroxidases (Daudi et al., 2012). The fact that knock-out of *DROP2* results in impairment of callose deposition, but not stomatal closure constitutes a difference to the action of the thylakoid-localized Ca^{2+}-modulator CAS. CAS is supposed to act upstream of the ROS production leading to stomatal closure during PTI, has an influence on callose deposition and also on the expression of defense genes (Nomura et al., 2012). To clearly identify the position of DROP2 in the signalling network, additional experiments, like the determination of flg22-induced ROS production or the expression of defense genes in *drop2* mutants will have to be performed. One experiment in the current study showed that callose deposition on leaves of seedlings was abolished by applying EGTA to remove extracellular Ca^{2+} (Fig. 25). This indicates that callose deposition is

dependent on Ca^{2+} influx across the plasma membrane. Stomatal closure induced by flg22 also depends on this influx. Therefore DROP2 cannot be involved in this initial Ca^{2+} signal, otherwise both reactions should have been impaired in *drop2* mutants. Taken together, the results obtained in the current study suggest that the putative ligand-gated channel and Ca^{2+} modulator DROP2 is part of the signalling network leading to plant immune response, acting downstream of the initial Ca^{2+} influx, with an influence on the signalling cascade leading to callose deposition during PTI but not on stomatal closure. Involvement of DROP2 in plant immunity is confirmed by experiments showing that *drop2* mutants accumulate higher fresh weights than wild type plants when grown in liquid culture supplemented with 1 µM flg22 (K. Thor, unpublished).

4.3.2 Is DROP3 involved in responses to drought stress?

Drought stress induces a range of physiological and biochemical responses in plants, including the closure of stomata induced by the plant hormone ABA (Acharya and Assmann, 2009). Microarray data from an experiment performed by Kilian *et al.* (2007) suggest that *DROP3* is upregulated under drought stress (Fig. 24). Kilian *et al*. (2007) exposed seedlings to a stream of air in a laminar flow hood for 15 minutes to induce the drought stress. Plants lost 10% of their fresh weight during this treatment. Performing the same assay with *PrDROP3::*GUS seedlings confirmed that *DROP3* expression is upregulated under these conditions (Fig. 15). However, the stress, which is perceived by the plants in such an experiment, might also be wind or touch rather than drought. In stomatal aperture assays, ABA-induced closure of stomata was not significantly different in *drop3-1* and *drop3-2* mutants and wild type plants (Fig. 22 c), indicating that DROP3 is not involved in this pathway. However, in those *in vitro* assays *drop3-1* mutants had higher stomatal aperture values under non-stress conditions (Fig. 22 d). In another drought stress experiment performed in this study, stomatal conductance of plants grown on soil was measured during seven days (Fig. 24). Here, stomatal conductance of *drop3-1* mutants was decreased compared to wild-type plants, but only slightly. More investigations will be needed to clearly say

if DROP3 is playing a role in regulating transpiration under drought stress. In addition, DROP3 may interfere in drought responses other than stomatal regulation, such as the transcriptional regulation of drought-responsive genes.

5. Summary

Calcium signals play an important role in many plant responses, yet the identity of many of the proteins responsible for their generation is still unknown. The current thesis deals with the characterization of a family of three potential Ca^{2+} signal modulators from *Arabidopsis thaliana* referred to as DROPs (DMI1-like RCK Domain Proteins). Confocal microscopy of transiently transformed mesophyll protoplasts revealed that the DROP1-EYFP fusion protein localizes to the ER, while DROP2-EYFP and DROP3-EYFP fusion proteins localize to chloroplasts, probably, as suggested by proteomics data, to the chloroplast envelope. As determined by analysis of microarray data and promoter-GUS studies, *DROP1* seems to be generally expressed at a very low level only. In contrast, expression of *DROP2* and *DROP3* could be detected in seedlings, roots, leaves, siliques, and flowers, particularly in stigmata and pollen. Pollen germination assays then showed that *drop2* and *drop3* knockout mutants as well as the *drop2 drop3* double mutant have a lower pollen germination rate and reduced pollen tube growth. Therefore it can be concluded that the two proteins play a role in these processes, possibly by modulating the essential Ca^{2+} gradient via influx of Ca^{2+} from plastids. Moreover, the mutants also exhibited a reduced silique length and defects in seed setting. This effect in principle could result from the reduced pollen tube growth alone, but a random distribution of aborted seeds points to an additional involvement of DROP2 and DROP3 in other processes with influence on proper silique and seed development, such as seed nutrient delivery or Ca^{2+} signals generated in stigmatic cells. The current thesis has also shown that *DROP2* is upregulated by flg22 treatment. *drop2* mutants accumulate less callose in response to flg22 than wild type plants, but do not show any difference in stomatal aperture. Thus, DROP2 could be shown to be part of the plant immune signalling pathway, probably acting downstream of the initial Ca^{2+} signal. Expression analysis and mutant phenotyping also indicate an involvement of DROP3 in root growth and possibly in acclimation to drought stress. In conclusion, the current thesis provides evidence for diverse roles of the as yet uncharacterized proteins DROP2 and DROP3 in

fertilization, root growth, and the plant immune response, and might imply a more important role of plastids in Ca^{2+} signalling as currently assumed. An important next step will now be to determine the precise function of DROP2 and DROP3 in those processes, to investigate their channel characteristics and finally to determine, if they really contribute to the generation of Ca^{2+} signals.

6. Zusammenfassung

Calcium-Signale spielen in vielen pflanzlichen Reaktionen eine wichtige Rolle. Die Identität der meisten Proteine, die an ihrer Entstehung beteiligt sind, ist jedoch noch unbekannt. Die vorliegende Arbeit befasst sich mit der Charakterisierung einer Familie von drei potentiellen Ca^{2+}-Signal-Modulatoren aus *Arabidopsis thaliana*. Diese werden hier als DROPs (DMI1-like RCK Domain Proteins) bezeichnet. Mithilfe konfokaler Mikroskopie von transient transformierten Mesophyllprotoplasten konnten DROP1-EYFP-Fusionsproteine am ER lokalisiert werden, während DROP2- und DROP3-Fusionsproteine eine chloroplastidäre Lokalisierung aufwiesen. Proteomanalysen deuten auf eine Position in der Chloroplastenhülle hin. Wie durch Analyse von Microarray-Daten und mithilfe des Promotor-GUS-Reportersystems gezeigt werden konnte, ist *DROP1* insgesamt nur sehr schwach exprimiert. Im Gegensatz dazu konnte die Expression von *DROP2* und *DROP3* in Keimlingen, Wurzeln, Blättern, Schoten und Blüten, hier besonders im Pollen und im Stigma, nachgewiesen werden. Anschließende Pollenkeimungsversuche zeigten, dass *drop2* und *drop3* Einzel- und Doppelmutanten eine geringere Pollenkeimungsrate und ein verringertes Pollenschlauchwachstum aufweisen. Daraus kann geschlossen werden, dass die beiden Proteine in diesen Prozessen eine Rolle spielen, möglicherweise indem sie durch einen Einstrom von Ca^{2+} aus Plastiden zur Regulierung des essentiellen Ca^{2+}-Gradienten beitragen. Darüber hinaus sind die Schoten der Mutanten verkürzt und zeigen Defekte in der Samenbildung. Im Prinzip könnte dies allein durch das verringerte Pollenschlauchwachstum erklärt werden. Die zufällige Verteilung der nicht entwickelten Samen innerhalb der Schoten deutet aber darauf hin, dass DROP2 und DROP3 auch noch an anderen für die Samen- und Schotenentwicklung wichtigen Prozessen beteiligt sind, z.B. der Versorgung mit Nährstoffen oder der Erzeugung von Ca^{2+}-Signalen in Zellen des Stigmas. Die vorliegende Arbeit konnte des Weiteren zeigen, dass die Expression von *DROP2* durch flg22-Behandlung hochreguliert wird und dass *drop2*-Mutanten weniger Callose als Reaktion auf flg22 akkumulieren als Wildtyppflanzen. Ihr Stomataschluss in Reaktion auf

flg22 unterscheidet sich jedoch nicht von der des Wildtyps. Somit konnte gezeigt werden, dass DROP2 Teil der Signalweiterleitung innerhalb der pflanzlichen Immunantwort ist, aber vermutlich dem ersten Ca^{2+}-Signal nachgeschaltet agiert. Die Ergebnisse der Expressionsanalyse und Phänotypisierung der Mutanten deuten außerdem darauf hin, dass DROP3 eine Rolle im Wurzelwachstum und möglicherweise auch in der Akklimation gegenüber Trockenstress spielt. Zusammenfassend liefert die vorliegende Arbeit Beweise dafür, dass die bis dahin noch nicht charakterisierten Proteine DROP2 und DROP3 in so unterschiedlichen Prozessen wie der Befruchtung, dem Wurzelwachstum und der pflanzlichen Immunantwort involviert sind, und impliziert eine möglicherweise stärkere Rolle von Plastiden in der Ca^{2+}-abhängigen Signalübertragung als bisher angenommen. Wichtige nächste Schritte sollten daher sein, die genaue Funktion von DROP2 und DROP3 in diesen Prozessen zu bestimmen, ihre Kanaleigenschaften zu untersuchen und zu klären, ob sie tatsächlich an der Entstehung von Ca^{2+}-Signalen mitwirken.

7. References

Abel,S. and Theologis,A. (1994) Transient transformation of Arabidopsis leaf protoplasts: a versatile experimental system to study gene expression. The Plant Journal **5**:421-427.

Acharya,B.R. and Assmann,S.M. (2009) Hormone interactions in stomatal function. Plant Molecular Biology **69**:451-462.

Ali,R., Ma,W., Lemtiri-Chlieh,F., Tsaltas,D., Leng,Q., von Bodman,S., and Berkowitz,G.A. (2007) Death don't have no mercy and neither does calcium: Arabidopsis CYCLIC NUCLEOTIDE GATED CHANNEL2 and innate immunity. The Plant Cell **19**:1081-1095.

Ané,J.M., Kiss,G.B., Riely,B.K., Penmentsa,R.V., Oldroyd,G.E.D., Ayax,C.A., Debellé F., Baek,J.M., Kalo,P., Rosenberg,C., Roe,B.A., Long,S.R., Denarie,J., and Cook,D.R. (2004) *Medicago truncatula* DMI1 required for bacterial and fungal symbioses in Legumes. Science **303**:1364-1367.

Arabidopsis Genome Initiative (2000) Analysis of the genome sequence of the flowering plant *Arabidopsis thaliana*. Nature **408**:796.

Ariizumi,T., Hatakeyama,K., Hinata,K., Sato,S., Kato,T., Tabata,S., and Toriyama,K. (2003) A novel male-sterile mutant of *Arabidopsis thaliana*, faceless pollen-1, produces pollen with a smooth surface and an acetolysis-sensitive exine. Plant Molecular Biology **53**:107-116.

Bennett,E.J., Roberts,J.A., and Wagstaff,C. (2011) The role of the pod in seed development: strategies for manipulating yield. New Phytologist **190**:838-853.

Bevan,M. (1984) Binary Agrobacterium vectors for plant transformation. Nucleic Acids Research **12**:8711-8721.

Bevan,M.W., Flavell,R.B., and Chilton,M.D. (1983) A chimaeric antibiotic resistance gene as a selectable marker for plant cell transformation. Nature **304**:184-187.

Björkman,T. and Cleland,R.E. (1991) The role of extracellular free-calcium gradients in gravitropic signalling in maize roots. Planta **185**:379**-**384.

References

Boller,T. and Felix,G. (2009) A renaissance of elicitors: perception of microbe-associated molecular patterns and danger signals by pattern-recognition receptors. Annual Review of Plant Biology. **60**:379-406.

Bölter,B., Soll,J.r., Hill,K., Hemmler,R., and Wagner,R. (1999) A rectifying ATP-regulated solute channel in the chloroplastic outer envelope from pea. The EMBO Journal **18**:5505-5516.

Bölter,B. and Soll,J. (2001) Ion channels in the outer membranes of chloroplasts and mitochondria: open doors or regulated gates? The EMBO Journal **20**:935-940.

Boudsocq,M. and Sheen,J. (2010) Stress signaling II: calcium sensing and signaling. In Abiotic Stress Adaptation in Plants, Springer Netherlands: pp. 75-90.

Bray,E.A., Bailey-Serres,J., and Weretilnyk,E. (2000) Responses to abiotic stress. In Biochemistry and Molecular Biology of Plants, B.B.Buchanan, W.Gruissem, and R.L.Jones, eds. American Society of Plant Physiologists Rockville: pp. 1158-1203.

Brown,I., Trethowan,J., Kerry,M., Mansfield,J., and Bolwell,G.P. (1998) Localization of components of the oxidative cross-linking of glycoproteins and of callose synthesis in papillae formed during the interaction between non-pathogenic strains of *Xanthomonas campestris* and French bean mesophyll cells. The Plant Journal **15**:333-343.

Capoen,W., Sun,J., Wysham,D., Otegui,M.S., Venkateshwaran,M., Hirsch,S., Miwa,H., Downie,J.A., Morris,R.J., and Ané,J.M. (2011) Nuclear membranes control symbiotic calcium signaling of legumes. Proceedings of the National Academy of Sciences, USA **108**:14348-14353.

Catoira,R., Galera,C., de Billy,F., Penmetsa,R.V., Journet,E.P., Maillet,F., Rosenberg,C., Cook,D., Gough,C., and Dénarié,J. (2000) Four genes of *Medicago truncatula* controlling components of a Nod factor transduction pathway. The Plant Cell **12**:1647-1665.

Chakrapani,S. and Perozo,E. (2007) How to gate an ion channel: lessons from MthK. Nature Structural & Molecular Biology **14**:180-182.

References

Chandra,S., Chabot,J.F., Morrison,G.H., and Leopold,A.C. (1982) Localization of calcium in amyloplasts of root-cap cells using ion microscopy. Science **216**:1221-1223.

Charles,S.A. and Halliwell,B. (1980) Action of calcium ions on spinach (Spinacia oleracea) chloroplast fructose bisphosphatase and other enzymes of the Calvin cycle. Biochemical Journal **188**:775-779.

Charpentier,M., Bredemeier,R., Wanner,G., Takeda,N., Schleiff,E., and Parniske,M. (2008) *Lotus japonicus* CASTOR and POLLUX are ion channels essential for perinuclear calcium spiking in Legume root endosymbiosis. The Plant Cell **20**:3467-3479.

Charpentier,M., Martins,T.V., Granqvist,E., Oldroyd,G., and Morris,R. (2013) The role of DMI1 in establishing Ca^{2+} oscillations in legume symbioses. Plant Signaling & Behavior **8**:e22894.

Chen,C., Fan,C., Gao,M., and Zhu,H. (2009) Antiquity and function of CASTOR and POLLUX, the twin ion channel-encoding genes key to the evolution of root symbioses in plants. Plant Physiology **149**:306-317.

Cheung,A.Y. (1996) Pollen pistil interactions during pollen-tube growth. Trends in Plant Science **1**:45-51.

Clough,S.J. and Bent,A.F. (1998) Floral dip: a simplified method for Agrobacterium-mediated transformation of *Arabidopsis thaliana*. The Plant Journal **16**:735-743.

Daudi,A., Cheng,Z., O´Brien,J.A., Mammarella,N., Khan,S., Ausubel,F.M., and Bolwell,G.P. (2012) The apoplastic oxidative burst peroxidase in Arabidopsis is a major component of pattern-triggered immunity. The Plant Cell **24**:275-287.

Dreger,M. (2003) Subcellular proteomics. Mass Spectrom Reviews **22**:27-56.

Edwards,A., Heckmann,A.B., Yousafzai,F., Duc,G., and Downie,J.A. (2007) Structural implications of mutations in the pea SYM8 symbiosis gene, the DMI1 ortholog, encoding a predicted ion channel. Molecular Plant-Microbe Interactions **20**:1183-1191.

Farquhar,G.D. and Sharkey,T.D. (1982). Stomatal conductance and photosynthesis. Annual Review of Plant Physiology **33**:317-345.

Fasano,J.M., Massa,G.D., and Gilroy,S. (2002) Ionic signaling in plant responses to gravity and touch. Journal of Plant Growth Regulation **21**:71-88.

Feijó,J.A., Malhó,R., and Obermeyer,G. (1995) Ion dynamics and its possible role during in vitro pollen germination and tube growth. Protoplasma **187**:155-167.

Felix,G., Duran,J.D., Volko,S., and Boller,T. (1999) Plants have a sensitive perception system for the most conserved domain of bacterial flagellin. The Plant Journal **18**:265-276.

Ferrándiz,C., Pelaz,S., and Yanofsky,M.F. (1999) Control of carpel and fruit development in Arabidopsis. Annual Review of Biochemistry **68**:321-354.

Ferro,M., Salvi,D., Brugière,S., Miras,S.p., Kowalski,S.n., Louwagie,M., Garin,J., Joyard,J., and Rolland,N. (2003) Proteomics of the chloroplast envelope membranes from *Arabidopsis thaliana*. Molecular & Cellular Proteomics **2**:325-345.

Ferro,M., Brugière,S., Salvi,D., Seigneurin-Berny,D., Moyet,L., Ramus,C., Miras,S.p., Mellal,M., Le Gall,S., and Kieffer-Jaquinod,S. (2010) AT_CHLORO, a comprehensive chloroplast proteome database with subplastidial localization and curated information on envelope proteins. Molecular & Cellular Proteomics **9**:1063-1084.

Footitt,S., Dietrich,D., Fait,A., Fernie,A.R., Holdsworth,M.J., Baker,A., and Theodoulou,F.L. (2007) The COMATOSE ATP-Binding cassette transporter is required for full fertility in Arabidopsis. Plant Physiology **144**:1467-1480.

Frietsch,S., Wang,Y.F., Sladek,C., Poulsen,L.R., Romanowsky,S.M., Schroeder,J.I., and Harper,J.F. (2007) A cyclic nucleotide-gated channel is essential for polarized tip growth of pollen. Proceedings of the National Academy of Sciences, USA **104**:14531-14536.

Froehlich,J.E., Wilkerson,C.G., Ray,W.K., McAndrew,R.S., Osteryoung,K.W., Gage,D.A., and Phinney,B.S. (2003) Proteomic study of the *Arabidopsis thaliana* chloroplastic envelope membrane utilizing alternatives to traditional two-dimensional electrophoresis. Journal Proteome Research **2**:413-425.

Fujiwara,M.T., Hashimoto,H., Kazama,Y., Hirano,T., Yoshioka,Y., Aoki,S., Sato,N., Itoh,R.D., and Abe,T. (2010) Dynamic morphologies of pollen plastids visualised by vegetative-specific FtsZ1-GFP in *Arabidopsis thaliana.* Protoplasma **242**:19-33.

Garay-Arroyo,A., Sánchez, M.D.L.P., García-Ponce,B., Azpeitia,E., and Álvarez-Buylla,E.R. (2012) Hormone symphony during root growth and development. Developmental. Dynamics. **241**:1867-1885.

Gleave,A. (1992) A versatile binary vector system with a T-DNA organisational structure conducive to efficient integration of cloned DNA into the plant genome. Plant Molecular Biology **20**:1203-1207.

Gómez-Gómez,L. and Boller,T. (2000) FLS2: an LRR receptor-like kinase involved in the perception of the bacterial elicitor flagellin in Arabidopsis. Molecular Cell **5**:1003-1011.

Gómez-Gómez,L., Felix,G., and Boller,T. (1999) A single locus determines sensitivity to bacterial flagellin in *Arabidopsis thaliana*. The Plant Journal **18**:277-284.

Grant,M., Brown,I., Adams,S., Knight,M., Ainslie,A., and Mansfield,J. (2000) The RPM1 plant disease resistance gene facilitates a rapid and sustained increase in cytosolic calcium that is necessary for the oxidative burst and hypersensitive cell death. The Plant Journal **23**:441-450.

Han,S., Tang,R., Anderson,L.K., Woerner,T.E., and Pei,Z.M. (2003) A cell surface receptor mediates extracellular Ca^{2+} sensing in guard cells. Nature **425**:196-200.

Hepler,P.K. (2005) Calcium: A central regulator of plant growth and development. The Plant Cell **17**:2142-2155.

Hetherington,A.M. and Woodward,F.I. (2003). The role of stomata in sensing and driving environmental change. Nature **424**:901-908.

Hirsch,S., Kim,J., Muñoz,A., Heckmann,A.B., Downie,J.A., and Oldroyd,G.E. (2009) GRAS proteins form a DNA binding complex to induce gene expression during nodulation signaling in *Medicago truncatula*. The Plant Cell **21**:545-557.

Holdaway-Clarke,T.L., Feijó,J.A., Hackett,G.R., Kunkel,J.G., and Hepler,P.K. (1997) Pollen tube growth and the intracellular cytosolic

calcium gradient oscillate in phase while extracellular calcium influx is delayed. The Plant Cell **9**:1999-2010.

Hruz,T., Laule,O., Szabo,G., Wessendorp,F., Bleuler,S., Oertle,L., Widmayer,P., Gruissem,W., and Zimmermann,P. (2008) Genevestigator V3: a reference expression database for the meta-analysis of transcriptomes. Advances in Bioinformatics **2008**:420747.

Imaizumi-Anraku,H., Takeda,N., Charpentier,M., Perry,J., Miwa,H., Umehara,Y., Kouchi,H., Murakami,Y., Mulder,L., Vickers,K., Pike,J., Downie,J.A., Wang,T., Sato,S., Asamizu,E., Tabata,S., Yoshikawa,M., Murooka,Y., Wu,G.J., Kawaguchi,M., Kawasaki,S., Parniske,M., and Hayashi,M. (2005) Plastid proteins crucial for symbiotic fungal and bacterial entry into plant roots. Nature **433**:527-531.

Inaba,T. and Ito-Inaba,Y. (2010) Versatile roles of plastids in plant growth and development. Plant and Cell Physiology **51**:1847-1853.

Inoue,K. (2007) The chloroplast outer envelope membrane: the edge of light and excitement. Journal of Integrative Plant Biology **49**:1100-1111.

Irish,V.F. (2010) The flowering of Arabidopsis flower development. The Plant Journal **61**:1014-1028.

Iwano,M., Entani,T., Shiba,H., Kakita,M., Nagai,T., Mizuno,H., Miyawaki,A., Shoji,T., Kubo,K., Isogai,A., and Takayama,S. (2009) Fine-tuning of the cytoplasmic Ca^{2+} concentration is essential for pollen tube growth. Plant Physiology **150**:1322-1334.

Iwano,M., Shiba,H., Miwa,T., Che,F.S., Takayama,S., Nagai,T., Miyawaki,A., and Isogai,A. (2004) Ca^{2+} dynamics in a pollen grain and papilla cell during pollination of Arabidopsis. Plant Physiology **136**:3562-3571.

Jakab,G., Ton,J., Flors,V., Zimmerli,L., Métraux,J.P., and Mauch-Mani,B. (2005) Enhancing Arabidopsis salt and drought stress tolerance by chemical priming for its abscisic acid responses. Plant Physiology **139**:267-274.

Jammes,F., Hu,H.C., Villiers,F., Bouten,R., and Kwak,J.M. (2011) Calcium-permeable channels in plant cells. FEBS Journal **278**:4262-4276.

Jefferson,R.A., Burgess,S.M., and Hirsh,D. (1986) beta-Glucuronidase from Escherichia coli as a gene-fusion marker. Proceedings of the National Academy of Sciences, USA **83**:8447-8451.

Johnson,C.H., Knight,M.R., Kondo,T., Masson,P., Sedbrook,J., Haley,A., and Trewavas,A. (1995) Circadian oscillations of cytosolic and chloroplastic free calcium in plants. Science **269**:1863-1865.

Jiang,Y., Lee,A., Chen,J., Cadene,M., Chait,B.T., and MacKinnon,R. (2002) The open pore conformation of potassium channels. Nature **417**:523-526

Jones,J.D. and Dangl,J.L. (2006) The plant immune system. Nature **444**:323-329.

Jung,E., Heller,M., Sanchez,J.C., and Hochstrasser,D.F. (2000) Proteomics meets cell biology: the establishment of subcellular proteomes. Electrophoresis **21**:3369-3377.

Kaupp,U.B. and Seifert,R. (2002) Cyclic nucleotide-gated ion channels. Physiological Reviews **82**:769-824.

Kerppola,T.K. (2006) Design and implementation of bimolecular fluorescence complementation (BiFC) assays for the visualization of protein interactions in living cells. Nature **1**:1278-1286.

Kilian,J., Whitehead,D., Horak,J., Wanke,D., Weinl,S., Batistic,O., D´A ngelo,C., Bornberg-Bauer,E., Kudla,J., and Harter,K. (2007) The AtGenExpress global stress expression data set: protocols, evaluation and model data analysis of UV-B light, drought and cold stress responses. The Plant Journal **50**:347-363.

Kim,T.H., Böhmer,M., Hu,H., Nishimura,N., and Schroeder,J.I. (2010) Guard cell signal transduction network: advances in understanding abscisic acid, CO_2, and Ca^{2+} signaling. Annual Review of Plant Biology **61**:561-591.

Knight,H., Trewavas,A.J., and Knight,M.R. (1997) Calcium signalling in *Arabidopsis thaliana* responding to drought and salinity. The Plant Journal **12**:1067-1078.

Knight,M.R., Campbell,A.K., Smith,S.M., and Trewavas,A.J. (1991) Transgenic plant aequorin reports the effects of touch and cold-shock and elicitors on cytoplasmic calcium. Nature **352**: 524-526.

Kreimer,G., Melkonian,M., Holtum,J.A.M., and Latzko,E. (1985) Characterization of calcium fluxes across the envelope of intact spinach chloroplasts. Planta **166**:515-523.

Kudla,J., Batistič,O., and Hashimoto,K. (2010) Calcium signals: the lead currency of plant information processing. The Plant Cell **22**:541-563.

Kwak,J.M., Mäser,P., and Schroeder,J.I. (2008) The clickable guard cell, version II: interactive model of guard cell signal transduction mechanisms and pathways. The Arabidopsis Book/American Society of Plant Biologists **6**:e0114.

Lecourieux,D., Mazars,C., Pauly,N., Ranjeva,R., and Pugin,A. (2002) Analysis and effects of cytosolic free calcium increases in response to elicitors in Nicotiana plumbaginifolia cells. The Plant Cell **14**:2627-2641.

Lecourieux,D., Ranjeva,R., and Pugin,A. (2006) Calcium in plant defence-signalling pathways. New Phytologist **171**:249-269.

Lee,J.S., Mulkey,T.J., and Evans,M.L. (1983) Reversible loss of gravitropic sensitivity in maize roots after tip application of calcium chelators. Science **220**:1375-1376.

Levy,J., Bres,C., Geurts,R., Chalhoub,B., Kulikova,O., Duc,G., Journet,E.P., Ane,J.M., Lauber,E., Bisseling,T., Denarie,J., Rosenberg,C., and Debelle,F. (2004) A putative Ca^{2+} and calmodulin-dependent protein kinase required for bacterial and fungal symbioses. Science **303**:1361-1364.

Limpens,E., Franken,C., Smit,P., Willemse,J., Bisseling,T., and Geurts,R. (2003) LysM domain receptor kinases regulating rhizobial Nod factor-induced infection. Science **302**:630-633.

Logemann,E., Birkenbihl,R., Ulker,B., and Somssich,I. (2006) An improved method for preparing Agrobacterium cells that simplifies the Arabidopsis transformation protocol. Plant Methods **2**:16.

Lu,X., Tintor,N., Mentzel,T., Kombrink,E., Boller,T., Robatzek,S., Schulze-Lefert,P., and Saijo,Y. (2009) Uncoupling of sustained MAMP receptor signaling from early outputs in an Arabidopsis endoplasmic reticulum glucosidase II allele. Proceedings of the National Academy of Sciences, USA **106**:22522-22527.

Luna,E., Pastor,V., Robert,J., Flors,V., Mauch-Mani,B., and Ton,J. (2011) Callose deposition: a multifaceted plant defense response. Molecular Plant-Microbe Interactions **24**:183-193.

Ma,Y. and Berkowitz,G.A. (2012) Biotic Stress Signalling: Calcium-Mediated Pathogen Defence Programmes. In Plant Stress Physiology, S.Shabala, ed CABI: pp. 291-309.

Madsen,E.B., Madsen,L.H., Radutoiu,S., Olbryt,M., Rakwalska,M., Szczyglowski,K., Sato,S., Kaneko,T., Tabata,S., Sandal,N. and Stougaard,J. (2003) A receptor kinase gene of the LysM type is involved in legumeperception of rhizobial signals. Nature **425**:637-640.

Malhó,R., Read,N.D., Pais,M.S., and Trewavas,A.J. (1994) Role of cytosolic free calcium in the reorientation of pollen tube growth. The Plant Journal **5**:331-341.

Malhó,R. and Trewavas,A.J. (1996) Localized apical increases of cytosolic free calcium control pollen tube orientation. The Plant Cell **8**:1935-1949.

McAinsh,M.R. and Hetherington,A.M. (1998) Encoding specificity in Ca^{2+} signalling systems. Trends in Plant Science **3**:32-36.

McAinsh,M.R. and Pittman,J.K. (2009) Shaping the calcium signature. New Phytologist **181**:275-294.

Meinke,D.W., Cherry,J.M., Dean,C., Rounsley,S.D., and Koornneef,M. (1998) *Arabidopsis thaliana*: A model plant for genome analysis. Science **282**:662-682.

Melotto,M., Underwood,W., Koczan,J., Nomura,K., and He,S.Y. (2006) Plant stomata function in innate immunity against bacterial invasion. Cell **126**:969-980.

Messerli,M.A., Créton,R., Jaffe,L.F., and Robinson,K.R. (2000) Periodic increases in elongation rate precede increases in cytosolic Ca^{2+} during pollen tube growth. Developmental Biology **222**:84-98.

Miller,D.D., Callahm,D.A., Gross,D.J., and Hepler,P.K. (1992) Free Ca^{2+} gradient in growing pollen tubes of Lillium. Journal of Cell Science **101**:7-12.

Mitra,R.M., Gleason,C.A., Edwards,A., Hadfield,J., Downie,J.A., Oldroyd,G.E., and Long,S.R. (2004) A Ca^{2+}/calmodulin-dependent

protein kinase required for symbiotic nodule development: gene identification by transcript-based cloning. Science **101**:4701-4705.

Monshausen,G.B., Bibikova,T.N., Messerli,M.A., Shi,C., and Gilroy,S. (2007) Oscillations in extracellular pH and reactive oxygen species modulate tip growth of Arabidopsis root hairs. Proceedings of the National Academy of Sciences, USA **104**:20996-21001.

Mott,K.A., Gibson,A.C., and O'Leary,J.W. (1982) The adaptive significance of amphistomatic leaves. Plant, Cell & Environment **5**:455-460.

Muthamilarasan,M. and Prasad,M. (2013) Plant innate immunity: An updated insight into defense mechanisms. Journal of Biosciences **38**:1-17.

Newman,M.A., Sundelin,T., Nielsen,J.T., and Erbs,G. (2013) MAMP (microbe-associated molecular pattern) triggered immunity in plants. Frontiers in Plant Science **4**:139.

Nicaise,V., Roux,M., and Zipfel,C. (2009) Recent advances in PAMP-triggered immunity against bacteria: pattern recognition receptors watch over and raise the alarm. Plant Physiology **150**:1638-1647.

Nomura,H., Komori,T., Kobori,M., Nakahira,Y., and Shiina,T. (2008) Evidence for chloroplast control of external Ca^{2+}-induced cytosolic Ca^{2+} transients and stomatal closure. The Plant Journal **53**:988-998.

Nomura,H., Komori,T., Uemura,S., Kanda,Y., Shimotani,K., Nakai,K., Furuichi,T., Takebayashi,K., Sugimoto,T., and Sano,S. (2012) Chloroplast-mediated activation of plant immune signalling in *Arabidopsis*. Nature Communications **3**:926.

Oláh,B., Briére,C., Béard,G., Dénarié,J., and Gough,C. (2005) Nod factors and a diffusible factor from arbuscular mycorrhizal fungi stimulate lateral root formation in *Medicago truncatula* via the DMI1/DMI2 signalling pathway. The Plant Journal **44**:195-207.

Oldroyd,G.E.D. (2013) Speak, friend, and enter: signalling systems that promote beneficial symbiotic associations in plants. Nature Reviews Microbiology **11**:252-263.

Oldroyd,G.E.D. and Downie,J.A. (2008) Coordinating nodule morphogenesis with rhizobial infection in Legumes. Annual Review of Plant Biology **59**:519-546.

Overvoorde,P., Fukaki,H., and Beeckman,T. (2010). Auxin control of root development. Cold Spring Harbor Perspectives in Biology **2** (6).

Palanivelu,R. and Tsukamoto,T. (2012) Pathfinding in angiosperm reproduction: pollen tube guidance by pistils ensures successful double fertilization. Wiley Interdisciplinary Reviews: Developmental Biology **1**:96-113.

Palmer,E. and Freeman,T. (2004) Investigation into the use of C-and N-terminal GFP fusion proteins for subcellular localization studies using reverse transfection microarrays. Comparative and Functional Genomics **5**:342-353.

Pau,V.P., Smith,F.J., Taylor,A.B., Parfenova,L.V., Samakai,E., Callaghan,M.M., Abarca-Heidemann,K., Hart,P.J., and Rothberg,B.S. (2011) Structure and function of multiple Ca^{2+}-binding sites in a K^+ channel regulator of K^+ conductance (RCK) domain. Proceedings of the National Academy of Sciences, USA **108**:17684-17689.

Peiter,E., Maathuis,F.J.M., Mills,L.N., Knight,H., Pelloux,J., Hetherington,A.M., and Sanders,D. (2005) The vacuolar Ca^{2+}-activated channel TPC1 regulates germination and stomatal movement. Nature **434**:404-408.

Peiter,E., Sun,J., Heckmann,A.B., Venkateshwaran,M., Riely,B., Otegui,M.S., Edwards,A., Freshour,G., Hahn,M.G., Cook,D.R., Sanders,D., Oldroyd,G.E.D., Downie,J.A., and Ané,J.M. (2007) The *Medicago truncatula* DMI1protein modulates cytosolic calcium signaling. Plant Physiology **145**:192-203.

Peiter,E. (2011) The plant vacuole: Emitter and receiver of calcium signals. Cell Calcium **50**:120-128.

Pierson,E.S., Miller,D.D., Callaham,D.A., Van Aken,J., Hackett,G., and Hepler,P.K. (1996) Tip-localized calcium entry fluctuates during pollen tube growth. Developmental Biology **174**:160-173.

Pierson,E.S., Miller,D.D., Callaham,D.A., Shipley,A.M., Rivers,B.A., Cresti,M., and Hepler,P.K. (1994) Pollen tube growth is coupled to the extracellular calcium ion flux and the intracellular calcium gradient: effect of BAPTA-type buffers and hypertonic media. The Plant Cell **6**:1815-1828.

Pilet,P.E. (1989) Differential growth and hormone redistribution in gravireacting maize roots. Environmental and Experimental Botany **29**:37-45.

Platt, A. R., Woodhall, R. W., and George, A. L. (2007) Improved DNA sequencing quality and efficiency using an optimized fast cycle sequencing protocol. Biotechniques **43**(1):58.

Plieth,C., Hansen,U.P., Knight,H., and Knight,M.R. (1999) Temperature sensing by plants: the primary characteristics of signal perception and calcium response. The Plant Journal **18**:491-497.

Plieth,C. and Trewavas,A.J. (2002) Reorientation of seedlings in the earth's gravitational field induces cytosolic calcium transients. Plant Physiology **129**:786-796.

Poovaiah,B.W., McFadden,J.J., and Reddy,A.S.N. (1987) The role of calcium ions in gravity signal perception and transduction. Physiologia Plantarum **71**:401-407.

Portis Jr,A.R. and Heldt,H.W. (1976) Light-dependent changes of the Mg^{2+} concentration in the stroma in relation to the Mg^{2+} dependency of CO_2 fixation in intact chloroplasts. Biochimica et Biophysica **449**:434-446.

Punta,M., Coggill,P.C., Eberhardt,R.Y., Mistry,J., Tate,J., Boursnell,C., Pang,N., Forslund,K., Ceric,G., and Clements,J. (2012) The Pfam protein families database. Nucleic Acids Research **40**:290-301.

Qi,Z., Stephens,N.R., and Spalding,E.P. (2006) Calcium entry mediated by GLR3.3, an Arabidopsis glutamate receptor with a broad agonist profile. Plant Physiology **142**:963-971.

Radutoiu,S., Madsen,L.H., Madsen,E.B.r., Felle,H.H., Umehara,Y., Grønlund,M., Sato,S., Nakamura,Y., Tabata,S., and Sandal,N. (2003) Plant recognition of symbiotic bacteria requires two LysM receptor-like kinases. Nature **425**:585-592.

Ranf,S., Eschen-Lippold,L., Pecher,P., Lee,J., and Scheel,D. (2011) Interplay between calcium signalling and early signalling elements during defence responses to microbe- or damage-associated molecular patterns. The Plant Journal **68**:100-113.

Reski,R. (1998) Physcomitrella and Arabidopsis: the David and Goliath of reverse genetics. Trends in Plant Science **3**:209-210.

Riely,B.K., Lougnon,G., Ané,J.M., and Cook,D.R. (2007) The symbiotic ion channel homolog DMI1 is localized in the nuclear membrane of *Medicago truncatula* roots. The Plant Journal **49**:208-216.

Roitsch,T. (1999) Source-sink regulation by sugar and stress. Current Opinion in Plant Biology **2**:198-206.

Rounds,C.M., Winship,L.J., and Hepler,P.K. (2011) Pollen tube energetics: respiration, fermentation and the race to the ovule. AoB Plants **2011**:plr019. doi:10.1093/aobpla/plr019.

Sai,J. and Johnson,C.H. (2002) Dark-stimulated calcium ion fluxes in the chloroplast stroma and cytosol. The Plant Cell **14**:1279-1291.

Salinas,J. and Sanchez-Serrano,J.J. (2006) Arabidopsis protocols. Methods in Molecular Biology 323. Humana Press, Springer.

Sanger,F., Nicklen,S., and Coulson,A.R. (1977) DNA sequencing with chain-terminating inhibitors. Proceedings of the National Academy of Sciences, USA **74**:5463-5467.

Schiøtt,M., Romanowsky,S.M., Baekgaard,L., Jakobsen,M.K., Palmgren,M.G., and Harper,J. (2004) A plant plasma membrane Ca^{2+} pump is required for normal pollen tube growth. Proceeding National Academy Sciences, USA **101**:9502-9507.

Schroeder,J.I. and Keller,B.U. (1992) Two types of anion channel currents in guard cells with distinct voltage regulation. Proceedings of the National Academy of Sciences, USA **89**:5025-5029.

Schroeder,J.I., Kwak,J.M., and Allen,G.J. (2001). Guard cell abscisic acid signalling and engineering drought hardiness in plants. Nature **410**:327-330.

Schwacke,R., Schneider,A., van der Graaff,E., Fischer,K., Catoni,E., Desimone,M., Frommer,W.B., Flügge,U.I., and Kunze,R. (2003) ARAMEMNON, a novel database for Arabidopsis integral membrane proteins. Plant Physiology **131**:16-26.

Smyth,D.R., Bowman,J.L., and Meyerowitz,E.M. (1990). Early flower development in Arabidopsis. The Plant Cell **2**:755-767.

Subbaiah,C.C., Bush,D.S., and Sachs,M.M. (1998) Mitochondrial contribution to the anoxic Ca^{2+} signal in maize suspension-cultured cells. Plant Physiology **118**:759-771.

Takahashi,H., Scott,T.K., and Suge,H. (1992) Stimulation of root elongation and curvature by calcium. Plant Physiology **98**:246-252.

Tamura,K., Dudley,J., Nei,M., and Kumar,S. (2007) MEGA4: molecular evolutionary genetics analysis (MEGA) software version 4.0. Molecular Biology and Evolution **24**:1596-1599.

Tang,L.Y., Nagata,N., Matsushima,R., Chen,Y., Yoshioka,Y., and Sakamoto,W. (2009) Visualization of plastids in pollen grains: involvement of FtsZ1 in pollen plastid division. Plant and Cell Physiology **50**:904-908.

Tunc-Ozdemir,M., Rato,C., Brown,E., Rogers,S., Mooneyham,A., Frietsch,S., Myers,C.T., Poulsen,L.R., Malhó,R., and Harper,J.F. (2013a) Cyclic nucleotide gated channels 7 and 8 are essential for male reproductive fertility. PloS One **8**:e55277.

Tunc-Ozdemir,M., Tang,C., Ishka,M.R., Brown,E., Groves,N.R., Myers,C.T., Rato,C., Poulsen,L.R., McDowell,S., Miller,G., Mittler,R., and Harper,J.F. (2013b) A cyclic nucleotide-gated channel (CNGC16) in pollen is critical for stress tolerance in pollen reproductive development. Plant Physiology **161**:1010-1020.

Umezawa,T., Nakashima,K., Miyakawa,T., Kuromori,T., Tanokura,M., Shinozaki,K., and Yamaguchi-Shinozaki,K. (2010) Molecular basis of the core regulatory network in ABA responses: sensing, signaling and transport. Plant and Cell Physiology **51**:1821-1839.

Vainonen,J.P., Sakuragi,Y., Stael,S., Tikkanen,M., Allahverdiyeva,Y., Paakkarinen,V., Aro,E., Suorsa,M., Scheller,H.V., and Vener,A.V. (2008) Light regulation of CaS, a novel phosphoprotein in the thylakoid membrane of *Arabidopsis thaliana*. FEBS Journal **275**:1767-1777.

Venkateshwaran,M., Cosme,A., Han,L., Banba,M., Satyshur,K.A., Schleiff,E., Parniske,M., Imaizumi-Anraku,H., and Ané,J.M. (2012) The recent evolution of a symbiotic ion channel in the legume family altered ion conductance and improved functionality in calcium signaling. The Plant Cell **24**:2528-2545.

Vitha,S., Yang,M., Sack,F.D., and Kiss,J.Z. (2007) Gravitropism in the starch excess mutant of *Arabidopsis thaliana*. American Journal of Botany **94**:590-598.

References

Vothknecht,U.C. and Soll,J. (2005) Chloroplast membrane transport: Interplay of prokaryotic and eukaryotic traits. Gene **354**:99-109.

Weinl,S., Held,K., Schlücking,K., Steinhorst,L., Kuhlgert,S., Hippler,M., and Kudla,J. (2008) A plastid protein crucial for Ca^{2+}-regulated stomatal responses. New Phytologist **179**:675-686.

Winter,D., Vinegar,B., Nahal,H., Ammar,R., Wilson,G.V., and Provart,N.J. (2007) An electronic fluorescent pictograph browser for exploring and analyzing large-scale biological data sets. PLoS One **2**:e718.

White,P.J. and Broadley,M.R. (2003) Calcium in Plants. Annals of Botany **92**:487-511.

Wyatt,S.E., Tsou,P.L., and Robertson,D. (2002) Expression of the high capacity calcium-binding domain of calreticulin increases bioavailable calcium stores in plants. Transgenic Research **11**:1-10.

Young,J.J., Mehta,S., Israelsson,M., Godoski,J., Grill,E., and Schroeder,J.I. (2006) CO_2 signaling in guard cells: calcium sensitivity response modulation, a Ca^{2+}-independent phase, and CO_2 insensitivity of the *gca2* mutant. Proceedings of the National Academy of Sciences, USA **103**:7506-7511.

Zhao,L.N., Shen,L.K., Zhang,W.Z., Zhang,W., Wang,Y., and Wu,W.H. (2013) Ca^{2+}dependent protein kinase11 and 24 modulate the activity of the inward rectifying K^+ channels in Arabidopsis pollen tubes. The Plant Cell **25**:649-661.

Zimmermann,P., Hirsch-Hoffmann,M., Hennig,L., and Gruissem,W. (2004) GENEVESTIGATOR. Arabidopsis microarray database and analysis toolbox. Plant Physiology **136**:2621-2632.

Zipfel,C., Robatzek,S., Navarro,L., Oakeley,E.J., Jones,J.D., Felix,G., and Boller,T. (2004) Bacterial disease resistance in Arabidopsis through flagellin perception. Nature **428**:764-767.

8. Appendix

Table S 1. Primers used for sequencing of EYFP fusion constructs

Primer name	Sequence (5'->3')	Binds in
pART7-MCS_F	CAATCCCACTATCCTTCGCAAGA	pART7
DMI1-CO2-RP	CCGAATCCGCTACAAAAGT	*DROP1*
DMI1_259_RP	GGTTGAAGAGCGCATTGTATC	*DROP1*
DMI1-135_RP	TGTGGTTGTGTTAGCAGAACG	*DROP1*
DMI1fw1	ACTAGCTTATTCGTTGGATGTG	*DROP1*
DMI1_seq_FW	GGTTCCAGATCAAGAAAGAGAGA	*DROP1*
DMI2_seq_RV	TGCCAATGTTCTTCTCAAGC	*DROP2*
DMI2-200-RP	TTCCTTGGAGTATCGGACATG	*DROP2*
DMI2_E05_RP	GCTTGAGAAGAACATTGGCAC	*DROP2*
DMI2fw2	TCCGCTTAGGTACCGCCACAG	*DROP2*
DMI2fw3	TTGTTTGTCCAATGCTCACG	*DROP2*
DMI2fw4	TCATATCGGATCGTGACTGG	*DROP2*
DMI3_415_LP	CTAGGACTTGCATATGTGCCC	*DROP3*
DMI3_415_RP	AGGACAGGAGATACAGAGCCG	*DROP3*
DMI3_095_LP	CGTACGCCAAAGATTTTGATC	*DROP3*
DMI3fw1	TGTGGGATTTTAAGAGATGG	*DROP3*
DMI3fw2	AGGACAGAAGAGGAGTGGACC	*DROP3*

Table S 2. Primers used for sequencing of *PrDROPx::*GUS constructs

Primer name	Sequence (5'->3')	Binds in
pBI101.3_F	GCGGATAACAATTTCACACAGGA	PBI103.3
pBI101.3	CGGGTTGGGGTTTCTACAGG	*DROP1*
DMI1fw_BamHI_N	AAAAAAGGATCCTGCCACACTAAGACCAGCCAAT	*DROP1*
pDMI1_seq2_RV	TCCAATCACCACCACTCCCAAT	*DROP1*
pDMI1_seq_RV	GCATGGTGTTACTGCCAGGTCTAC	*DROP1*
DMI1rv_BamHI_N	AAAAAAGGATCCCGGGTTGAAGTAAGTAAATTGAGAAACAG	*DROP1*
DMI2fw_BamHI_N	AAAAAAGGATCCAGTGAAAGATTATGCCCTCCACATG	*DROP2*
pDMI2_SEQ_fw3	CTCTCTGTGGTAATGTGCACGATC	*DROP2*
pDMI2fw1	CTTGTGGATGAGGTTTTAACGATAG	*DROP2*
pDMI2rv	TCTTCTTCCACTCACTTCTCTCGTT	*DROP2*
pDMI2fw2	ATGTTTATATGGTCTAGGGCTGTGC	*DROP2*
DMI2rv_BamHI_N	AAAAAAGGATCCTTATCTCTTCTCCTCGCTCTCTCTTTGT	*DROP2*
DMI3fw_BamHI	AAAAAAGGATCCTCGCATCATAGCAAGGAAAGCAAG	*DROP3*
pDMI3_seq2_RV	GCGATGAGGCACTTCAAGA	*DROP3*
pDMI3_seq_FW	CGACTCCTTCTGGTTCCGTAG	*DROP3*
pDMI3_seq_RV	TCTTCGTCTCTCGTATGATGTACTGT	*DROP3*
pDMI3_seq2_FW	GCTCTCTCAATGGTCAAAA	*DROP3*
DMI3rv_BamHI	AAAAAAGGATCCCTTTCTTAATCTTCTCCTTGATTTATCTTACGC	*DROP3*

Appendix

Table S 3. Details on promoter-GUS photos presented in this thesis

Construct	Figure	Age of plants	Tissue	line	Incubation time
*prDROP1::*GUS	Fig. 8 b c Fig. 8 d	4 week-old plants 18 d seedlings	Rosette base Seedling	1-6	16 hrs
*prDROP1::*GUS	Fig. 8 a	4 week-old plants	Root	1-8	16 hrs
*prDROP2::*GUS	Fig. 13 Fig. 14	10 d seedlings 30 d plants	Leaves under flg22-stress	2-1 2-7	12 hrs
*prDROP2::*GUS	Fig. 8 h Fig. 11	12 d seedlings 6-7 week-old plants	Leaves of seedling Flowers	2-6	16 hrs 16 hrs
*prDROP2::*GUS	Fig. 9 a	7-8 week-old plants	Inflorescence	2-1	16 hrs
*prDROP2::*GUS	Fig. 8 f	30 d plants	Leaf	2-6	16 hrs
*prDROP2::*GUS	Fig. 9 b	6-7 week-old plants	Stigma	2-7	16 hrs
*prDROP2::*GUS	Fig. 9 c Fig. 8 e Fig. 9 d Fig. 8 g	6-7 week-old plants 12 d seedlings 7-8 week-old plants 12 d seedlings	Stigma Root Silique Roots of seedling	2-5	16 hrs 16 hrs 16 hrs 16 hrs
*prDROP3::*GUS	Fig. 15	18 d seedlings	Seedlings under drought stress	3-1 3-3 3-2	8 hrs
*prDROP3::*GUS	Fig. 8 i,l Fig. 8 j Fig. 9 h	15 d seedling 30 d plants 7-8 week-old plants	Root tip, seedling Leaf Silique	3-2	16 hrs 16 hrs 16 hrs
*prDROP3::*GUS	Fig. 12 Fig. 9 g	6-7 week-old plants 6-7 week-old plants	Flowers Stigma	3-8	16 hrs 16 hrs
*prDROP3::*GUS	Fig. 9 e	7-8 week-old plants	Inflorescence	3-3	16 hrs
*prDROP3::*GUS	Fig. 9 f	6-7 week-old plants	Stigma	3-7	16 hrs
*prDROP3::*GUS	Fig. 8 k	18 d seedlings	Roots of seedling	3-1	16 hrs

Table. S 4 Manufacturers' addresses

Company	Address
Apolda	Apolda, Germany
Biozym	Oldendorf, Germany
Carl Roth	Karlsruhe, Germany
Duchefa	Haarlem, The Netherlands
Finnzymes	Espoo, Finland
Fluka	Buchs, Switzerland
Formedium	Hunstanton, England
Invitrogen	Darmstadt, Germany
Macherey-Nagel	Düren, Germany
MBI Fermentas	Waltham, MA U.S.A
New England Biolabs (NEB)	Ipswich, U.K
Sigma-Aldrich	St. Louis, USA
Promega	Madison,WI U.S.A
Qiagen	Venlo, The Netherlands

Eidesstattliche Erklärung / *Declaration under Oath*

Ich erkläre an Eides statt, dass ich die Arbeit selbstständig und ohne fremde Hilfe verfasst, keine anderen als die von mir angegebenen Quellen und Hilfsmittel benutzt und die den benutzten Werken wörtlich oder inhaltlich entnommenen Stellen als solche kenntlich gemacht habe.

I declare under penalty of perjury that this thesis is my own work entirely and has been written without any help from other people. I used only the sources mentioned and included all the citations correctly both in word or content.

_____ _____ _____

Datum / Date Unterschrift des Antragstellers / *Signature of the applicant*

Acknowledgements

I would like to express my great appreciation to everyone who helped me during studying towards my PhD in Halle. It was my dream since I was a teenager to study abroad. As a master student I realized that my interest really was in lab research about plant molecular biology. I was very lucky that everything came true during my PhD.

First, I would like to thank the CSC (China Scholarship Council, my financial support) for giving me the opportunity to spend several years for studying abroad and the Land Sachsen-Anhalt (Ministerium für Landwirtschaft und Umwelt) for funding parts of this project.

Many thanks to all outstanding colleagues of Prof. Peiter´s group. In my PhD journey, we used to work together every day, even on weekends. How can I forget every lab member! We were working with the same PCR machines, touching the same plates and sharing the same clean bench each day. The relationship between us therefore got close without needing German language. I learned a lot from all of you.

Special thanks to PD Dr. agr. Feng Yan from Gießen. He recommended and introduced me to Prof. Dr. Edgar Peiter.

I wish to thank Tina Peiter-Volk, the first person I knew in Halle. She gave me a lot of help for my life here. It was her to teach me cloning technology at the very beginning of my study.

I am very grateful to Dr. Kathrin Thor and thank her for giving me an excellent scientific supervision. It is clear that without her, my PhD work would have been impossible. Her exceptional ideas, profound knowledge and continuous guidance supported me to finish my PhD thesis.

I would like to sincerely thank Prof. Dr. Edgar Peiter for introducing me to the scientific fields of plant nutrition and molecular biology and for providing me the opportunity to work under his supervision in this group. His excellent advices, unlimited encouragement and support throughout the graduate study will always be remembered.

Finally, also many thanks to my Chinese friends who stayed with me when I felt lonely; encouraged me when I was not brave to face problems; cared for me when I was upset. Therefore, I cannot imagine my life without all of you.

Last but not least, I wish to thank all my family members for their support. They encouraged me to achieve my dream no matter when or where I am. Thanks to my mother and to my Yong Chen who always stand by and accepted me when I was wayward, petulant, and disagreeable.

Curriculum Vitae

Personal data

Name	Xuefeng Gong
Date of birth	6th of February 1983
Place of birth	Xi´an, VR China
Address	Northwest A & F University, No.3 Taicheng Road, Yangling, Shaanxi, 712100 VR China (In China) Wolfgang-Langenbeck-Str. 5, 06120 Halle (Saale) (In Germany)

Education

September, 2000 - July, 2004	Undergraduate studies in Agronomy (Horticulture), Northwest Agriculture & Forestry University, China.
September, 2005 - July, 2008	Masters Degree (MSc) in Agronomy (Tea Science), Northwest Agriculture & Forestry University, China.
Since November, 2009	PhD studies at the Institut für Agar- und Ernährungswissenschaften, Naturwissenschaftliche Fakultät III, Martin-Luther-Universität Halle-Wittenberg, Germany

Occupations

July, 2004 – July, 2005	working for logistics group of Northwest Agriculture & Forestry University

Halle (Saale), 15 August 2013 Signature:_____

Publications and contributions to meetings

Poster presentations

Gong, X., Kiep, V., Janssen, A., Peiter, E., Thor, K.
Characterization of Arabidopsis homologs to a leguminous Ca^{2+} signal modulator.
International Workshop and Meeting of the German Society of Plant Nutrition, Bonn 2012

Thor, K., **Gong, X.**, Kiep, V., Janssen, A., Peiter, E.
From nodules to stress response – towards the function of Arabidopsis homologues to a leguminous Ca^{2+} signal modulator
International Symposium "Communication in Plants and their Responses to the Environment", Halle 2011

Thor, K., **Gong, X.**, Kiep, V., Janssen, A., Peiter, E.
More than nodules? Investigating *Arabidopsis* homologues to a leguminous Ca^{2+} signal modulator
International Symposium “Plant Calcium Signaling”, Münster 2010

Thor, K., **Gong, X.**, Kiep, V., Janssen, A., Peiter, E.
More than nodules? Investigating Arabidopsis homologues to a leguminous Ca2+ signal modulator
Meeting of the German Society of Plant Nutrition "Genetics of Plant Mineral Nutrition", Hannover 2010